

Fall 2013

Analysis Strategies for Bioactive, Polar Fatty Amides in Complex Samples

Erin Blaine Divito

Follow this and additional works at: <https://dsc.duq.edu/etd>

Recommended Citation

Divito, E. (2013). Analysis Strategies for Bioactive, Polar Fatty Amides in Complex Samples (Doctoral dissertation, Duquesne University). Retrieved from <https://dsc.duq.edu/etd/489>

This Immediate Access is brought to you for free and open access by Duquesne Scholarship Collection. It has been accepted for inclusion in Electronic Theses and Dissertations by an authorized administrator of Duquesne Scholarship Collection. For more information, please contact phillips@duq.edu.

ANALYSIS STRATEGIES FOR BIOACTIVE, POLAR FATTY AMIDES IN
COMPLEX SAMPLES

A Dissertation

Submitted to the Bayer School of Natural and Environmental Sciences

Duquesne University

In partial fulfillment of the requirements for
the degree of Doctor of Philosophy

By

Erin Blaine Divito

December 2013

Copyright by
Erin Blaine Divito

2013

ANALYSIS STRATEGIES FOR BIOACTIVE, POLAR FATTY AMIDES IN
COMPLEX SAMPLES

By

Erin Blaine Divito

Approved August 9, 2013

Michael Cascio, Ph.D.
Professor of Chemistry and Biochemistry
(Committee Chair)

Jeffry Madura, Ph.D.
Professor of Chemistry and Biochemistry
(Committee Member)

Stephanie Wetzel, Ph.D.
Professor of Chemistry and Biochemistry
(Committee Member)

Jelena Janjic, Ph.D.
Professor of Pharmacy
(Committee Member)

Philip Reeder, Ph.D.
Dean, Bayer School of Natural and
Environmental Science
Professor of Chemistry and
Biochemistry

Ralph Wheeler, Ph.D.
Chair, Department of Chemistry and
Biochemistry
Professor of Chemistry and Biochemistry

ABSTRACT

ANALYSIS STRATEGIES FOR BIOACTIVE, POLAR FATTY AMIDES IN COMPLEX SAMPLES

By

Erin Blaine Divito

December 2013

Dissertation supervised by Michael Cascio

Bioactive lipids are known to exert physiological effects and interact with neuroreceptors. Little is known about the bioregulation of primary fatty acid amides, though N-acyl glycines are thought to be their anabolic precursors. Chapter 1 details the current metabolic, physiological, and receptor interactions of primary fatty acid amides and their related congeners and reviews current strategies for isolation and detection. Chapter 2 outlines mass spectrometry collision induced fragmentation assignments pertaining to method development of multiple reaction monitoring detection of these species. Chromatographic separation methods of fatty acyls, with a focus on primary fatty acid amides and N-acyl glycines, are outlined in chapter 3 and these results are used to develop a two dimensional liquid chromatography tandem mass spectrometry analysis method. Multiple reaction monitoring was utilized as the detection mode due to the

enhanced limit of detection obtained from mass filtering background and matrix components. The implementation of our developed analytical separation and detection approach for quantitation of these bioactive lipids in vertebrate samples and future implications of primary fatty acid amide and N-acyl glycine analysis are reviewed in chapter 4. In addition, the appendix summarizes a method for selective, sensitive multiple reaction monitoring detection of palmitoylethanolamine, an N-acylethanolamine with analgesic and anti-inflammatory properties.

DEDICATION



This thesis work is dedicated to the late Dr. Mitchell E. Johnson.

ACKNOWLEDGEMENT

Foremost, I would like to express my deep gratitude to Dr. Michael Cascio for his close mentorship, scientific and personal support after the unexpected passing of my graduate mentor, Dr. Mitch Johnson. I am grateful for the time and thoughtfulness Mike has added to my PhD experience. He exudes enthusiasm for both life and science which proved to be contagious in our lab environment.

Thanks to my committee members Dr. Stephanie Wetzel, Dr. Jeffry Madura, and Dr. Jelena Janjic. Each of you has provided invaluable advice, time, and support to me while in pursuit of my PhD. Special thanks to Stephanie for the mentorship on instrumentation trouble shooting and maintenance she has given throughout my time at Duquesne.

Great thanks to both the Cascio and Johnson lab group members. I won't name all of you, there are simply too many! You have made my time at Duquesne an enjoyable experience. I will always remember our group lunches, brewing discussions, practical jokes, bad science movie Fridays, and long rides home. I could not have asked for better friends to share this time with. You are truly the ideal 'science family'. Best of luck to those of you who are still making your PhD journey.

To my family and friends, thank you. You have given me unending support, love, and encouragement throughout my life which has made me the person I am today.

Lastly, I would like to thank my husband. You have been a constant in this crazy time.

Thank you for the support, early morning car rides home from lab, all our scientific

discussions, and your wonderful sense of humor. I am so excited to see what the next steps in our journey hold.

Erin Divito

Duquesne University

2013

TABLE OF CONTENTS

	Page
Abstract.....	iv
Dedication.....	vi
Acknowledgement.....	vii
List of Tables.....	xiii
List of Figures.....	xiv
List of Abbreviations.....	xvi
Chapter 1: Metabolism, Physiology, and Analyses of Primary Fatty Acid Amides.....	1
1.1 Introduction.....	1
1.2. Biosynthesis.....	3
1.2. Degradation by Fatty Acid Amide Hydrolase.....	9
1.3. Fatty Acid Amide Effects on Physiology.....	11
1.3. Serotonin Receptors.....	13
1.3.2. Cannabinoid Receptors.....	15
1.3.3. GABA and Glycine Receptors.....	17
1.3.4. Glycine Transporters.....	18
1.3.5. Gap Junction and Ca ²⁺ Signaling.....	19
1.3.6. Transient Receptor Potential Vanilloid Receptors.....	21
1.3.7. Interaction with Orphan G-protein Coupled Receptors.....	24
1.4. Analyses Methods.....	25
1.4.1. Chromatographic Separation Techniques.....	25

1.4.2. Detection Methods.....	27
1.5 . Summary and Outlook.....	28
Chapter 2: Electrospray Ionization and Collision Induced Dissociation Mass Spectrometry of Primary Fatty Acid Amides and N-acyl Glycines.....	
2.1 .Abstract.....	31
2.2 Introduction.....	32
2.3 Materials and Methods.....	34
2.3.1. Chemicals.....	34
2.3.2. PFAM Synthesis.....	35
2.3.3. Mass Spectrometry.....	36
2.4 Results.....	36
2.5 Discussion and Conclusion.....	46
Chapter 3: Chromatographic Separation Methods for Fatty Acyls.....	
3.1 .Abstract.....	49
3.2 Introduction.....	49
3.3 Materials and Methods.....	53
3.3.1. Chemicals.....	53
3.3.2. Normal Phase Separation.....	54
3.3.3. Silver Ion Chromatography.....	54
3.3.4. Reversed Phase Separation of N-acyl Glycines.....	55
3.3.5. Reversed Phase Separation of Primary Fatty Acid Amides.....	56
3.4 Results.....	57

3.4. Normal Phase Chromatography.....	56
3.4.2 Silver Ion Chromatography.....	59
3.4.3. Reversed Phase Separation of N-acyl Glycines.....	61
3.4.4. Reversed Phase Separation of Primary Fatty Acid Amides.....	64
3.5. Discussion and Conclusion.....	66

Chapter 4: PFAM and NAG Detection in Tissue Samples and

Implications for Future Studies	70
4.1. Abstract.....	70
4.2. Introduction.....	71
4.3. Materials and Methods.....	72
4.3.1. Chemicals.....	72
4.3.2. Lipid Extraction and Normal Phase Separation.....	73
4.3.3. Reversed Phase Separation with MRM Detection of PFAMs and NAGs.....	74
4.4 Results.....	75
4.5. Discussion and Conclusion.....	79
4.6. Project Outlook and Concluding Remarks.....	82

Appendix 1: Palmitoylethanolamine Stability in Fluorocarbon Emulsions: A Delivery

System for Treatment of Chronic Pain.....	85
A.1. Abstract.....	85
A.2. Introduction.....	85
A.3 Materials and Methods.....	92

A.3.1. Chemicals.....	92
A.3.2 Methods.....	93
A.4. Results.....	93
A.5. Discussion and Conclusion.....	97
References.....	101

LIST OF TABLES

	Page
1-1. Representative structures from the FA, PFAM, NAG, and NAE subclasses of lipids.....	2
1-2. Summary of effects of oleamide, N-arachidonoylglycine, and anandamide on various receptors, transporters, and gap junction proteins.....	13
3-1. LOD and LOQ for several commercially available NAGs.....	63
3-2. LOD and LOQ for select PFAMs	66
A-1. Quantitation of PEA in nano-emulsions.....	97

LIST OF FIGURES

	Page
1-1. Proposed pathways of PFAM anabolism.....	9
1-2. Degradation scheme of oleamide and anandamide with enzyme FAAH.....	10
2-1. CID of stearamide, oleamide, and oleoylglycine.....	40
2-2. Product ion scans of saturated PFAMs.....	41
2-3. Product ion scans of palmitamide and 13C-1-palmitamide.....	42
2-4. Product ion scans of monounsaturated PFAMs.....	43
2-5. Proposed mechanism for the loss of ammonia and water from PFAMs.....	44
2-6. Product ion scans of oleamide and 13C2-9, 10-oleamide.....	44
2-7. CID pattern of oleoylglycine.....	45
3-1. Chromatogram of seven fatty acyl subclasses separated by normal phase chromatography.....	57
3-2. Example chromatogram of fractional PFAM elution from normal phase chromatography.....	58
3-3. FAPE elution by silver ion chromatography.....	60
3-4. FAPE elution by silver ion chromatography.....	61
3-5. Separation of NAGs.....	62
3-6. Separation of very long chain PFAMs.....	64
4-1. Analysis of contamination and use of inhibitors in tissue extracts.....	76
4-2. Analysis of individual Sprague-Dawley rat hearts and Swiss-Webster mouse brain with mid-brain removed.....	77
4-3. Time dependent extraction of individual Sprague-Dawley rat heart samples.....	78

4-4. Analysis of Sprague-Dawley rat liver.....	79
A-1. CID of PEA.....	94
A-2. Linear range, LOD and LOQ determination of PEA.....	95

LIST OF ABBREVIATIONS

5-HT.....	5-hydroxytryptamine
5HTR.....	5-hydroxytryptamine receptor
ADH.....	alcohol dehydrogenase
AEA.....	arachidonylethanolamine
APCI.....	atmospheric pressure chemical ionization
BAAT.....	bile acid CoA: amino acid N-acyl transferase
cAMP.....	cyclic adenosine monophosphate
CB.....	cannabinoid receptor
CE.....	collision energy
CID.....	collision induced dissociation
CSF.....	cerebral spinal fluid
DAG.....	diacylglycerol
DRG.....	dorsal root ganglion
ESI.....	electrospray ionization
FA.....	fatty acid
FAAH.....	fatty acid amide hydrolase
FAPE.....	fatty acid phenacylester
GABA.....	γ -aminobutyric acid
GAT.....	γ -aminobutyric acid transporter
GC.....	gas chromatography
GLYAT.....	glycine N-acyl transferase

GLYATL.....	glycine N-acyl transferase like
GlyR.....	glycine receptor
GLYT.....	glycine transporter
GPR.....	G protein receptor
HPLC.....	high pressure liquid chromatography
IL-1 β	interleukin-1 beta
LC.....	liquid chromatography
LOD.....	limit of detection
LOQ.....	limit of quantitation
MAG.....	monoacylglycerol
MDLC.....	multidimensional liquid chromatography
MRM.....	multiple reaction monitoring
MS.....	mass spectrometry
MS/MS.....	tandem mass spectrometry
NAAA.....	N-acylethanolamine-hydrolyzing acid amidase
NAE.....	N-acylethanolamine
NAG.....	N-acyl glycine
NMR.....	nuclear magnetic resonance
OEA.....	oleoylethanolamine
PAL.....	peptidyl- α -hydroxyglycine- α -amidating lyase
PAM.....	peptidylglycine α -amidating monooxygenase
PCR.....	polymerase chain reaction
PEA.....	palmitoylethanolamine

PFAM.....primary fatty acid amide
PPAR.....peroxisome proliferator activated receptor
QToF.....quadrupole time of flight
QqQ.....triple quadrupole
SEA.....stearoylethanolamine
SPE.....solid phase extraction
TAG.....triacylglycerol
THC.....tetrahydrocannabinol
TLC.....thin layer chromatography
TRPV.....transient receptor potential vanilloid receptor
UPLC.....ultra-high pressure liquid chromatography
UV.....ultraviolet

Chapter 1

Metabolism, Physiology, and Analyses of Primary Fatty Acid Amides

Adapted from: Divito, E. B.; Cascio, M. Metabolism, Physiology, and Analysis of Primary Fatty Acid Amides. Chemical Reviews. (In Press)

1.1 INTRODUCTION

Primary fatty acid amides (PFAMs) are a group of lipids that have been identified as bioactive lipid signaling molecules. In this introductory chapter we review the progress in identifying metabolism pathways, pharmacological properties, and receptor interactions for this group of lipids. In addition, various modes of separation and detection have been developed to study both their biological content and alterations in their metabolism, and these studies are also reviewed.

Lipids are loosely defined as hydrophobic molecules, typically containing an acyl chain or ring structure, that are soluble in organic solvents. Recently a new classification system was developed allowing for a broad definition of lipids that is based on similarity in structure and biosynthetic pathways¹. This system ultimately divided lipid molecules into eight different classes, including numerous subclasses. It is easily observed from the number of subclasses in each category that lipids comprise a broad range of molecules. A few subclasses of the fatty acyls group relevant to this review are shown in Table 1-1. A new subclass of lipids, the PFAMs, has been recently identified. This group consists of a carboxamide head group and an acyl tail of various length and unsaturation. The first report of PFAMs was in luteal phase plasma reported in 1989 by Arafat and coworkers². Since this initial discovery, many studies have been published on their interaction with

various receptors, including the 5-hydroxytryptamine (5-HT)³⁻⁸, cannabinoid⁹, and γ -aminobutyric acid (GABA) receptors^{10,11}. Interactions of PFAMs with cannabinoid receptors are still somewhat controversial, as oleamide has been shown to weakly potentiate (1 μ M) or to have no effect on cannabinoid receptors *in vitro*^{12,13}. Additionally, many observations of behavioral effects upon subcutaneous or intravenous injection of oleamide (octahexanoamide, denoted C18:1⁹) have been reported. These responses include analgesic and anti-anxiety¹⁴ phenotypes, sleep induction¹⁵⁻¹⁷, and increased food uptake.¹⁸ There also is an implied link between oleamide and mood due to the observed potentiation of 5-HT receptors (5-HTR) with exogenous application of oleamide^{14,19}.

Although studies indicate PFAMs are bioactive signaling molecules, little is known about their metabolism or localization *in vivo*. This is possibly due to their low concentrations in tissue and biological fluids, typically in the nM range^{2,16,20,21}, which makes analyses challenging. Their structural similarity to other lipid subclasses and occurrence of isomers within the subclass can make isolation and structural identification more complicated. This review will examine some of the progress made towards identifying PFAM metabolic pathways, their physiology and receptor interactions, and current methods of analyses.

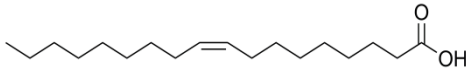
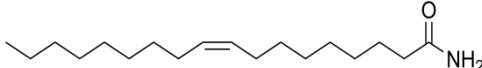
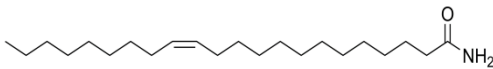
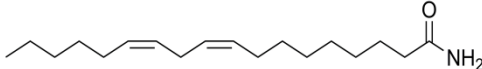
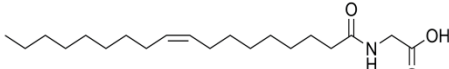
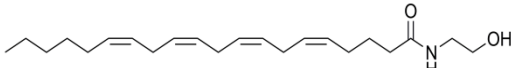
Lipid Subclass	Common Name (CX:Y ^z)	Structure
Fatty Acids (FA)	Oleic acid (C18:1 ⁹)	
Primary Fatty Acid Amides (PFAMs)	Oleamide (C18:1 ⁹)	
	Erucamide (C22:1 ¹³)	
	Linoleamide (C18:2 ^{9,12})	
N-acyl Glycines (NAGs)	Oleoylglycine (C18:1 ⁹)	
N-acyl Ethanolamines (NAEs)	Anandamide (C20:4 ^{5,8,11,14})	

Table 1-1. Representative structures from the FA, PFAM, NAG, and NAE subclasses of lipids. The common name is given for each structure along with the typical lipid abbreviation CX:Y^z. C indicates the carbon acyl chain starting from the head group position with X being the number of carbon atoms in the chain. Y is the number of unsaturation points and z indicates the position(s) of

1.2. BIOSYNTHESIS

The identification of PFAMs in human plasma in 1989² went largely unrecognized until 1995 when Cravatt *et al.*¹⁵ reported increased levels of three PFAMs in the cerebral spinal fluid (CSF) of sleep deprived cats. This finding, in conjunction with several other reports on oleamide (C18:1⁹) and 5-HTR interaction³⁻¹¹, increased interest in the anabolic pathways of PFAMs. An enzyme involved in the post-translational modification of peptides, peptidylglycine α -amidating monooxygenase (PAM), converts peptidyl glycines to their active amidated form. Merkler *et al.*²² were

the first to report that PAM also converts N-myristoylglycine (C14:0) to the primary amide, myristamide. This led the authors to hypothesize that PAM could amidate other fatty glycines to their corresponding primary amide form. In a subsequent work, a broad range of fatty glycines, from formylglycine to linoleoylglycine, were converted to the primary amide form by purified recombinant type A rat PAM^{23,24}. The apparent affinity of these substrates for PAM varied widely, but generally increased as the acyl chain length of the substrate increased. The K_m for longer chain length substrates were generally equal or greater than that of a previously characterized “good” peptide substrate, D-Tyr-Val-Gly. Oxygen and glyoxylate levels were measured to quantitate activity of PAM, and NMR studies confirmed the conversion of the fatty glycine to its PFAM. During monitoring of oxygen and glyoxylate, oxygen levels depleted rapidly while glyoxylate production, from the oxidative cleavage of the fatty glycine, accumulated more slowly. This supported a hypothesis that the fatty glycine first goes through an intermediate form before oxidative cleavage by peptidyl- α -hydroxyglycine α -amidating lysase (PAL), the second domain of PAM. The intermediate was identified by NMR analysis as N-acyl- α -hydroxyglycine²³. *In vitro* reactions of PAM and various fatty glycines were analyzed by liquid chromatography and UV detection, and the resulting three peaks were identified as the fatty glycine, the N-acyl- α -hydroxyglycine, and the PFAM. When a PAL inhibitor was added to the incubation mixture the levels of fatty glycine and the intermediate N-acyl- α -hydroxyglycine increased and PFAM levels were decreased as compared to the incubation mixtures without inhibitor²⁵. Similar results were observed in N₁₈TG₂ mouse neuroblastoma cells²⁶. The authors proposed a biosynthesis pathway where a fatty acid is converted to a fatty-CoA by acyl-CoA

transferase. The fatty-CoA then is converted to a fatty glycine by glycine N-acyl transferase (GLYAT) and the fatty glycine proceeds to the PFAM through the actions of PAM (see Scheme 1).

Mueller and coworkers have reported enzymatic conversion of both oleoyl-CoA and oleoyl glycine to oleamide by cytochrome *c*^{27,28}. In both cases, the presence of oleamide was confirmed by TLC separation, liquid chromatography with UV detection, and tandem mass spectrometry. In regard to conversion of oleoyl-CoA to oleoyl glycine, maximal conversion rates were observed with 300 μ M glycine and 2 mM hydrogen peroxide under physiological conditions (37°C and pH 7.6)²⁸. Similar conditions were reported for the synthesis of oleamide from oleoyl-CoA, except that ammonium chloride was 125 mM for maximal activity²⁷. Similar experiments were conducted by McCue *et al.* demonstrating that arachidonoyl-CoA could also be converted to the fatty glycine by cytochrome *c*²⁹. Ammonium has been implicated as the source of nitrogen in the amidation reaction producing PFAMs³⁰, however the enzyme responsible for the conversion was not identified. Additionally, oleic acid was unable to be converted directly to either oleoylglycine or oleamide, consistent with the proposed pathway of Merkle and coworkers²⁴ wherein the fatty-CoA is an essential component in oleamide biosynthesis.

Bile acid CoA:amino acid N-acyl transferase (BAAT) has also been found to catalyze the conversion of fatty-CoA substrates to fatty glycines³¹. This enzyme displayed highly variable activity for acyl chain lengths of 16 to 22, and its activity was markedly decreased when any degree of unsaturation was present. The relative enzymatic activity increased for saturated fatty-CoAs of 22 to 26 carbon length. This

enzyme, therefore, might not aid in the formation of oleamide, but of other long chain PFAMs.

In 2010, Waluk *et al.*³² demonstrated that glycine N-acyltransferase-like 2 (GLYATL2) showed specificity with glycine conjugation of fatty-CoAs of medium chain length (C8 to C18). GLYAT is known to have highest activity with benzoyl-CoA, but is also capable of conjugating glycine to short chain fatty-CoAs (less than C8)³³. GLYATL2 showed the highest activity with C18:1-CoA ($K_m = 4 \mu\text{M}$) to produce oleoylglycine. Little to no activity was observed with substrates with fewer than an 8 carbon acyl chain, in the absence of conjugated glycine, and with alanine, serine, or taurine substituted for the glycine moiety. Additionally, some inhibition was observed with substrate concentrations above 50 μM . Interestingly, this enzyme was found in the endoplasmic reticulum localized in the salivary gland, trachea, spinal cord, and skin. Measurement of levels of NAGs by LC-MS in selected ion mode found highest NAG levels in the spinal cord and skin³⁴, similar to reports of GLYATL2 localization, providing evidence that this is a good candidate enzyme for *in vivo* synthesis. It is important to note that rodents do not possess the ortholog to hGLYATL2. They do express the orthologs for hGLYAT and hGLYATL3, however the latter has not yet been characterized for acyl-glycine conjugating activity.

Several other reports have identified a relatively new pathway for synthesis of NAGs from NAE precursors. The first report, by Burstein and co-workers³⁵, identified via radiochromatograms that liver cell extracts produced N-arachidonoylglycine when anandamide was present. In experiments with RAW 264.7 murine macrophage cells, it was established that a deuterium labeled anandamide produced a likewise deuterium

labeled N-arachidonoylglycine as determined with LC-MS/MS studies³⁶. The authors also demonstrated that incubation of cells with arachidonic acid did not produce N-arachidonoylglycine. Application of N-arachidonoylglycine to cell cultures also did not result in the production of neither arachidonic acid nor anandamide. To support that alcohol dehydrogenase (ADH) was the enzyme responsible for the conversion of anandamide to N-arachidonoylglycine; the ethanolamide moiety of anandamide was deuterium labeled. Analysis of the products showed deuterium labeling of N-arachidonoylglycine consistent with the mechanistic actions of ADH. Incubations of anandamide, glycine, and recombinant FAAH were unable to produce N-arachidonoylglycine, therefore ruling out this enzyme as a participant in the conversion.

These findings have been further supported by *in vitro* studies of purified ADH isoforms. ADH7 was used with anandamide (1-8 M) to determine if this enzyme catalyzes the production of N-arachidonoylglycine from anandamide³⁷. Products analyzed by LC-MS/MS in MRM mode revealed a match to the standard N-arachidonoylglycinal. In incubations of ADH7 with N-arachidonoylglycinal, N-arachidonoylglycine product was only detected in the presence of enzyme. ADH5 was found to be inactive for conversion of anandamide to the glycinal or glycine derivative. However, these studies were conducted under non-physiological conditions.

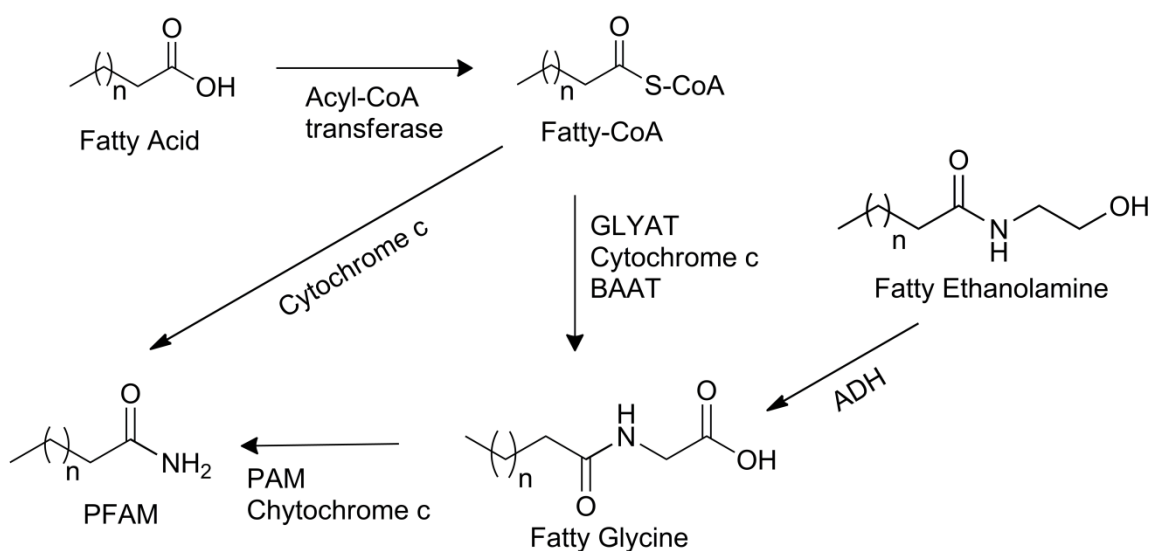
ADH3 was found to convert NAEs (C2 – C20) to their corresponding N-acylglycinals with K_m and V_{max} values generally decreasing with increasing chain length³⁸. These studies were confirmed with analysis by HPLC, GC-MS, and carbon NMR. K_m and V_{max} values were unable to be determined for carbon chains above 12 due to low solubility. However, acetylethanolamine values were $V_{max}/K_m = 2.7 \text{ sec}^{-1}\text{M}^{-1}$, K_m

= 450 mM, $V_{\max} = 1.9 \mu\text{mol}/\text{min}\times\text{mg}$ and lauroylethanolamine were $V_{\max}/K_m = 160 \text{ sec}^{-1}\text{M}^{-1}$, $K_m = 0.033 \text{ mM}$, $V_{\max} = 0.14 \mu\text{mol}/\text{min}\times\text{mg}$. The fatty-glycinal was found to be the primary product and conversion to the fatty-glycine was determined to be due to non-enzymatic aldehyde dismutation. Docking experiments indicate the hydroxyl group of the NAE coordinating with Zn(II) of the active site akin to previously studied ADH3 substrates^{39,40}. The authors suggest that the relatively low K_m and V_{\max} values make it unlikely that this enzyme plays a significant role during *in vivo* conversion of NAEs.

The proposed intermediate of oleamide, oleoylglycine, was studied to determine the physiological effects and the effect on oleamide levels⁴¹. Injection reduced locomotion and core body temperature. After euthanasia, oleamide levels were found to not increase in serum, suggesting oleoylglycine has the ability to induce similar physiological effects as those observed with oleamide. Fatty glycines might not be requisite intermediates in the metabolic pathway of PFAMs. However, it is still unclear how this pathway is regulated *in vivo*.

Thus, current evidence suggests that PFAM synthesis does not proceed directly from the free fatty acid, but must first be converted to a fatty-CoA substrate for further modification. The next step in the proposed biosynthetic pathway is controversial, as it is not known at this time if GLYAT, cytochrome c, BAAT, an unidentified enzyme, or a combination is responsible for the conversion to the fatty glycine. If the fatty glycine is the anabolic intermediate, then conversion to the PFAM has been demonstrated with both PAM and cytochrome c. However, the results of Mueller *et al.*²⁸ suggest that an alternative pathway, to that proposed by Merkler²², could also exist leading from the fatty-CoA directly to the PFAM (see Scheme 1-1 for a pathway summary). It is also

unclear if glycine, ammonia, or some other molecule may be the source of nitrogen in the amidation reaction of PFAMs. For example, addition of glutamine to rat brain homogenate resulted in modest increase in levels of oleamide³⁰. Further studies are essential to provide a better understanding of the anabolic pathway for PFAMs, as defects in their metabolism may contribute to disease states and PFAMs clearly play an important role in health and fitness.

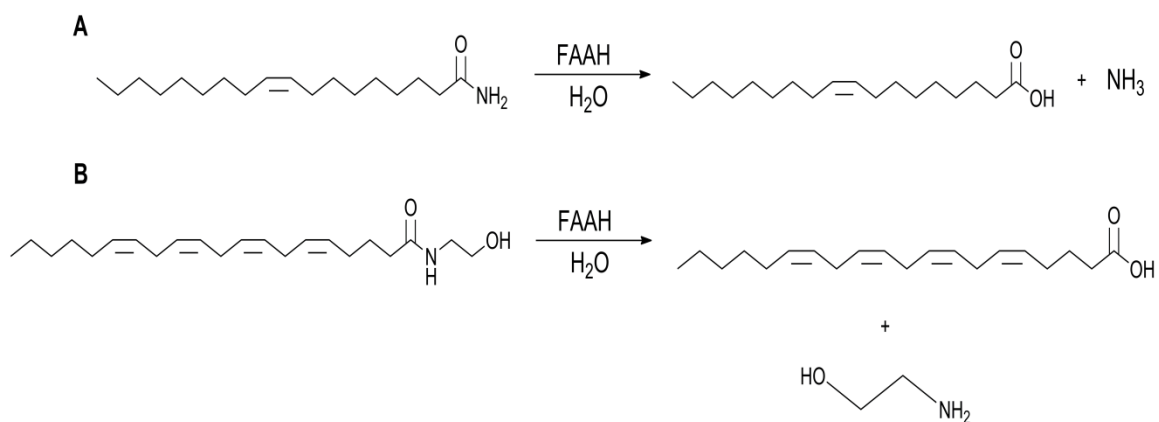


Scheme 1-1. Proposed pathways of PFAM anabolism suggest a starting product of a fatty acyl CoA substrate being converted to either to the related N-acyl glycine intermediate or directly to the PFAM. The substrates shown are of ambiguous length; however note that n (the number of carbons) does not change according to any of the proposed mechanisms. The enzymes shown (GLYAT, cytochrome c, PAM, and BAAT) in the conversion of the fatty-CoA to the fatty glycine or fatty amide are still debated *in vivo*.

1.2.1. Degradation by Fatty Acid Amide Hydrolase (FAAH)

FAAH activity has been extensively reviewed⁴²⁻⁴⁶, and is, therefore, only briefly discussed. FAAH is a 65 KDa integral membrane protein that enzymatically degrades fatty acid amides, such as anandamide and oleamide, to their respective fatty acid^{47,48} (Scheme 1-2). Site directed mutagenesis studies have identified three consensus amino

acids (K142, S217, and S241 in *rFAAH*) that are essential for enzyme activity, and these have been termed the Ser-Ser-Lys catalytic triad⁴⁹. Rat FAAH has been co-crystallized with inhibitor methoxy arachidonyl phosphonate and solved to a 2.8 Å resolution⁵⁰. In 2006, FAAH-2, another enzyme that degrades fatty acid amide substrates, was identified and has 20% sequence identity with FAAH. FAAH-2 has similar hydrolysis rates with oleamide (FAAH-1 9.7±0.8 and FAAH-2 8.4±0.8 nmol/min×mg, respectively) but could not degrade anandamide as efficiently as FAAH-1 (FAAH-1: 17 ± 1, and FAAH-2: 0.46 ± 0.04 nmol/min×mg, respectively)⁵¹. These two enzymes were found to have slightly different substrate selectivity, with FAAH-1 preferentially degrading poly-unsaturated substrates while FAAH-2 degraded mono-unsaturated substrates. The two enzymes seem to respond similarly to known inhibitors of FAAH-1 (see references 42-46 for lists of inhibitors). Interestingly, FAAH-2 sequence matches were found in humans but not in mice or rats, thus care should be taken in direct pharmacological comparisons across species and subtypes.



Scheme 1-2. Degradation scheme of (A) oleamide and (B) anandamide with enzyme FAAH. The amide substrates are degraded via hydrolysis to their corresponding fatty acid. For a catabolic mechanism involving FAAH see references 42 and 45.

1.3. FATTY ACID AMIDE EFFECTS ON PHYSIOLOGY

The most well-known physiological effect of PFAMs is their sleep inducing properties. Lerner *et al.* initially reported the increased concentration of a lipophilic molecule in the cerebrospinal fluid of sleep deprived cats, which they termed cerebrodien¹⁶. The structure was later verified as oleamide, and a second component was identified as erucamide¹⁵. Similar studies have also shown an increase in oleamide in the cerebral spinal fluid in hibernating squirrels⁵². Injection of 5 mg/kg of oleamide in rats induced hypolocomotion and sleep-like behaviors. Other reports have shown that oleamide injection in mice increases sleep latency and hypomobility^{11,14,19,53,54}. Oleic acid and elaidamide (C18:1^{9trans}) did not cause the sleep inducing properties of oleamide, consistent with specific allosteric interactions of this PFAM with a target receptor. The sleep induction process was not accompanied with changes in heart rate or blood pressure, however a concentration dependent decrease in body temperature (2°C at 20 mg/kg dose) was observed as soon as 30 minutes after injection^{17,54}. The mechanism by which oleamide acts to induce sleep is currently unknown.

Due to the structural similarity of oleamide and anandamide, other physiological effects of oleamide related to cannabinoid receptor interaction were investigated. Similar to the effects of anandamide, oleamide was found to induce overeating in Wistar rats at all doses tested (0.5-4 mg/kg). It is still uncertain if oleamide is able to interact directly with cannabinoid receptors *in vivo* or if the presence of oleamide increases the relative half-life of anandamide to yield secondary physiological effects.

Erucamide, also found in cerebral spinal fluid with oleamide, was previously isolated and purified from bovine omentum⁵⁵. This lipid was found to promote

angiogenesis in regenerating skeletal muscle, chick chorioallantoic membrane, rat cornea, and mouse dorsal air-sac when applied in microgram quantities. Related PFAMs, with varied acyl chain length, were also tested to determine their ability to promote angiogenesis. Similar to other reports previously discussed, amides with acyl chains shorter than 16 carbons showed weak or no angiogenesis, while longer chains approached activity comparable to erucamide. The increase in angiogenesis was explored to determine if this property was an effect of increased cellular proliferation. No increase in proliferation was observed with erucamide levels < 0.1 mg/mL. These effects were not affected by addition of glucocorticoid, suggesting that erucamide-induced angiogenesis is not due to an inflammatory response. These observations were later replicated by Mitchell *et al.* when studying the effect of erucamide on regenerating skeletal muscle⁵⁶. In samples where erucamide seemed to increase angiogenesis in skeletal muscle the standard deviation was large making interpretation difficult. Additionally, erucamide application did not change the type of cells present or increase regeneration, consistent with observations of Wakamatsu *et al.*⁵⁵.

NAGs have also been shown to have biological effects similar to PFAMs. Oleoylglycine has been shown to induce hypothermia and hypomotility in rats to a comparable potency as oleamide⁴¹. N-arachidonoylglycine has been demonstrated to dose dependently attenuate T lymphocyte proliferation³⁵. This substrate was also found to reduce IL-1 β secretion from human peripheral blood mononuclear cells with treatment at 1 and 10 μ M. Additionally, 0.43 μ g palmitoylglycine administered via intradermal injection suppressed the response to heat stimulus at 45-52°C⁵⁷ and 275 nmol of N-arachidonoylglycine reduced formalin-induced pain response. In the following sections

we focus on the observed effects of PFAMs and NAGs on metabotropic and ionotropic receptors, transporters, and gap junction proteins. These results are also summarized in Table 1-2.

Target	Substrate	Effect	Maximal Response	EC ₅₀	Reference
5-HT _{1A} R	Oleamide	Potentiates	100 nM	-	3
5-HT _{2A} R	Oleamide	Potentiates	100 nM	-	3, 7
5-HT _{2C} R	Oleamide	Potentiates	100 nM	-	5, 3
5-HT ₃ R	Oleamide	No effect	-	-	5
5-HT ₇ R	Oleamide	Inhibits	100 nM	-	7
CB ₁ R	Oleamide	No effect	-		13
		Potentiates		10 μM*	12
GABA _A R	Oleamide	No effect			5
		Potentiates (α1β1γ2s)	500 nM		66
		Potentiates (α1β2γ2L)		28 μM	64
		Potentiates		15 μM	10
α1 GlyR	Oleamide	Potentiates	-	22 μM	64
Gap Junction	Oleamide	Inhibits	100 μM	50 μM	71
GLYT2a	Arachidonoylglycine	Inhibits	-	5.1 μM*	67
GLYT1b	Arachidonoylglycine	No effect	-	-	67
GAT1	Arachidonoylglycine	No effect	-	-	67
TRPV1	Anandamide	Potentiates	-	5-12 μM	73, 77

Table 1-2. Summary of effects of oleamide, N-arachidonoylglycine, and anandamide on various receptors, transporters, and gap junction proteins. The * denotes values reported as an IC₅₀. Orphan receptors were excluded due to incomplete characterization at present time.

1.3.1. Serotonin Receptors

After the discovery that oleamide accumulates in the cerebral spinal fluid of sleep deprived mammals^{15,16} many reports were published on the effect of oleamide on serotonin (5-hydroxytryptamine) receptors (5HTRs), due to the link between 5-HTR activity and sleep⁵⁸⁻⁶⁰. c-Fos, a protein that regulates transcription, is found to be upregulated in specific brain regions of rat during night hours⁷. Intraperitoneal injections

of oleamide administered to rats induced a normal sleep-like state during daytime hours. Immunohistochemical staining and *in situ* hybridization indicated that c-Fos expression was increased in rat brain 45 minutes to 2 hours after injection with oleamide⁷. Expression of 5-HT₇R was identified in the same regions as c-Fos upregulation. The most prevalent areas of c-Fos upregulation as a result of oleamide treatment were the cerebral cortex, hypothalamus, and thalamus. Injections of oleic acid increased c-Fos expression as well; however the increase was not as significant as that observed with oleamide.

Huidobro-Toro *et al.* reported the effects of oleamide on *Xenopus* oocytes expressing either 5HT_{2A}R or 5HT_{2C}R by observing chloride currents produced by downstream signaling via two electrode recordings. Oleamide reversibly potentiated both serotonin subtypes via altered efficacy of 5HT_{2A}R and reduction of the EC₅₀ of 5HT_{2C}R. Co-treatment of the oocytes with kainate or carbachol, competitive inhibitors of 5HT₂R, did not alter the effects of oleamide suggesting oleamide acts at an allosteric site. Changing the *cis*- double bond to a *trans*- configuration, altering the head group to a carboxylic acid from the carboxamide, or movement of the double bond eliminates the potentiation effect observed with oleamide (stearamide (C18:0) exhibits inhibitory effects).

Boger *et al.* reported maximal potentiation of subtypes 5HT_{1A}R and 5HT_{2A}R when 100 nM oleamide was co-administered with 5HT³. Receptor activity was measured by calorimetric assay for β -galactosidase in NIH 3T3 cells expressing 5-HT_{2A}R, or in RAT-1 cells expressing 5-HT_{1A}R and the β -galactosidase gene. Of the lipid variants tested, oleamide was found to have the highest activity. Patterns in activity were

discerned by systematic alternation of oleamide's structure, as compounds containing an olefin at a $\Delta 9$ from the methyl terminus showed small potentiation while compounds with the olefin at $\Delta 9$ from the head group position were inactive. Movement of the double bond further from the carboxamide produced inactive compounds, while positioning the double bond closer to the carboxamide resulted in inhibitory effects. An overall increase in unsaturation points typically decreased potentiation. These results were mimicked in both receptor subtypes, however, 1A receptor subtypes were more tolerant of structural changes to oleamide than 2A receptor subtypes.

Oleamide was also found to increase phosphoinositide hydrolysis in 5HT_{2AR} when co-administered with 5HT⁶. As in previous reports, in the absence of 5HT oleamide had no substantial effect on phosphoinositide hydrolysis and increased cAMP accumulation. However, oleamide induced inhibition of cAMP in the presence of high concentrations of 5-HT (1 mM). Oleamide was shown to inhibit cAMP accumulation and radiolabeled 5-HT binding to 5HT_{7R} in a concentration-dependent manner^{6,8}. Clozapine, a high affinity inhibitor of 5-HT_{7R}, was unable to block the increase in cAMP in response to oleamide treatment. It was, thus, concluded that oleamide acts at an allosteric site, which is in agreement with the results previously discussed⁴.

1.3.2. Cannabinoid Receptors

Because PFAMs are structurally similar to the N-acylethanolamine (NAE) fatty acyl subclass, such as the endocannabinoid anandamide, efforts have been made to determine if oleamide is an endogenous ligand for cannabinoid (CB) receptors. Reports on oleamide interaction with CB₁ receptors have provided conflicting results thus far.

Oleamide causes concentration-dependent vasorelaxation of rat mesenteric resistance arteries^{9,61,62}. In the presence of AM251, a CB₁ receptor subtype inhibitor, but not AM630, a CB₂ subtype receptor inhibitor, the vasorelaxation was attenuated, suggesting that oleamide may induce these effects partially through action of CB₁ receptors⁹. These effects were also reduced in the presence of O-1918, an inhibitor of the non-CB₁/CB₂ receptor, and with inhibitors of the vanilloid receptor 1 (TRPV1). The attenuation was not observed in the presence of CB₁ receptor inhibitor when the mesenteric arteries were denuded of endothelium. The vasorelaxation effect was also reduced in the presence of nitric oxide synthase inhibitor, L-NAME, and with K⁺ and Ca⁺ channel inhibitors, indicating that oleamide may have several modes of action with respect to vasorelaxation^{9,62}. Addition of a fatty acid amide hydrolase inhibitor had no effect on the ability of oleamide to induce vasorelaxation⁹. Since formation of the catabolic metabolite, oleic acid, is inhibited in these studies it is concluded that carboxamide functionality is necessary for the vasorelaxation response. As expected from the FAAH study, exogenous application of oleic acid to rat mesenteric resistance arteries had no observable effect⁹. Several other reports have shown low affinity (IC₅₀ 10 μM¹²) or negligible binding of oleamide to CB₁ receptor¹³. It is unclear if solubility is contributing to the conflicting results, as some samples are prepared in an organic solvent-containing solution while others dissolved the lipid agent in saline. However, the physiological concentration of oleamide and other PFAMs in mesenteric arteries or heart, as well as other organ systems, is not reported. Interestingly, PAM activity was found to be 1000 times higher in the atrium, while no amidated peptides have been reported in that region. Since PAM is the proposed anabolic enzyme for PFAMs it is possible that PFAM levels

in heart may be higher than previously reported in cerebral spinal fluid or plasma (nM). Knowledge of these levels will aid in determining if PFAMs are endogenous endocannabinoids that can invoke signaling in vasorelaxation pathways. Additionally, this information may provide insight to other physiological roles as well as their anabolism *in vivo*.

1.3.3. GABA and Glycine Receptors

Oleamide administration via intraperitoneal injection in mice shows analgesic-like effects¹⁹ and, as previously stated, is shown to increase in the cerebral spinal fluid of animals subjected to 6 or more hours of sleep deprivation¹⁵. GABA receptors (GABAR) are targets for various sedatives, such as barbiturates and anesthetic steroids⁶³, raising speculation that oleamide may well interact with GABARs. In GABA_AR $\beta 3$ subunit knockout mice, intraperitoneal injection of oleamide (0.8 mg/kg or 1.6 mg/kg) did not produce a decrease in sleep latency that is typically observed in wild type mice treated with oleamide as compared to wild-type controls¹¹. Additionally, no other hypnotic effects were observed in the knockout mice versus controls not injected with oleamide. Therefore, it seems that GABAR may play a role in the oleamide-induced signaling pathway that causes sleep. Other reports have also shown that oleamide's effects may be subunit-dependent. Electrophysiological measurements have shown that oleamide potentiates chloride currents in $\alpha 1\beta 1\gamma 2$ or $\alpha 1\beta 2\gamma 2$ GABARs with an EC₅₀ of approximately 20 μM ^{10,64-66}. Oleamide alone had no effect on current as compared to controls, and current enhancement was not observed with the $\alpha 1\beta 2$ receptor type¹⁰. Radiolabeled binding assays indicated that binding of GABA was not affected by

oleamide application^{19,64}. The EC₅₀ for GABA was reduced, while the Hill slope was unaffected by exogenous application of oleamide, suggesting that oleamide works through an allosteric-type mechanism⁶⁴. Oleamide was found to potentiate $\alpha 1$ glycine receptor homopentamers, with a similar EC₅₀ to GABAR, but overall current enhancement was less marked than with GABARs. It has been suggested that receptor potentiation could be affected by second messenger signaling or altered receptor phosphorylation⁵³. Such changes in phosphorylation have been observed in $\alpha 1$ connexins⁶⁷ (see **3.5 Gap Junctions and Ca²⁺ Signaling**). However, these possibilities are unexplored for GABARs and GlyRs.

1.3.4. Glycine Transporters

In studies of the glycine transporter 2a (GLYT2a), co-application of glycine (30 μ M) and N-arachidonoylglycine (10 μ M) to *Xenopus* oocytes reduced the amplitude of the glycine mediated current measured by two electrode voltage clamp^{68,69}. Washout of N-arachidonoylglycine and subsequent application of glycine produced current levels similar to those observed before exposure to N-arachidonoylglycine. No difference in current amplitude was observed with treatment with staurosporine, thus, the observed inhibition by N-arachidonoylglycine is not linked to protein kinase C activation. In addition, N-arachidonoylglycine treatment also reduced the amount of glycine uptake. Given these observations, it was concluded that reduction in glycine currents was a result of N-arachidonoylglycine inhibition of GLYT2a activity. Concentration response data for glycine in the presence and absence of 10 μ M N-arachidonoylglycine revealed that the substrate acts as a reversible, non-competitive inhibitor with an IC₅₀ = 5.1 \pm 3.1 μ M.

Similar experiments show that N-arachidonoylglycine is not a substrate for GAT1 and GLYT1b.

1.3.5. Gap Junctions and Ca²⁺ Signaling

Oleamide, and another structurally similar PFAM, linoleamide (C18:2^{9,12}), were studied to determine their effect on gap junction communication and Ca²⁺ signaling. Application of 50 μM oleamide abolished gap junction transfer of Lucifer Yellow dye and conductance in cultured rat glial cells^{67,70}. Oleic acid and elaidamide (C18:1^{9 trans}) had no effect on dye transfer, nor conductance, even at concentrations greater than 50 μM. Other structural analogs, such as *cis*-8-octadecenamide, *cis*-11-octadecenamide, or the ethanolamine derivative, were effective at blocking gap junction communication, but with less potency than oleamide⁶⁷. Subsequent studies using a broad range of analogs found that the *cis*-9 olefin position and stereochemistry determined the magnitude of PFAM effect on gap junction activity in glial cells⁷⁰. Moving the double bond “up or down” the chain, as well as changing the stereochemistry from *cis*- to *trans*-, reduced the observed inhibition of gap junctions. Erucamide (C22:1¹³), a natural PFAM containing the typical positional isomer of C22:1, had negligible inhibitory effects, while a synthetic derivative, *cis*-9-docosenamide (C22:1⁹), inhibited gap junction activity to levels comparable to oleamide. Variations in the acyl tail length were tolerable within a narrow range (C16 to C20). Shortening the acyl tail length to C14 reduced the inhibitory effect, while acyl tails longer than C20 also showed diminished inhibition. All of the polyunsaturated fatty acids studied were less potent than oleamide, with the exception of arachidonamide (C20:4^{8,11,14, 16}) which showed 90-100% inhibition at 20-100 μM⁷⁰.

Some tolerance was observed when the head group of oleamide was altered. The ethyl ester and a sarcosine derivative retained a portion of activity, but the NAG, oleoylglycine (a suspected anabolic precursor to oleamide), did not inhibit gap junction communication. This data supports the hypothesis that amidation of these species confers biological activity. Other derivatives also retained similar inhibitory properties with respect to gap junctions if the structural alterations contained a π -electron system at the $\Delta 9$ position and/or were perturbed such that the molecule adopted a “hairpin” configuration⁷⁰.

Calcium signaling can traffic through gap junctions, therefore calcium wave propagation was investigated in rat glial cells treated with oleamide, a gap junction inhibitor⁶⁷. Oleamide and anandamide were found to have no effect on calcium wave propagation, suggesting that gap junction inhibition is not caused by molecular “blocking” or insertion into the junction. Oleamide was found to block gap junction communication of cells with $\alpha 1$ and $\beta 1$ connexin similarly, while oleic acid and elaidamide (C18:1^{trans}) had no effect. Since $\alpha 1$ connexin may be either non-, mono- or di-phosphorylated, changes in phosphorylation were tested in response to oleamide pretreatment. In cells exposed to oleamide, there was a significant decrease in the di-phosphorylated isoform. After washing the cells to remove oleamide, the di-phosphorylated isoform returned to basal levels. To our knowledge this is the sole report of PFAMs altering protein phosphorylation.

50 μ M oleamide caused an increase in internal calcium of T24 and BFTC bladder cancer cells, human MG63 osteoblast-like cells, canine MDCK renal tubular cells and rat PC12 pheochromocytoma cells⁷¹. T24 cells had the largest oleamide-induced internal calcium increase of these cell lines. The effect was concentration dependent between 10-

100 μM with an EC_{50} of 50 μM . Linoleamide, a congener of oleamide, was found to be more potent, with an EC_{50} of 30 μM . The source of internal calcium increase was found to be mainly from influx, as determined by removing external calcium^{71,72}. However, this concentration increase was found to be partially due to release of endoplasmic reticulum stores, as cell pretreatment with thapsigargin, an endoplasmic reticulum pump inhibitor, blocked the oleamide or linoleamide-elicited effect.

Palmitoylglycine treatment (10 μM) of F-11 cells was found to increase calcium influx ($\text{EC}_{50} = 5.5 \mu\text{M}$) as measured by fluorescence with the calcium fluorophore, Fura-2⁵⁷. Stearoylglycine and stearic acid were found to marginally elevate calcium influx. Other related fatty glycines such as, oleoylglycine, N-arachidonoylglycine, docosahexaenoylglycine, as well as free glycine were unable to affect calcium levels at concentrations up to 50 μM . 10 μM of ruthenium red and 1 mM La^{3+} , abolished calcium response due to palmitoylglycine treatment and pertussis toxin attenuated the effect. 2 μM treatment with ω -conotoxin MVIIC or ω -conotoxin GVIA, voltage-gated calcium blockers, did not affect the influx of calcium.

1.3.6. Transient Receptor Potential Vanilloid Receptors

Transient receptor potential (TRP) cation channels are key receptors in the perception of pain and are activated by noxious stimuli including heat, cold, pH, and lipidergic substances. Here we will discuss briefly their interaction with various N-acyl ethanolamines and N-acyl amino acid derivatives. For a more complete picture of TRP receptors, please see the following reviews⁷³⁻⁷⁶.

Anandamide (C20:4 NAE) was found to induce vasodilation in rat hepatic and small mesenteric arteries and guinea-pig basilar artery, as well as increase calcitonin gene-related peptide (CGRP) and increase tissue content of cAMP in rat hepatic artery⁷⁷. Pretreatment with capsaicin and 8-37 CGRP (vasodilator neuropeptide antagonist) abolished anandamide induced relaxation and capsazepine (vanilloid receptor antagonist), inhibits vasodilation and attenuates release of CGRP. These effects were shown to be TRPV specific, as SR141716A (CB1 receptor antagonist), ω -conotoxin GVIA, MVIIC, nor nimodipine (voltage-gated calcium blockers) did not block anandamide induced relaxation. 2-arachidonylglycerol and palmitylethanolamide were unable to elicit a response. Similar activity with other NAEs on TRPV has been reported. Linolenylethanolamine (C18:3), linoleylethanolamine (C18:2), and oleylethanolamine (C18:1) were found to induce concentration dependent vasodilation in rat mesenteric artery, which was blocked by capsazepine and arteries pretreated with capsaicin⁷⁸. The observed relaxation of arteries treated with oleylethanolamine was nearly absent in TRPV1 knockout mice. Linolenylethanolamine, linoleylethanolamine, oleylethanolamine, anandamide, and N-Docosatetraenylethanolamine (C22:4) dose-dependently increased intracellular calcium. LC-MS/MS experiments revealed that stearylethanolamine (C18:0), oleylethanolamine, and linoleylethanolamine were found in higher levels in mesenteric arteries compared to anandamide (21, 16, and 19 pmol/mg protein respectively), however activity in calcium assays required at least one unsaturation point.

While the above experiments with NAEs required low micromolar quantities, some N-acyl dopamines were found to have a much higher potency. N-arachidonoyl

dopamine was found to increase intracellular calcium in HEK293 cells overexpressing hVR1 ($EC_{50} = 40$ nM) and rVR1 ($EC_{50} = 48$ nM)⁷⁹. This increase was abolished by iodoresiniferatoxin. Intradermal injection of N-arachidonoyl dopamine (1.5 μ g) in the hind paw of Sprague-Dawley rats resulted in thermal hyperalgesia. Analysis via MS showed the highest concentrations of N-arachidonoyl dopamine in the striatum, hippocampus, and cerebellum. Similar experiments were conducted with N-oleoyl dopamine, N-palmitoyl dopamine (C16:0), and N-stearoyl dopamine (C18:0)⁸⁰. In agreement with previous trends, the saturated compounds, N-palmitoyl dopamine and N-stearoyl dopamine, were found to be inactive in calcium mobilization and thermal hyperalgesia assays. N-oleoyl dopamine increased calcium mobilization ($EC_{50} = 36$ nM) and thermal hyperalgesia ($EC_{50} = 0.72$ μ g) with a somewhat greater potency than N-arachidonoyl dopamine.

Recently Bradshaw and colleagues have reported striking similarities between the activity profiles of palmitoylglycine, an NAG, and TRPC5 and this hypothesis is currently under investigation by their group⁷⁴. Though not data currently exists for activation of TRP receptors and NAGs or PFAMs, the striking similarity of these lipid subclasses and the above lipidergic ligands makes it intriguing to speculate that these compounds may, too, be endogenous activators.

1.3.7. Interaction with Orphan G-protein Coupled Receptors

Recently there has been an effort to identify and match orphan receptors to physiologically relevant ligands. GPR92 is an orphan receptor that is part of the rhodopsin-like GPCR family. It has been shown by reversed transcription PCR to have

the highest mRNA levels in dorsal root ganglia in the nervous system, spleen, stomach, intestine, thymus, and kidney^{69,81,82}. As previously mentioned, N-arachidonoylglycine shows similar distribution levels as GPR92³⁴. In studies of CV-1 cells, addition of N-arachidonoylglycine increased levels of inositol phosphate in a concentration dependent manner, with an $EC_{50} > 50 \mu\text{M}$ as measured in radioactivity assays⁸¹. This increased inositol phosphate production was abolished by treatment with a phospholipase C inhibitor, U73122. Additionally, N-arachidonoylglycine caused a dose-dependent increase in intracellular calcium concentration that was not blocked by treatment with pertussis toxin, as measured in DRG neurons. N-arachidonoylglycine was not, however, able to affect levels of cAMP. Molecular modeling and site-directed mutagenesis identified residues Thr97, Gly98, and Phe101 on transmembrane domain 3 of GPR92 as interacting with N-arachidonoylglycine.

N-arachidonoylglycine was also found to interact with GPR18, an orphan receptor expressed in T and B cells^{69,83}. Treatment with $10 \mu\text{M}$ N-arachidonoylglycine increased intracellular calcium release in L929 cells, and this effect was also observed in K562 and CHO cells with a 2 to 3 fold higher response⁸³. Unlike GPR92, treatment of cells expressing GPR18 with 100 nM N-arachidonoylglycine had a 70% inhibition of cAMP production ($IC_{50} = 20 \text{ nM}$). However, other groups using techniques like PathHunter assays and electrophysiology have disputed N-arachidonoylglycine activation of GPR18^{84,85}.

1.4. ANALYSES METHODS

PFAMs and NAGs have shown a wide variety of physiological effects on receptor activity and animal behavior. However, it is often difficult to analyze the content and identity of these bioactive lipids. PFAMs are generally found at nM levels at physiological levels and absorb very weakly in the UV-Visible region making detection and identification using conventional methods challenging. Additionally, NAGs have been reported in ranges of pmol of amide per gram of tissue analyzed. In the following sections we review methods for the isolation, separation, and detection of PFAMs and NAGs from biological samples.

1.4.1. Chromatographic Separation Techniques

Sample preparation, in terms of extraction and/or isolation of PFAMs, is the preceding step in any chromatographic separation technique. This step can be challenging, as many of the fatty acyl subclasses share similar properties with PFAMs. The most common extraction for PFAMs is a Folch-Pi extraction⁸⁶, which isolates the fatty acyls, triacylglycerols (TAGs), diacylglycerols (DAGs), monoacylglycerols (MAGs), N-acyl glycines (NAGs), PFAMs, and N-acylethanolamines (NAEs). A toluene:acetone (4:2) solvent mixture was used to extract erucamide from various organ tissue⁸⁷. Extraction is sometimes accompanied by an isolation step, typically utilizing solid phase extraction (SPE) methods⁸⁸⁻⁹⁰. An SPE method for isolation of only PFAMs from standard lipid mixture and N₁₈TG₂ mouse neuroblastoma cells was detailed by Sultana *et al.*⁸⁹ PFAM recoveries were 70% or greater for 0.2-20 µg of amide loaded onto the SPE columns and fractional lipid content was verified by TLC. This method

could be used for isolation of any of the nine lipid subclasses (fatty acids, PFAMs, NAG, NAE, MAG, DAG, TAG, cholesterol, and cholesterol esters) tested. Likewise, the TLC method outlined could be employed for qualitative composition studies.

Gas chromatography has been used to identify PFAMs isolated from luteal phase plasma², N₁₈TG₂ mouse neuroblastoma cells^{20,89}, oleamide in plasma and cerebral spinal fluid²¹, and erucamide in pig organs and blood⁸⁷. All of the listed analyses employed a 5HP-MS capillary column for separation. The temperature elution profile differed slightly if the sample was trimethylsilyl derivatized or analyzed as the native structure. An alternative column, BPX-70, was able to resolve 6 C18:1 PFAM trimethylsilyl stereoisomers⁸⁹. The *trans* isomers eluted at least a minute prior to their corresponding *cis* isomers. Additionally, the retention time was found to increase as the double bond position was closer to the carbonyl group. The elution trends observed could aid in identification of stereoisomers even if mass spectrometry detection is not available.

Liquid chromatography is a viable alternative to gas chromatography, especially with the recent increases in column technology. Reversed phase C18 stationary phases are the most common choice for separation of PFAMs^{20,25,55}. However, if resolution of short chain amides (C2-C12) are desired a C8 column can be employed²⁵. Separation is typically achieved by gradient elution with acetonitrile/water or methanol/water solvent mixtures. Gradient elution programs vary depending on the resolution of analytes desired, the column properties and experimental details are provided in the cited publications. These methods were used to purify erucamide from biological samples⁸⁷, PFAM content in tallow⁹⁰, and to examine PFAM content and anabolism in N₁₈TG₂ mouse neuroblastoma cells²⁰.

For separation of NAEs and NAGs, Burstein *et al.* employed silica gel TLC of radiolabeled NAE and NAG substrates³⁵. Separation was achieved by a chloroform, methanol, acetic acid mixture and retention visualization was accomplished by scintillation counting. Separation of NAGs from complex mixtures has been accomplished by primarily C18 reversed phase chromatography with water and acetonitrile or methanol gradients^{34,57,91}. Tissue studies were carried out in rat tissue and bovine brain^{34,57}.

1.4.2. Detection Methods

UV-Visible spectroscopy and mass spectroscopy (MS) detection methods were utilized in conjunction with the above separations. Carpenter *et al.* used liquid chromatography with UV detection at 210 nm to assess PAM mediated changes in PFAM levels of mouse neuroblastoma cells²⁵. Because PFAMs do not absorb UV light readily, the limit of detection (100 μ M) for this method was relatively high. At this limit of detection, trace analysis is not possible unless a large amount of sample is processed and concentrated. However, this method is useful, as an LC with a UV-Vis detector is ubiquitous in most institutions. Other analysis systems for PFAM detection typically use a mass spectrometer because it is compatible with gas or liquid chromatography. Additionally, modes such as selected ion monitoring, or multiple reaction monitoring (MRM) in tandem mass spectrometers, can allow for lower detection limits, enabling trace analysis⁹². When using electron ionization, as found in gas chromatography instruments, the fragmentation pattern can be matched to standard databases for component identification. If PFAM fragmentation patterns are not provided in the

database software, reports have been published of electron ionization fragmentation assignment of PFAM-TMS derivatives⁹³ or post-column mass spectra of collision induced dissociation of PFAMs⁹⁴. PFAM content in tallow was investigated by liquid chromatography atmospheric pressure chemical ionization mass spectrometry with a reported limit of detection of 18.5 femtomoles⁹⁰.

Detection methods for NAGs have primarily been published on MS or tandem MS. For quantitation studies of bovine brain and rat tissue LC/MS and calibration curves were used to determine levels of NAGs³⁴. This study ranged from value of approximately 2 to 140 pmol per gram of dry tissue. Rimmerman *et al.* obtained quantitation of palmitoylglycine and N-arachidonoylglycine in Sprague-Dawley rat brain utilizing LC and tandem MS with a triple quadrupole operated in MRM mode⁵⁷. Quantitation levels were between 6 and 895 pmol per gram of tissue. Both reports demonstrate identification of NAGs in mixtures using accurate mass quadrupole time of flight mass spectrometers^{34,57}.

1.5. SUMMARY AND OUTLOOK

The knowledge gained on the metabolism and physiological interaction of PFAMs and biological systems has grown significantly since these molecules were first reported in 1989. The degradation of these lipid messengers by FAAH is well characterized, however there are still ample questions pertaining to their anabolism *in vivo*. The enzymes responsible for conversion of the fatty-CoA to the primary amide are still largely debated. Additionally, there is still not a clear picture of how these molecules are regulated in signaling, whether systemically or locally within specific tissue regions.

Intraperitoneal injection of oleamide in mice causes a sleep-like state characterized by hypomotility, hypothermia, and ptosis that are not blocked by treatment with a CB1 antagonist⁹⁵. Therefore, oleamide seems to exert physiological signaling effects that are independent of anandamide and the cannabinoid system. Exogenous application of oleamide to the serotonin and GABA receptor systems indicated that physiological effects may be modulated by receptor interaction as deletion of the $\beta 3$ subunit of the GABA receptor abolished the hypnotic effects observed with oleamide treatment¹¹. Interestingly, differential phosphorylation was observed in the cellular connexin protein with exogenous application of oleamide in gap junction studies⁶⁷. Therefore, PFAMs may modulate receptor function via downstream signaling or by changing phosphorylation states, although no further studies have been conducted. Nonetheless, PFAMs are an emerging class of bioactive signaling molecules whose wide range of modulatory activities are only recently becoming discovered. It is critical that the anabolic and signaling pathways for these physiologically-important effectors be elucidated. This knowledge may provide invaluable insight to disease states or provide pharmacological strategies and novel therapeutics for a wide-range of symptoms, such as in treatment of pain and inflammation⁴⁴.

There are established isolation procedures and relatively predictive elution profiles of this class of lipids due to their structural similarity with fatty acids. Future analyses of these classes of lipids will benefit from the rise in sophistication of column and mass spectrometry technology. UPLC and nano-HPLC are advantageous as they reduce band broadening and total analysis time, providing analysis that is fast and of increased sensitivity. Chipcube LC systems are available with an option of trapping

columns, thus, having the potential to increase sample load while reducing a portion of the matrix contaminants which can cause ion suppression in MS. Our laboratory, amongst others, is also currently investigating microfluidics and laser induced fluorescence platforms to aid in reducing sample requirements and increasing detection sensitivity. Initial findings indicate detection limits below those achievable by MS (unpublished work). PFAMs and NAGs, unfortunately, are not currently represented in LIPID Metabolites and Pathways Strategy (LIPID MAPS)⁹⁶, and MetLIN databases. However, several select PFAMs and NAGs are available in the Human Metabolome Database (HMDB). Current efforts to determine anabolic pathways, receptor-ligand interaction studies, and new quantitative analysis in biological samples leaves the field poised for advancement in broadening our knowledge of the effects of PFAMs *in vivo*.

Chapter 2

Electrospray Ionization and Collision Induced Dissociation Mass Spectrometry of Primary Fatty Acid Amides and N-acyl Glycines

Adapted from: Divito, E. B., A. P. Davic, et al. (2012). "Electrospray ionization and collision induced dissociation mass spectrometry of primary fatty acid amides." Analytical chemistry 84(5): 2388-2394.

2.1. ABSTRACT

Primary fatty acid amides are a group of bioactive lipids that have been linked with a variety of biological processes such as sleep regulation and modulation of monoaminergic systems. As novel forms of these molecules continue to be discovered, more emphasis will be placed on selective, trace detection. Prior to this report, there was no published experimental determination of collision induced dissociation of PFAMs. A select group of PFAM standards, 12 to 22 length carbon chains, were directly infused into an electrospray ionization source Quadrupole Time of Flight Mass Spectrometer. All standards were monitored in positive mode using the $[M+H]^+$ peak. Mass Hunter Qualitative Analysis software was used to calculate empirical formulas of the product ions. All PFAMs showed losses of 14 m/z indicative of an acyl chain, while the monounsaturated group displayed neutral losses corresponding to H_2O and NH_3 . The resulting spectra were used to propose fragmentation mechanisms. Isotopically labeled PFAMs were used to validate the proposed mechanisms. Patterns of saturated versus unsaturated standards were distinctive, allowing for simple differentiation. This determination will allow for fast, qualitative identification of PFAMs. Additionally, it

will provide a method development tool for selection of unique product ions when analyzed in multiple reaction monitoring mode.

2.2 INTRODUCTION

Primary fatty acid amides (PFAMs) are a subclass of fatty acyls containing a carboxamide head group and an acyl tail of varying carbon length and unsaturation. This group of lipids contains endogenous biomolecules, many of whose exact physiological role has not been identified. Although distinct metabolic pathways have yet to be elucidated for this class of biomolecules, they have been located in several specific tissues and biological fluids since the late 1980s. The first reported discovery of PFAMs was of palmitamide (hexadecanoamide, denoted C16:0), oleamide (C18:1⁹) and linoleamide (C18:2^{9,12}) in luteal phase plasma.² Oleamide and erucamide (C22:1¹³) were subsequently identified in the cerebral spinal fluid of sleep-deprived cats.^{15,16} Exogenous application of oleamide was shown to potentiate serotonin receptor subtypes 1A, 2A, and 2C, as well as to potentiate the class A type of γ -aminobutyric acid receptor, GABA_AR.^{3-6,10} Oleamide has also been found to inhibit gap junction communication when exogenously applied to glial cells.^{67,70} This lipid was reported to induce various physiological properties such as vasorelaxation, increased food uptake, anti-anxiety, and analgesic-like properties.^{9,14,17,18,62} While less well characterized than oleamide, the physiological properties of other PFAMs have been reported. For example, erucamide promotes angiogenesis and regulates water balance^{56,87}, and linoleamide induces sleep and increases cytosolic calcium levels in renal tubular cells.⁷² These effects have been ascribed to the carboxamide head group since the free fatty acid form does not produce,

or greatly reduces, the observed effects. There is also selectivity shown for the double bond position and acyl chain length.

PFAMs exhibit a broad range of physiological effects and, therefore, may be bioindicators for disease states. However this lipid class is typically found at low concentrations. Investigation of the levels of these amides in biological fluids and tissues suggests that physiological concentrations are in the nM range.^{2,16,20,21} This makes separation and detection of physiological levels of PFAMs challenging. Much of the separation and detection work to date has been conducted on the N-acylethanolamine, anandamide, though a few reports exist on other PFAMs. Separation of PFAMs has involved mainly gas chromatography (GC) and high performance liquid chromatography (HPLC) with either the endogenous species or a derivatized form as the analyte. PFAMs were analyzed in plasma², cerebral spinal fluid¹⁵, and mouse neuroblastoma cells^{20,89} by derivatization to trimethylsilylamides, followed by GC separation with mass spectrometry (MS). HPLC is an alternative to GC for separation of PFAMs since it does not require derivatization if a MS detector is used. HPLC-MS has been used to investigate the conversion of N-acylglycines to PFAMs *in vitro*²⁵.

In order to examine the presence and levels of PFAMs in biological samples it is necessary to first extract these lipids from the sample. Folch-Pi or Bligh-Dryer extraction techniques are common; however these methods may co-extract other subclasses of fatty acyls such as fatty acids, N-acylethanolamines, and N-acylglycines.⁸⁹ In addition, many of the fatty acyls are isobaric, further complicating the analyses. This makes front-end separation a necessity as many of the isobars can be resolved solely by chromatography. Additionally, tandem MS is becoming a prevalent tool for selective, sensitive detection of

lipids. The sensitivity has been reported as femtomoles in optimized systems.^{97,98} Additionally, no sample derivatization is needed in an LC-MSMS system, making it attractive for lipid analysis.

Some fatty amide fragmentation mechanisms have been investigated with electron ionization or collision induced dissociation.^{93,99} There are a few reports on endogenous PFAMs where tandem MS was utilized for structural identification.^{15,100,101} In order to enhance the selectivity and sensitivity of tandem MS using multiple reaction monitoring (MRM), knowledge of the fragmentation mechanism must be known. This is especially true when investigating the fatty acyl group as all of the subclasses will contain acyl chain fragments in CID spectra. It is, therefore, important to identify product ions that are unique to the fatty acyl subclass so that the selectivity and sensitivity of MRM can be utilized. In order to provide essential tools to allow for identification of these physiologically relevant class of lipids, we report proposed fragmentation mechanisms of various saturated and mono-unsaturated PFAMs based on the observed product ions obtained with a quadrupole time of flight (QToF) MS.

2.3. MATERIALS AND METHODS

2.3.1 Chemicals:

Methanol optima grade and ammonium hydroxide were purchased from Fisher Scientific (Fair Lawn, NJ, USA). Oxalyl chloride, ¹³C₂-9,10-oleic acid, oleic acid, erucic acid, petroselaidic acid, and anhydrous dichloromethane were from Sigma Aldrich (St Louis, MO, USA). N, N-dimethylformamide, ¹³C-1-hexadecanoic acid, heptadecanoic acid, and eicosanoic acid were purchased from Aldrich Chemical Company (Milwaukee,

WI, USA). Lauric acid, myristic acid, palmitic acid, stearic acid, formic acid, and docosanoic acid were purchased from Acros Organics (New Jersey, USA). Elaidic acid was from MP Biomedical Inc. (Solon, OH, USA) and linoleamide was purchased from Enzo Life Sciences (Ann Arbor, MI, USA). Oleoylglycine was purchased from Cayman Chemicals (Ann Arbor, MI, USA).

2.3.2 PFAM synthesis:

PFAMs were synthesized by a modified procedure described by Philbrook.¹⁰² Fatty acids were dissolved in anhydrous dichloromethane and converted to the acid chloride by reaction with oxalyl chloride under anhydrous argon atmosphere. Dichloromethane solvent was removed by rotary evaporation in vacuo, and the remaining acid chloride was subjected to ammonia gas by insertion of ammonium hydroxide filled syringes. Reactions were complete when the fatty acid chloride oil was completely converted to a white solid fatty acid amide product. Products were purified by liquid phase extraction with chloroform.

Purity of all synthesized amides was verified by GCMS on a Varian CP-3800 GC with Varian Saturn 2000 Ion Trap Mass Spectrometer. Gas chromatography was performed on a Varian Factor Four Capillary Column (VF-5ms, 30 m × 0.25 mm ID) with a flow of 1 mL/min helium carrier gas. Injector temperature was held at 250°C with split injection (ratio 10). Temperature gradient started at 55°C and ramped 40°C/min to 150°C with a hold of 3.62 minutes before ramping 10°C/min to 275°C and holding 6.50 minutes. The total run time was 25 minutes. Eluted fatty amides were ionized by chemical ionization with methanol and analyzed in selected ion mode. The peak area of

fatty acid substrate and PFAM product from GC-MS runs were used to determine purity. All PFAMs were found to be of 98% purity or greater.

2.3.3 Mass spectrometry:

PFAM fragmentation patterns were obtained on an Agilent Technologies 6530 Accurate Mass QToF LCMS with electrospray ionization source. Samples of 10 μ M of amide in 95:5 methanol/water solvent with 0.3% formic acid (v/v) were introduced by direct infusion at 500 μ L/min using a Harvard Apparatus 11 Plus syringe pump. Mass spectral parameters were as follows: gas temperature 300°C, drying gas 8 L, nebulizer pressure 35 psi, sheath gas temperature 350°C, sheath gas flow 11 L, capillary voltage 4000 V, fragmentor voltage 150 V, nitrogen collision gas, and collision energy 20-35 mV depending on sample identity. Each sample was infused and spectra collected for 1 minute, with a final average of 20 scans/spectra. Empirical formulas for product ions were generated using Mass Hunter Workstation Software Qualitative Analysis.

2.4. RESULTS

In order to understand the mechanism of PFAM CID a select group containing lauramide (C12:0), myristamide (C14:0), palmitamide (C16:0), oleamide (C18:1⁹), elaidamide (C18:1^{9t}), petroselaidamide (C18:1^{6t}), stearamide (C18:0), arachidamide (C20:0), erucamide (C22:1¹³), and behenamide (C22:0) were directly infused into an electrospray ionization source coupled to a QToF. N-acyl glycine (NAG) fragmentation patterns were obtained via direct infusion into an electrospray ionization source, operated in negative mode, coupled to a triple quadrupole mass spectrometer. All PFAM parent

ions were observed as the $[M + H]^+$ ion and NAGs as the $[M - H]^-$. Fragmentation patterns for both classes of fatty acyls were obtained at collision energies from 20 -100 V (Figure 2-1). As the collision energy increased the patterns were dominated by the occurrence of smaller product ions. Empirical formula generation suggested that the fragmentation pathways for all saturated PFAMs were similar regardless of the acyl chain length. All MS/MS spectra contained an acyl chain fragment observed at 57 m/z (Figure 2-2). Additionally, several fragment ions were identified by isotope ratio analysis to contain both nitrogen and oxygen. This is observable in both the parent ion mass and isotope distribution. The parent ion mass is an odd number value (if the additional proton charge is removed) which is attributed to the single nitrogen atom present in the structure. The major parent ion peak is comprised of the most stable atomic isotopes. Peaks of greater mass in the ion cluster are compounds containing the lesser abundant isotopes. In these examples a peak at 2 m/z greater than the parent ion is due to the 0.204% probability of the compound containing ^{18}O . In this way isotope ratio analysis was used to determine the empirical formulas for each major product ion. The product ions were interpreted to be fragments which contain the head group carboxamide but differ by the acyl chain fragmentation point. As the acyl tail length was increased, the occurrence of higher mass product ions increased, and differed by 14 m/z. This supported the hypothesis that the acyl chain fragmentation point was variable. An isotopically labeled palmitamide (^{13}C -1-hexadecanoamide) was used to confirm the identity of the proposed head group fragments. In this case the product ions containing the head group carbon would be mass shifted by 1 amu (Figure 2-3A), while the acyl chain fragment at 57 m/z would remain unchanged. These suspected product ion assignments were used to

propose a fragmentation mechanism for the saturated PFAMs. The head group fragments form by β -hydrogen rearrangement causing the product ion to terminate with a methyl, while the remainder of the acyl tail was lost as a neutral fragment (Figure 2-3B). An alternate fragmentation mechanism to that proposed is homolytic cleavage of the carbon-carbon bond with radical hydrogen transfer, as described by Wysocki and Ross.¹⁰³ This type of fragmentation was most common at carbons 3-6 from the carboxamide moiety (for collision energies of 20-35 V), producing the largest observed alkyl loss. The acyl chain fragment was proposed to form through bond rearrangement to produce a singly charged acyl fragment. The secondary product then undergoes a hydrogen rearrangement from the carboxamide ion to the alkene tail resulting in a neutral loss (Figure 2-3C). This was supported by product ion peaks, as no doubly charged head group fragment was observed. An alternative fragmentation mechanism for acyl tail formation could involve β -hydrogen rearrangement within the acyl tail, and a bond rearrangement at a position of 4 or less carbons away. This type of fragmentation would produce a neutral loss of an alkene chain, an acyl chain fragment of 57 m/z or less, and a doubly charged carboxamide fragment that would undergo hydrogen rearrangement previously described, to result in another neutral loss. Both acyl chain fragmentation pathways are probable, as product ions of 43 and 29 m/z can be observed on MS with mass scanning capabilities below 50 m/z (data not shown).

Monounsaturated PFAMs had a distinct fragmentation pattern when compared with saturated PFAMs (Figure 2-4). The major difference was the loss of 17 and 35 m/z indicating the loss ammonia, and both ammonia and water from the carboxamide. These losses were verified by empirical formula analysis, and have been previously reported.¹⁵

The remaining product ions were identified as alkyl chains of varying length, as well as the acyl fragment of 57 m/z that was observed in the saturated PFAM fragmentation patterns. Because all the product ions were identified as alkyl chains, it was postulated that the loss of water and ammonia was a fast process resulting in a positively charged alkyl fragment of m/z 247 (Figure 2-5A). The loss of ammonia and water gave rise to product ions 265 and 247 m/z. These ions have been observed in similar CID experiments conducted on phosphatidylcholines.¹⁰⁴ This 247 m/z alkyl carbocation would then fragment and give rise to the remaining product ions observed. Changing the length of the acyl chain or the position/stereochemistry of the double bond did not alter the observed product ion masses. This could be explained by hydrogen rearrangement causing double bond labiality, as depicted in Figure 4B. The product ions observed at 83 and 69 m/z arise from charge directed fragmentation of the 247 m/z alkyl carbocation, as depicted in Figure 4C. An isotopically labeled oleamide (¹³C₂₋₉, 10-octadecanoamide) fragmentation pattern was examined to determine bond cleavage points (Figure 2-5). 135 m/z product ion was calculated to have an empirical formula of C₁₀H₁₅ and to contain both isotope labels. This suggests that the fragmentation point was just to the left of the double bond position. Likewise, 121 m/z empirical formula was C₉H₁₃ and contained just one ¹³C label, indicating a cleavage at the double bond position. This result confirmed the proposed mechanism shown in Figure 2-4B. The product ions observed at 83 and 69 m/z were not mass shifted due to ¹³C labeling, confirming the proposed charge directed fragmentation mechanism (Figure 2-4C).

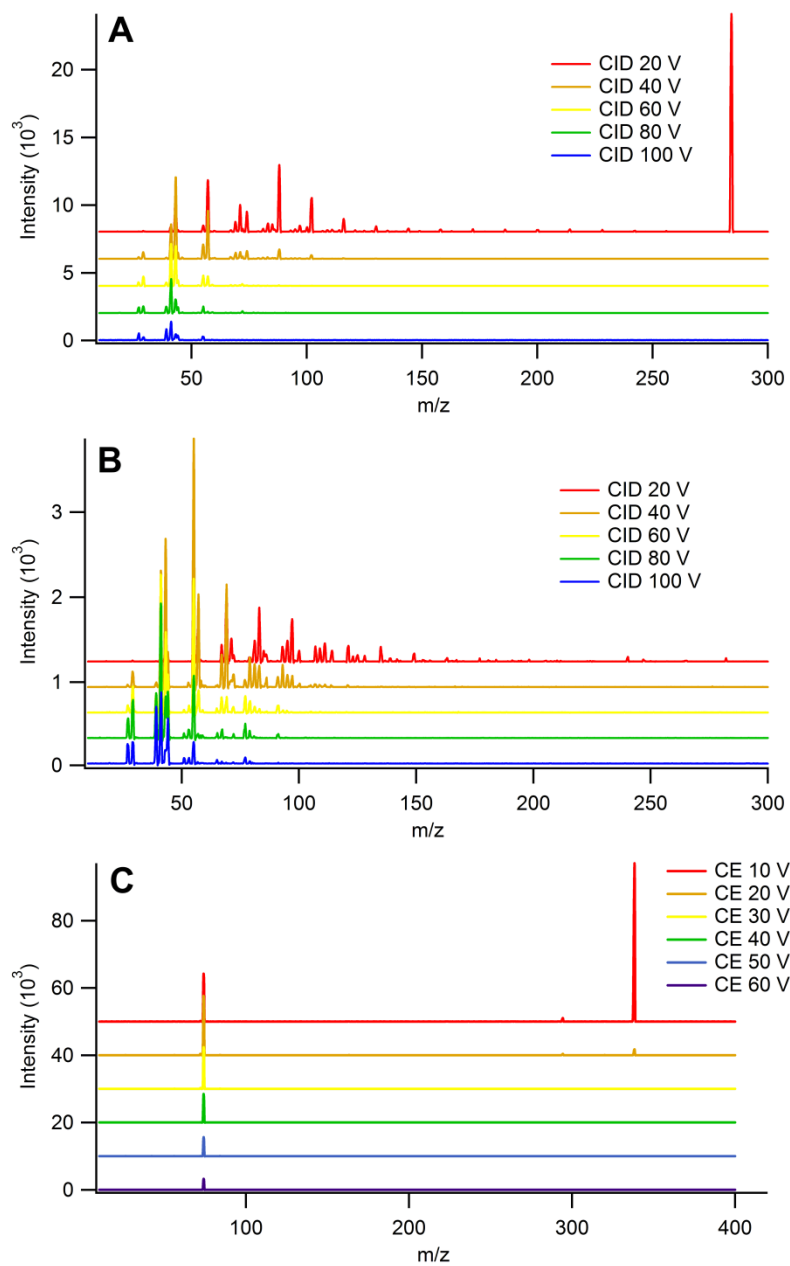


Figure 2-1. CID of 10 μ M standards of A: stearamide, B: oleamide, and C: oleoylglycine directly infused at 0.50 mL/minute using a Harvard A11 syringe pump into a Agilent 6460 triple quadrupole. The collision energy was varied and is depicted in the legend of each figure.

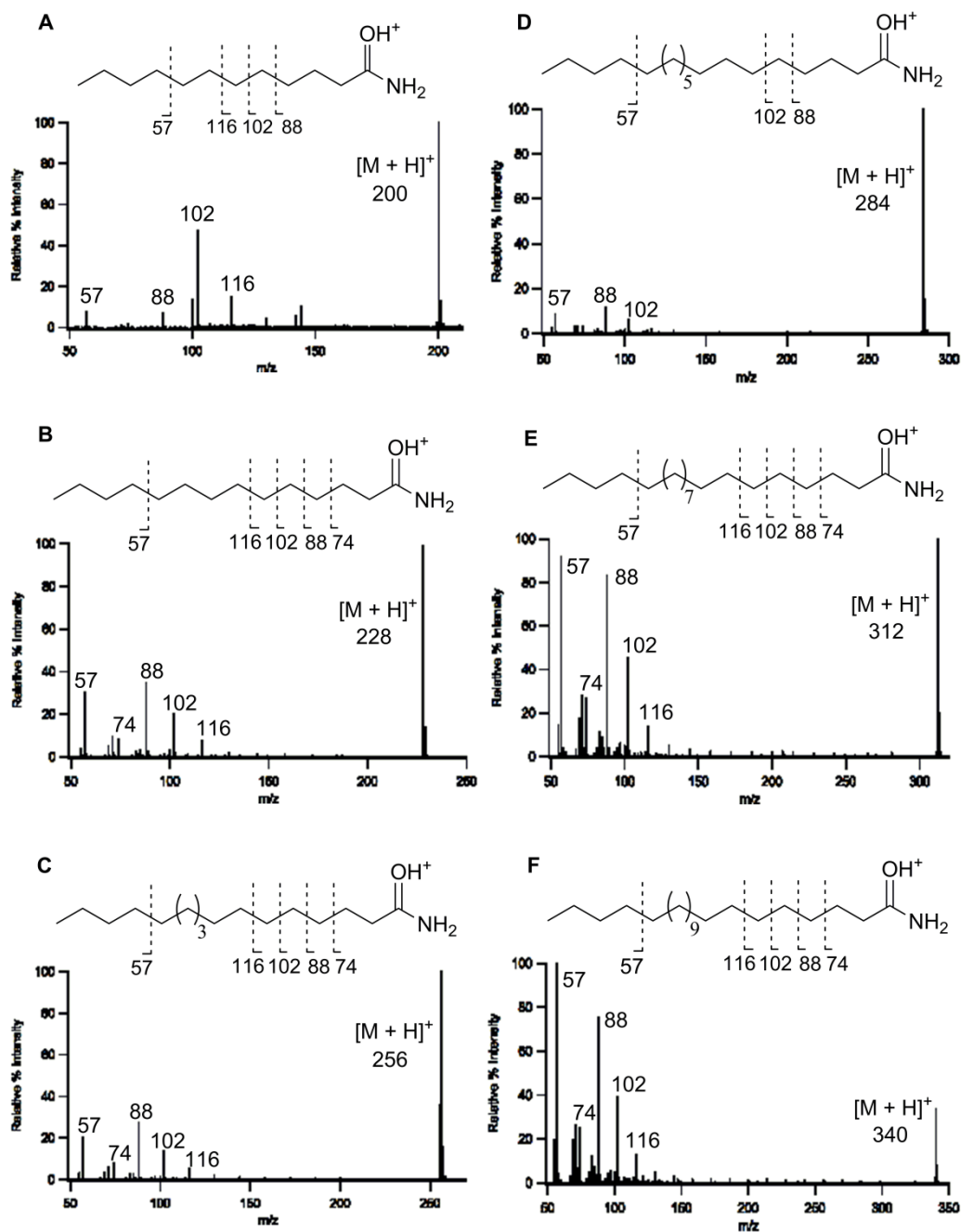


Figure 2-2. Product ion scans of saturated PFAMs from CID-MS. *A*: Lauramide (C12:0), *B*: myristamide (C14:0), *C*: palmitamide (C16:0), *D*: stearamide (C18:0), *E*: arachidamide (C20:0), and *F*: behenamide (C22:0). All samples were approximately 10 μ M and were directly infused into an ESI-QToF at a rate of 500 μ L/min. Collision energy was set to 20 V for each sample except behenamide (C22:0) which was collected at 35 V.

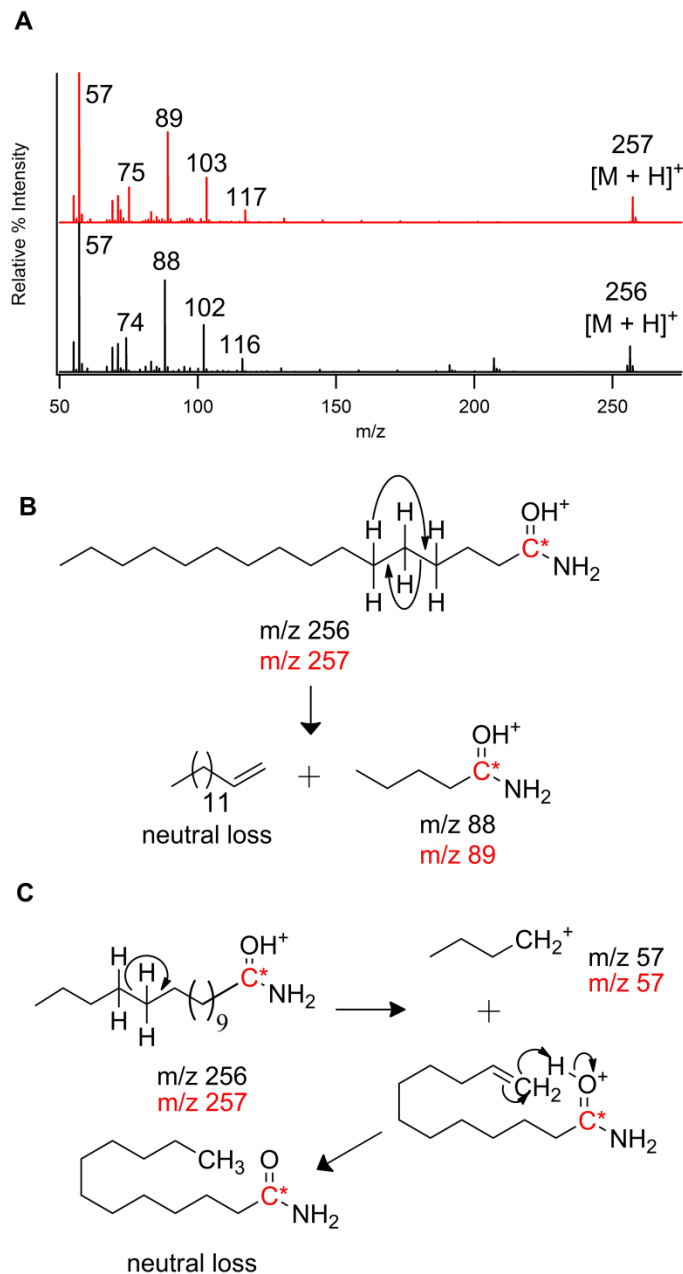


Figure 2-3. A: Product ion scans of palmitamide (black) and ^{13}C -1-palmitamide (red). All samples were approximately $10\ \mu\text{M}$ and were directly infused into an ESI-QToF at a rate of $500\ \mu\text{L}/\text{min}$ with a collision energy of $20\ \text{V}$. The top trace is offset on the y-axis by 100 units. B: Proposed β -hydrogen rearrangement resulting in the head group containing fragments. The * denotes the position of ^{13}C in case of isotopically labeled analyte. C: Proposed bond fragmentation to yield a $57\ \text{m/z}$ product ion.

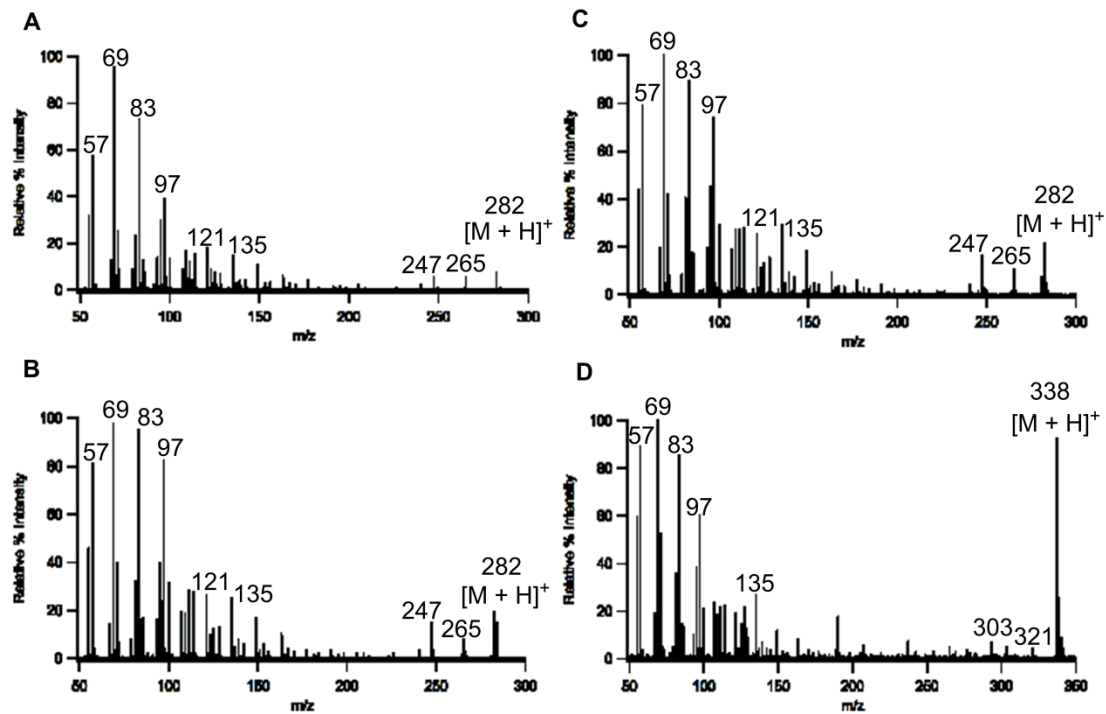


Figure 2-4. Product ion scans of monounsaturated PFAMs from collision induced dissociation MS at a CE of 20 V. *A*: oleamide (C18:1⁹), *B*: elaidamide (C18:1^{9t}), *C*: petroselaidamide (C18:1⁶), and *D*: erucamide (C22:1¹³). All samples were approximately 10 μ M and were directly infused into an ESI-QToF at a rate of 500 μ L/min.

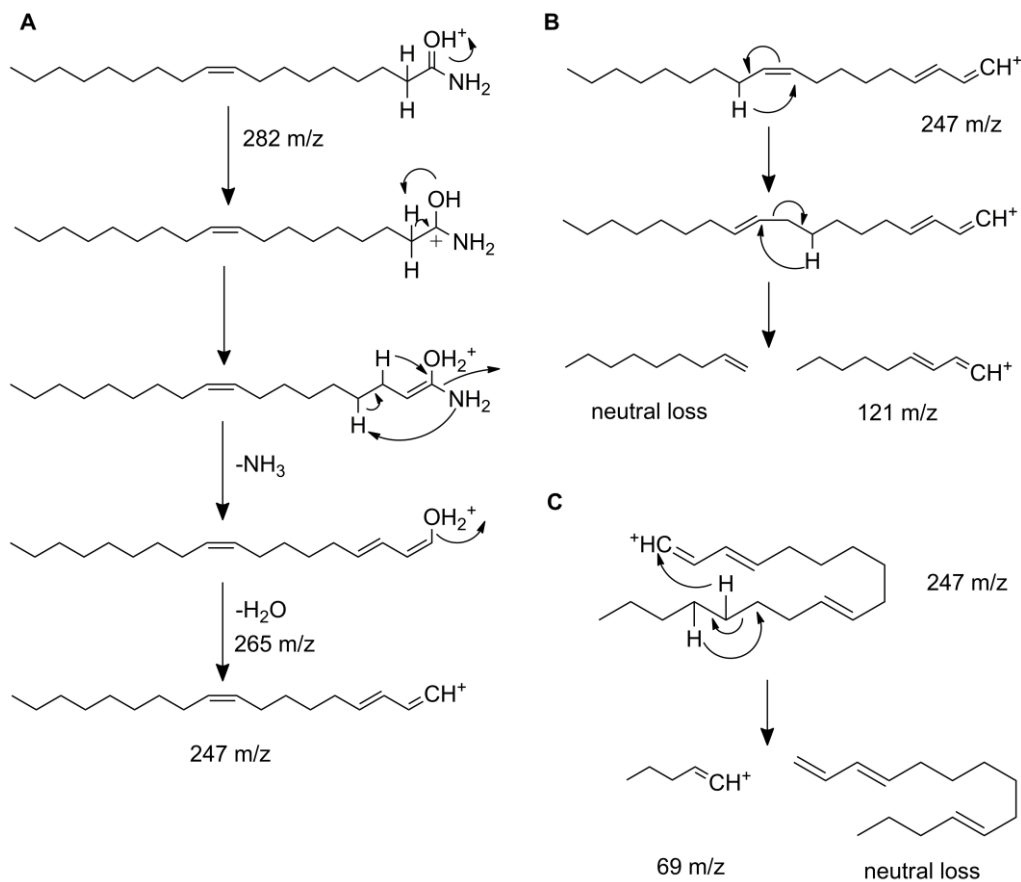


Figure 2-5. A: Proposed mechanism for the loss of ammonia and water from PFAMs. B: Hydrogen rearrangement resulting in double bond movement and fragmentation to yield the observed alkyl product ions. C: Charge directed fragmentation resulting in product ion 69 m/z and a neutral loss.

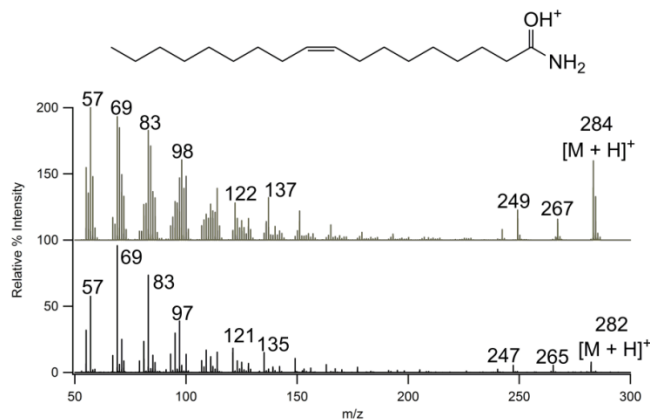


Figure 2-6. Product ion scans of oleamide (bottom trace) and $^{13}\text{C}_2$ -9, 10-oleamide (top trace). All samples were approximately 10 μM and were directly infused into an ESI-QToF at a rate of 500 $\mu\text{L}/\text{min}$. Both spectra were collected at 20 V collision energy. The top trace is offset on the y-axis by 100 units. The most abundant peak in the ion cluster was mass labeled.

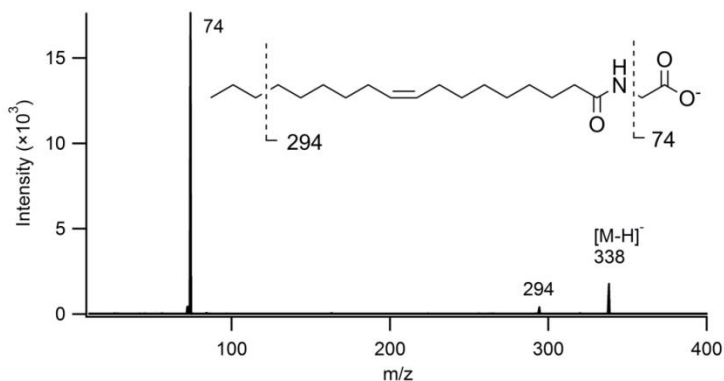


Figure 2-7. CID pattern of 10 μM oleoylglycine standard directly infused at 0.50 mL/minute using a Harvard A11 syringe pump into a Agilent 6460 triple quadrupole equipped with an ESI source operated in negative mode. The parent ion was observed as the $[\text{M} - \text{H}]^-$. The most abundant peak in the ion cluster was mass labeled. The molecular structure shows the proposed bond fragmentation site.

The group of product ions between 105 and 118 m/z was scrutinized because of the differences in relative intensity between isobars. In a double blind test the change in relative intensity between the product ions in the group, though not significant, was enough to obscure accurate identification (data not shown).

Oleoylglycine fragmentation pattern (Figure 2-7) has an $[\text{M} - \text{H}]^-$ parent ion and displayed major product ions of 294 and 74 m/z . Upon inspection of the molecular structure the product ion 74 m/z was proposed as the deprotonated form of the glycine head group. The remaining product ion revealed a similar fragment loss of 57 m/z that was observed in the saturated PFAM CID (Figure 2-2). This ion was not observed in the oleoylglycine spectra as the 57 m/z occurs as the positive ion.

2.5. DISCUSSION AND CONCLUSION

CID patterns of saturated and monounsaturated PFAMs, ranging in acyl chain length from 12 to 22, were collected and analyzed to determine the empirical formulas of the product ions. The saturated PFAMs were found to contain similar product ion peaks

containing carbon, oxygen, hydrogen, and nitrogen except for the product ion 57 m/z, which contain carbon and hydrogen. Product ion peaks containing nitrogen and oxygen were proposed to be fragments including the carboxamide head group and differing in the acyl fragmentation site. The 57 m/z product ion, present in both the saturated and monounsaturated PFAMs, was identified as an acyl chain fragment. The fragmentation patterns observed for saturated PFAMs are similar to patterns observed for fatty acids analyzed in positive mode as lithium adduct ions.^{103,105} Both display product ions separated by 14 m/z units which is characteristic of acyl chain lipids. Additionally, bond fragmentation within the acyl chain occurs by similar charge remote fragmentation mechanisms.^{103,106,107} One distinct difference between fatty acid and PFAM fragmentation is the charged fragment does not terminate in an alkene in the latter case. This change can either occur directly by β -hydrogen rearrangement before alkane bond cleavage or by radical hydrogen attachment after a homolytic bond fragmentation (Figure 2-2B). The product ions observed do not support the typical pericyclic 1,4 hydrogen elimination mechanism reported for fatty acid CID. Additionally, at the collision energy tested, no loss of water or ammonium was observed from the carboxamide of saturated PFAMs, as is sometimes seen in fatty acid or fatty amide CID.^{103,108,109}

The defining characteristic of the monounsaturated PFAM fragmentation patterns was the $[M + H - 17]$ and the $[M + H - 35]$ product ion peaks, indicating the loss of ammonia and water from the carboxamide head group. These two product ion peaks, as well as the acyl tail signature, can be diagnostic of PFAMs when observed in typical biological systems. The remaining fragments were identified as alkyl chain fragments. Increasing chain length increased the appearance of higher mass product ions when

exposed to constant collision energy. The product ions are expected to be terminal alkenes, however observed masses do not support a pericyclic fragmentation mechanism. A change in the position or stereochemistry of the double bond did not change the product ions observed, consistent with previously reports of unsaturated fatty acids.¹¹⁰ For this reason, the identity of isobaric compounds could not be differentiated. Therefore, if isomer identification by MS alone is necessary, the double bond should first be derivatized to prevent labiality¹¹⁰ or a front end LC method capable of separating isobars must be developed.

In contrast to the PFAMs, NAGs occur as $[M - H]^-$ parent ions. The major ions observed in the oleoylglycine fragmentation pattern 294 and 74 m/z . These ions were proposed to be the deprotonated form of glycine at 74 m/z . Product ion 294 m/z exhibited a loss of 57 m/z and was proposed to lose this fragment via hydrogen rearrangement similar to the mechanism proposed for saturated PFAMs. No charge rearrangement occurs in this case and the positive 57 m/z ion is not observed in negative ion mode.

The important role of lipids in biology and health, as well as the emergence of sensitive detection platforms utilizing mass spectrometry, have driven the field of lipidomics (recently reviewed in a special Chemical Review issue on “Lipid Biochemistry, Metabolism, and Signaling”).¹¹¹ Despite the physiological significance of PFAMs²⁻¹⁸ (see **Chapter 1: Metabolism, Physiology, and Analyses of Primary Fatty Acid Amides**), this class of lipids have not been extensively characterized and is not well represented in the LIPID Metabolites and Pathways Strategy (LIPID MAPS) consortium site (www.lipidmap.org).¹¹² In this work we have reported CID patterns for various saturated and monounsaturated PFAMs and successfully employed isotope

labeled compounds to elucidate fragmentation mechanisms, providing essential information necessary for further analytical studies on this class of lipids.

Chapter 3

Chromatographic Separation Methods for Fatty Acyls

3.1. ABSTRACT

The view of lipids in biochemistry is expanding as numerous fatty acyls are discovered to possess signaling properties. These signaling lipids are often found in quantities of pmol/g of tissue and are co-extracted with numerous lipophilic molecules, making their detection and identification challenging. Common analytical means involve chromatographic separation and MS techniques; however, a single step is typically inefficient due to the complexity of the sample. It is, therefore, essential to develop approaches that incorporate multiple dimensions of separation. Described in this chapter are normal phase, reversed phase, and silver ion separation strategies for fatty acyls that included tandem MS as a detection method and additional means of separation and identification. These approaches are intended to be used in concert to accommodate quantitation of highly complex samples.

3.2. INTRODUCTION

Lipids are typically viewed in terms of constituents of cellular membranes and modes of energy storage; however, many lipids exert bioactive properties through cellular signaling means. NAEs have a long history of physiological and G-protein receptor mediated effects that are directly related to, or reminiscent of, cannabinoid activation¹¹³⁻¹¹⁶. PFAMs and NAGs, however, are just beginning to be recognized as bioactive signaling lipids that have demonstrated interactions with serotonin receptors⁴⁻⁷, gap junction proteins and calcium signaling^{57,67,70-72}, and a myriad of physiological

effects^{11,15,17,19,52-54,56,117-119} (see **Chapter 1: Metabolism, Physiology, and Analyses of Primary Fatty Acid Amides**) . Of these documented effects, the most potent bioactive lipids consist of 16-22 chain length acyl tails and can be saturated or unsaturated species. In addition, it is hypothesized that aberrant endogenous levels of these species, either by down-stream modulation or alteration of their metabolic enzymes, could contribute to disease states. This is an intriguing consideration as PFAMs are known to have high affinity for serotonin receptors, though no reports exist for PFAM levels in this disease phenotype. Evidence for up-regulation of NAEs exists in studies of chronic pain¹²⁰, schizophrenia¹²¹, depression and anxiety¹²², yet the physiological relevance of these observations is still unclear. In light of this, it is of substantial importance to develop analysis strategies for bioactive fatty acyls. These methods, in combination with phenotype studies, will aid in the elucidation of the role of signaling lipids and disease states. The generated methodologies may provide additional tools for diagnosis and development of treatment strategies.

Lipid milieus of biological samples are often very complex mixtures. Even the most common lipid extraction methods, such as Folch-Pi⁸⁶, remove a mélange of several different lipid classes. Identification of isomers and isobars by standard separation methods, such as normal phase and reversed phase chromatography, is often insufficient for complete identification of all constituents. Silver ion chromatography has been used extensively for separation of lipid samples with a high variation of unsaturation numbers of geometrical configuration¹²³⁻¹³⁴. However, silver ion separations cannot differentiate between trans-unsaturated and saturated analytes.

Multidimensional liquid chromatography (MDLC) analysis is the process of injecting samples onto a liquid chromatography system where two different separation schemes (columns or dimensions) are used¹³⁵⁻¹³⁹. The main advantage of MDLC is the dramatic increase in peak capacity known as the “product rule”; where the maximum peak capacity becomes the product of the two individual chromatographic peak capacities. These different separation schemes must be orthogonal, or operate by different separation mechanisms, in order to achieve maximum capacity. Analysis by two different chromatographic dimensions allows for the separation of difficult to resolve components or samples with a high number of constituents.

There are several terms for describing multidimensional systems. The first is a distinction between online and off-line systems. An on-line system uses a switching valve to divert fractions of the 1st dimension flow directly to the 2nd dimension. Off-line systems use two different chromatography steps where the sample is collected from the first dimension, dried down and reconstituted for injection into a second system.

For online MDLC the 2nd dimension separation must be very fast so that extreme band broadening due to longitudinal diffusion is minimal in the 1st dimension. One option for shorter analysis times is the use of columns with particle sizes smaller than 3 μm . The reduction in particle sizes results in a decrease in the resistance to mass transfer between the two phases. This allows the analysis to be run at an increased linear velocity, thereby, reducing the analysis time. Additionally, the plate height is decreased as the square of the particle size according to the van Deemter relationship¹⁴⁰⁻¹⁴². Since plate height is inversely related to peak resolution, this produces a more efficient separation between analytes.

Additionally, the switching valve timing, the amount of time between loop switching (process that diverts small eluent fractions from the 1st dimension to the 2nd dimension for analysis), and loop size must be determined after successful method development of both dimensions. Both methods have the advantage that if separation mechanisms between dimensions are orthogonal then maximum peak capacity is achieved. Off-line systems are advantageous because there is no concern of sample solvent miscibility between separation dimensions. However, the analysis time is generally longer because samples have to be processed between separations.

Silver ion chromatography is a method for separating molecules with different degrees of unsaturation. The general mechanism of action in this separation scheme is unclear, though, Christie and co-workers propose a theory of silver ions forming weak, reversible charge transfer complexes with the analytes^{128,143-145}. Another possibility is an intermolecular ion-dipole interaction between the loaded silver ions on the chromatographic bed and the π bonds of the analyte. In general, elution order of analytes by this technique is saturated, trans-unsaturated, mono-unsaturated, and so on. A number of experimental parameters and analyte variables have been explored in relation to retention factor allowing implementation of this methodology in a predictable manner^{127,146,147}. One exception to typical chromatographic separations is that retention of analytes in silver ion chromatography is reduced at lower temperature¹⁴⁸.

Both online and offline MDLC separations have been demonstrated for TAGs in plant and animal samples¹³¹⁻¹³⁴. Each approach utilized a reversed phase separation with an isopropanol/acetonitrile gradient and an isocratic silver ion separation with 0.5-0.7% acetonitrile in hexane. Samples that were separated with an online MDLC approach

always had a reversed phase 2nd dimension separation with a total analysis time of less than 2 minutes^{131,133}. MDLC has not yet been demonstrated with PFAMs and NAGs, although our laboratory has utilized an SPE method prior to GC-MS analysis¹⁴⁹. The following sections demonstrate various separation methods for PFAMs, NAGs, and fatty acid phenacyl esters. We additionally propose an offline separation method for future utilization.

3.3. MATERIALS AND METHODS

3.3.1 Chemicals

Methanol optima grade, formic acid optima grade, ammonium acetate, silver nitrate, hexane, dichloromethane, acetonitrile, and ammonium hydroxide were purchased from Fisher Scientific (Fair Lawn, NJ, USA). Oxalyl chloride, oleic acid, erucic acid, petroselinic acid, heptane HPLC grade, methyl-tert-butyl-ether HPLC grade, isopropanol HPLC grade, acetic acid, and anhydrous dichloromethane were from Sigma Aldrich (St Louis, MO, USA). N, N-dimethylformamide, heptadecanoic acid, and eicosanoic acid were purchased from Aldrich Chemical Company (Milwaukee, WI, USA). Lauric acid, myristic acid, palmitic acid, stearic acid, and docosanoic acid were purchased from Acros Organics (New Jersey, USA). Elaidic acid was from MP Biomedical Inc. (Solon, OH, USA) and linoleamide was purchased from Enzo Life Sciences (Ann Arbor, MI, USA). Oleoylglycine, Linoleoylglycine, palmitoylglycine, arachidonoylglycine, and arachidoylglycine were purchased from Cayman Chemicals (Ann Arbor, MI, USA).

3.3.2 Normal Phase Separation

PFAM and NAG standards were prepared in a mixture at 1 mM concentration of each standard. The mixture was separated via normal phase chromatography utilizing a YMC PVA-Sil column (4.6 × 250 mm, 5 μm particle size). Gradient elution is carried out starting at 95 % mobile phase A (heptane with 0.5% v/v methyl-tert-butyl-ether) and increasing linearly to 50% mobile phase B (methyl-tert-butyl-ether with 10% v/v 2-propanol and 0.2% v/v acetic acid) over 40 minutes with a flow rate of 1 mL/minute (gradient developed by Kroniser and Johnson, unpublished). Fractions were collected at one minute intervals and the times corresponding to NAG and PFAM elution are determined by reversed phase chromatography and MS/MS detection.

3.3.3 Silver Ion Chromatography

Select saturated, monounsaturated, and di-unsaturated fatty acids were derivatized to fatty acid phenacyl esters (FAPEs) by reaction of excess 2-bromoacetophenone and a triethylamine catalyst in an acetone solvent carried out in sealed culture tubes that were placed in a boiling water bath for approximately 45 minutes¹⁵⁰. After 45 minutes the reaction was cooled to room temperature and then an acetic acid solution was used to convert any unused 2-bromoacetophenone reagent to phenacyl acetate. Prior to separation the reaction solution was dried under nitrogen and reconstituted in hexane.

The silver ion column was prepared from a Waters Spherisorb SCX column (4.6 × 150 mm, 5 μm particle size) by injection of 20 μL aliquots of 10% aqueous silver nitrate solution to a total volume of 1 mL. After the silver ions were loaded onto the

cation exchange column, the system was flushed for one hour, and then stored in a hexane solvent.

10 μ M FAPE samples were analyzed on the prepared silver-ion column connected to a Waters 600 HPLC system equipped with a Waters 2487 Dual λ Absorbance Detector operated at a wavelength of 250 nm. A 20 μ L loop was used for sample loading and elution was achieved using a solution of 59.7/39.8/0.5 hexane/dichloromethane/acetonitrile in isocratic mode with a flow rate of 1 mL/minute.

3.3.4 Reversed Phase Separation of N-acyl Glycines

Palmitoylglycine, linoleoylglycine, oleoylglycine, stearidonoylglycine, arachidonoylglycine, and arachidoylglycine were analyzed on an Agilent Technologies 1200 Liquid Chromatography system with a 6460 Triple Quadrupole Mass Spectrometry Detector. Mobile phase A was methanol and mobile phase B water both contained 10 mM ammonium acetate. Separations were carried out on a YMC Cartenoid column (4.6 \times 150 mm, 5 μ m particle size) with a linear gradient of 90% to 100% mobile phase A over 15 minutes with a 15 minute hold time. An additional separation method was developed on a Phenomenex C18 column (4.6 \times 100 mm, 2.6 μ m particle size) with a linear gradient of 80% to 100% mobile phase A over 5 minutes and a 2 minute hold time. A second gradient method was used and consisted of 70% mobile phase A hold for 7 minutes, a linear gradient increase to 80% for 7 minutes, a 1 minute hold at 80% before increasing to 100% mobile phase A over 5 minutes, and a final 5 minute hold for a total analysis time of 25 minutes.

Ionization was achieved with an ESI source operated in negative mode with optimized parameters: fragmentor voltage 135 V, sheath gas flow 11 L/minute, nebulizer pressure 55 psi, nozzle voltage 500 V, capillary voltage 3500 V, drying gas flow 9 L/minute, drying gas temperature 275°C, and dwell time of 500 ms. Multiple reaction monitoring parameters were set-up to analyze the $[M - H]^-$ parent ions and 74 m/z product ion.

3.3.5 Reversed Phase Separation of Primary Fatty Acid Amides

All primary fatty acid amide standards were synthesized in house at greater than 98% purity (**Chapter 2 Section 3.2 PFAM synthesis**). Lauramide (C12:0), myristamide (C14:0), linoleamide (C18:2^{9, 12}), palmitamide (C16:0), oleamide (C18:1⁹), elaidamide (C18:1^{9trans}), petroselaidamide (C18:1^{6trans}), heptadecanoamide (C17:0), stearamide (C18:0), arachidamide (C20:0), erucamide (C22:1¹³), and behenamide (C22:0) were separated on a Agilent RP C18 column (2.0 × 50 mm, 1.8 μm particle size) with a gradient elution of methanol, optima grade and water both containing 0.3% formic acid.

PFAMs were detected using an Agilent 6460 Triple Quadrupole Mass Spectrometer equipped with an atmospheric pressure chemical ionization (APCI) source. Optimized detection parameters are as follows: gas temperature 325°C, vaporization temperature 325°C, gas flow 4 L/minute, nebulizer pressure 22 psi, capillary voltage 3500 V, corona 4 μA, and fragmentor 125 V. Multiple reaction monitoring was used to detect the $[M + H]^+$ parent ions and product ions of 55 and 43 m/z for the monounsaturated and saturated compounds respectively.

3.4. RESULTS

3.4.1 Normal Phase Separation

A 975 nmol lipid mixture of fatty acids (FA), triacylglycerols (TAG), diacylglycerols (DAG), monoacylglycerols (MAG), NAGs, PFAMs, and NAEs standards were separated by normal phase chromatography (Figure 3-1. Kroniser and Johnson, unpublished).

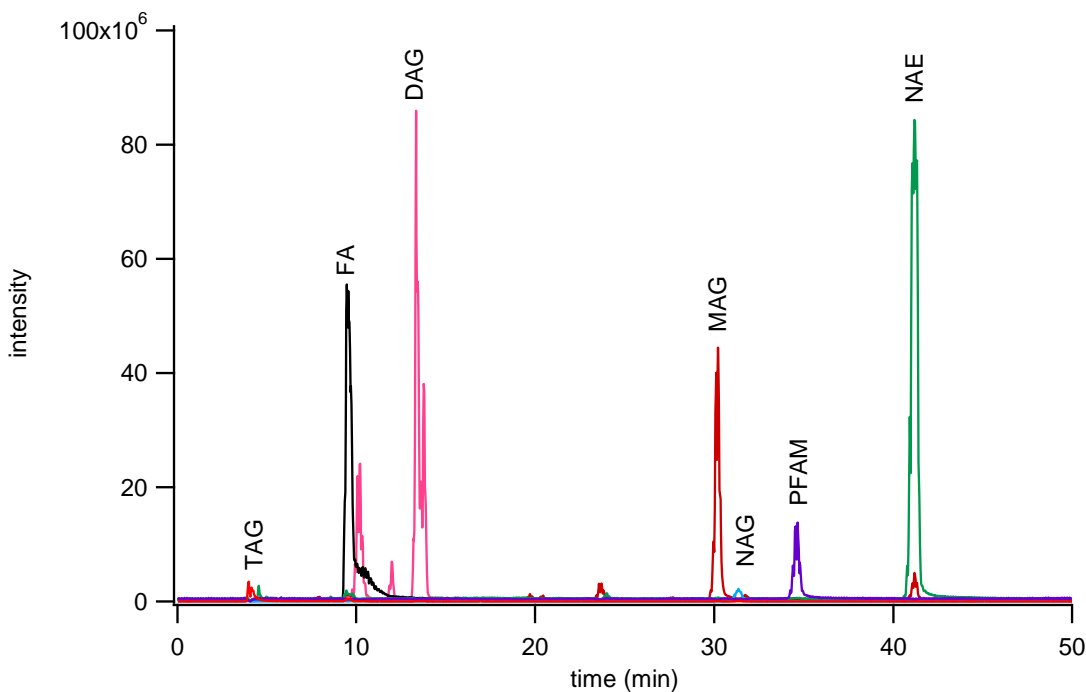


Figure 3-1. Chromatogram of seven fatty acyl subclasses separated by normal phase chromatography using a YMC PVA-Sil (4.6×250 mm, $5 \mu\text{m}$ particle size) on a Waters ZMD MS with an ESI probe with polarity switching. Separation was achieved with mobile phase A (heptane with 0.5 % methyl-tert-butyl ether) and mobile phase B (10% 2-propanol, 0.2% acetic acid in methyl-tert-butyl ether) run in gradient mode from 95% to 50% A over 40 minutes. The monoacylglycerol (MAG) were monitored as the $[\text{M}+\text{Na}]^+$ peak, PFAM as the $[\text{M}+\text{H}]^+$ peak, DAG as $[\text{M}+\text{Na}]^+$ peak, NAE as $[\text{M}+\text{Na}]^+$ peak, FA as $[\text{M}-\text{H}]^-$ peak, NAG as $[\text{M}-\text{H}]^-$ peak, and TAG $[\text{M}+\text{Na}]^+$ peak. Each class was monitored on a different channel on the MS.

Sample injection volume was increased from $20 \mu\text{L}$ to $200 \mu\text{L}$ to accommodate larger scale sample purification needs. The effect of the increased injection volume on elution was tested by collecting one fraction per minute over the total analysis time. These

fractions were dried down, reconstituted in methanol, and analyzed by reversed phase methods (Figure 3-2). The NAGs and PFAMs were found to co-elute from 31 to 38 minutes (Figure 3-2B, C). Co-elution was determined not to be problematic because these species ionize in different modes for reversed phase MRM analysis (see **3.4 Reversed Phase Separation of N-acyl Glycines** and **3.5 Reversed Phase Separation of Primary Fatty Acid Amides**).

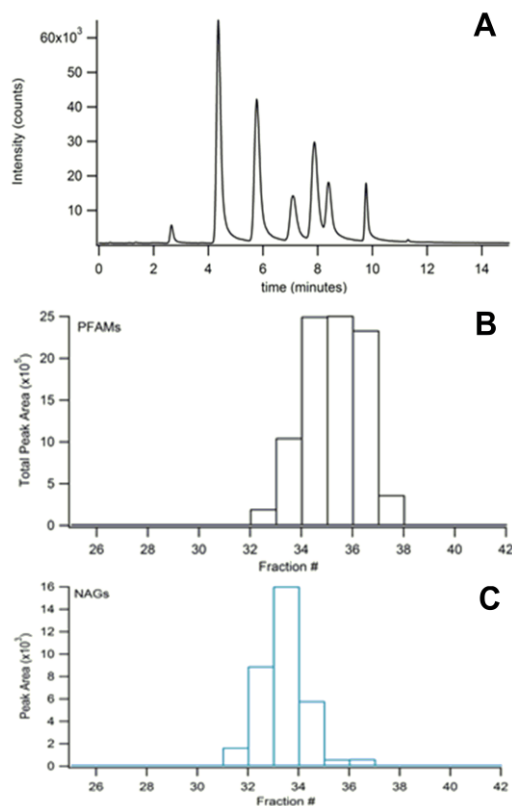


Figure 3-2. (A) Representative chromatogram of fractional PFAM elution from normal phase chromatography collected from 34-35 minutes. Fraction was dried down, reconstituted in methanol and analyzed on an Agilent RP C18 (2.0 × 50 mm, 1.8 μm particle size) with methanol/water gradient elution. 0.3% formic acid was added as an ionization aid and multiple reaction monitoring was used. (B) PFAM and (C) NAG standards eluted from the normal phase chromatography separation on a YMC PVA-Sil column (4.6 × 250 mm, 5 μm particle size) with gradient elution (see **3.2 Normal Phase Separation** for gradient information). Fractions were collected each minute, dried and reconstituted in methanol. Fractions were analyzed by reversed phase chromatography. All peaks observed in each fraction were summated and represented as the peak area per fraction.

3.4.2 Silver Ion Chromatography

FAPes were prepared from select fatty acids ranging in carbon chain length from 12 to 22 and 0 to 2 degrees of unsaturation. Successful derivatization was confirmed by UV-visible and FT-IR spectroscopy (data not shown). Thin layer chromatography also confirmed synthesis of the FAPE from oleic acid by an R_f value of 0.406 which was in good agreement with literature reports¹²⁹. Addition of acetic acid to the FAPE reaction mixture after heating was necessary to prevent excess 2-bromoacetophenone from degrading the FAPE products. A mixture of stearic, oleic, and linoleic acid phenacyl esters were prepared and separated on a strong cation exchange column loaded with silver ions (Figure 3-3A). Elution order was determined by individual injection of each of the FAPes. An additional peak was present in each of the chromatograms that was due to excess phenacyl bromide reagent, therefore, the individual products and mixture was spiked with phenacyl bromide to confirm elution time. Stearic acid phenacyl ester was found to elute first followed by excess phenacyl bromide, oleic acid phenacyl ester, and linoleic phenacyl ester.

The effect of chain length on separation was determined by injection of saturated FAPes from 14 to 20 carbons as both individual FAPes and as a mixture (Figure 3-3B). It was found that the saturated FAPes co-eluted as one peak with the longer chain FAPes eluting near the beginning of the mixture. This co-elution trend did not continue with increasing degrees of unsaturation as distinct peaks were observed for oleic acid phenacyl ester and erucic acid phenacyl ester (Figure 3-4).

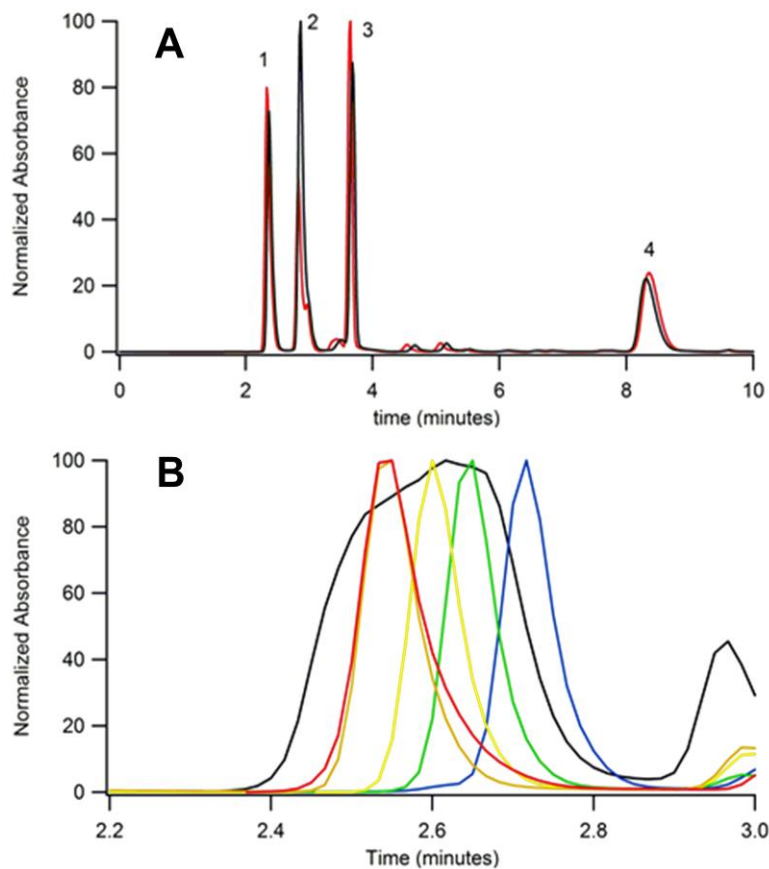


Figure 3-3. (A) FAPE elution by silver ion chromatography with an isocratic mobile phase of 59.7/39.8/0.5 hexane/dichloromethane/acetonitrile at a flow rate of 1 mL/minute and UV monitoring at 250 nm. (1) Stearic acid phenacyl ester, (2) phenacyl bromide, (3) oleic acid phenacyl ester, (4) linoleic acid phenacyl ester. The red trace is elution of the mixture of FAPes and the black trace shows the mixture that was spiked with phenacyl bromide reagent. Both traces were normalized to the intensity of (4) to account for absorption variability between runs. (B) Saturated FAPes elution by silver ion chromatography with an isocratic mobile phase of 59.7/39.8/0.5 hexane/dichloromethane/acetonitrile at a flow rate of 1 mL/minute and UV monitoring at 250 nm. Elution order is as follows: behenic acid phenacyl ester (C22:0, red), arachidic acid phenacyl ester (C20:0, orange), stearic acid phenacyl ester (C18:0, yellow), palmitic acid phenacyl ester (C16:0, green), myristic acid phenacyl ester (C14:0, blue). The mixture of C14:0 to C22:0 is shown in black.

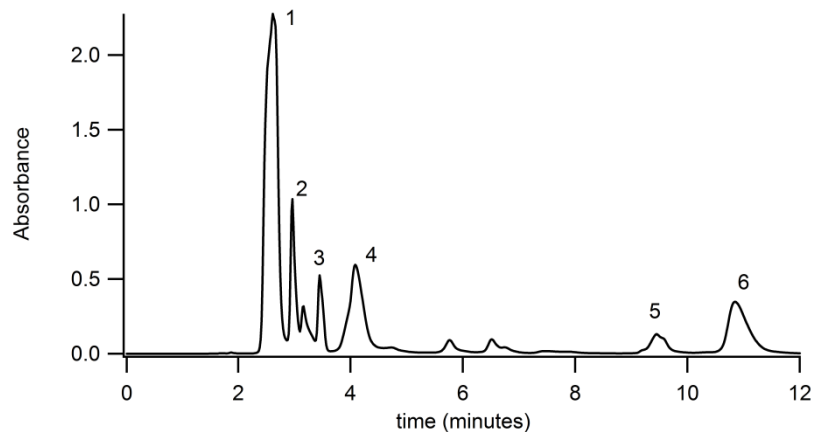


Figure 3-4. Elution of FAPEs by silver ion chromatography with an isocratic mobile phase of 59.7/39.8/0.5 hexane/dichloromethane/acetonitrile at a flow rate of 1 mL/minute and UV monitoring at 250 nm. (1) saturated FAPEs C14:0 to C22:0, (2) excess phenacyl bromide, (3) erucic acid phenacyl ester, (4) oleic acid phenacyl ester, (5) eicosadienoic acid phenacyl ester, (6) linoleic acid phenacyl ester.

3.4.3 Reversed Phase Separation of N-acyl Glycines

Palmitoylglycine (C16:0), oleoylglycine (C18:1⁹), linoleoylglycine (C18:2^{9,12}), stearidonoylglycine (C18:4^{6,9,12,15}), arachidonoylglycine (C20:4^{5,8,11,14}), and arachidoylglycine (C20:0) were separated utilizing a C30 YMC carotenoid column and a fused-core Phenomenex C18 column.

Separation of palmitoylglycine (C16:0), oleoylglycine (C18:1⁹), linoleoylglycine (C18:2^{9,12}), and arachidoylglycine (C20:0) was achieved on a C30 YMC carotenoid column (4.6 × 150 mm, 5 μm particles size) with gradient elution of methanol and water. Both mobile phases were modified with 10 mM ammonium acetate to aid in ionization. Elution was achieved by linear increase in methanol from 90-100% over 15 minutes, followed by a 15 minute hold. Elution of each component was determined by the parent mass (Figure 3-5A).

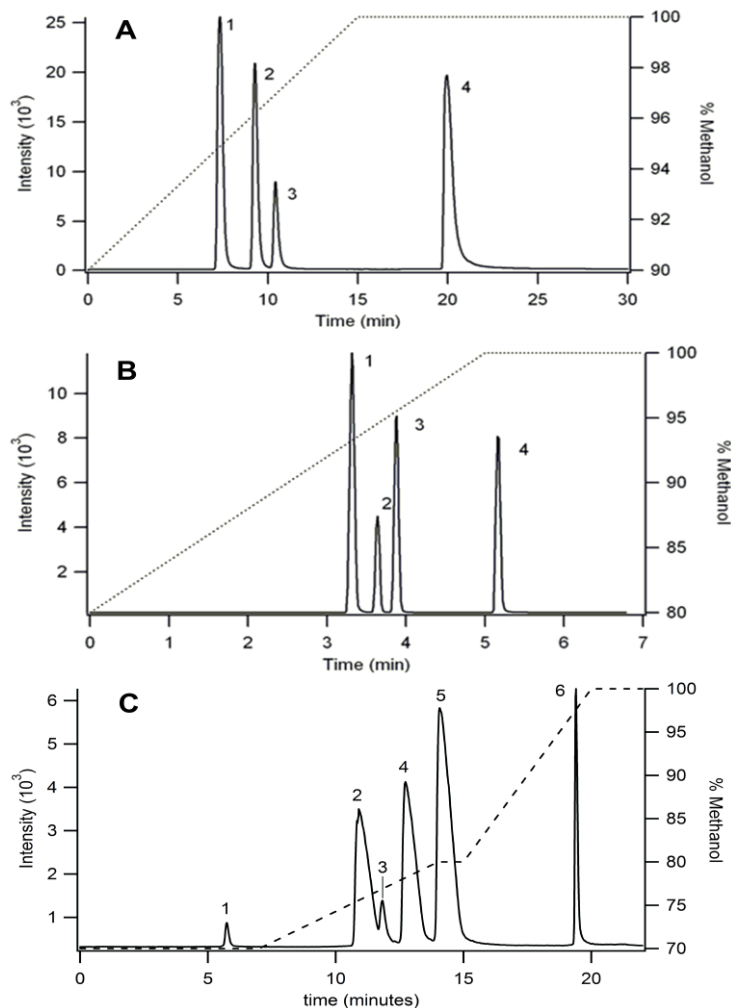


Figure 3-5. Separation of NAGs on (A) a C30 YMC carotenoid column (4.6×150 mm, 5 μ m particles size) and (B, C) Phenomenex C18 column (4.6×100 mm, 2.6 μ m particles size) using two different gradient separations. Ionized by ESI and detected in MRM mode as the $[M-H]^-$ parent and 74 m/z product at collision energy of 20 V. Flow rate was 1 mL/min. The right axis shows the gradient elution profile for % methanol. Peak identities in (A, B) are (1) linoleoylglycine C18:2, (2) palmitoylglycine C16:0, (3) oleoylglycine C18:1, (4) arichidoylglycine C20:0 and (C) are (1) stearidonoylglycine C18:4, (2) linoleoylglycine C18:2, (3) arachidonoylglycine C20:4, (4) palmitoylglycine C16:0, (5) oleoylglycine C18:1, (6) arachidoylglycine C20:0.

In an effort to reduce the analysis time, a fused-core Phenomenex C18 column (4.6×100 mm, 2.6 μ m particles size) was employed using methanol/water gradient elution (Figure 3-5B). The use of a fused-core particle C18 column reduced the experimental time by 6 fold compared to the C30 column separation while simultaneously increasing resolution.

A second elution method was developed (Figure 3-5C) using the fused-core C18 column to determine elution of two additional analytes, arachidonoylglycine (C20:4^{5,8,11,14}) and stearidonoylglycine (C18: 4^{6,9,12,15}). Although the total analysis time was increased 4 fold compared with the previous gradient method (Figure 3-5B); co-elution between linoleoylglycine (C18:2) and arachidonoylglycine (C20:4) was avoided.

Utilizing the method developed in Figure 3-5 the ionization parameters were optimized to yield the lowest detection limit possible (see **3.4 Reversed Phase Separation of N-acyl Glycines** for final parameters). The limit of detection for each analyte was determined by 5 μ L injection of standards between 100 nM and 10 μ M. The results for limit of detection (LOD = signal to noise ratio, S/N, 3) and limit of quantitation (LOQ = S/N 5) are shown in Table 3-1. The calibration curves were linear (see Table 3-1 R² value) between 1 – 10 μ M.

N-acyl glycine	Abbreviation	LOD (μM)	LOQ (μM)	R²
Stearidonoylglycine	C18:4 ^{6, 9, 12, 15}	0.475	1.00	0.999
Linoleoylglycine	C18:2 ^{9, 12}	0.499	1.00	0.999
Arachidonoylglycine	C20:4 ^{5, 8, 11, 14}	0.484	1.00	0.999
Palmitoylglycine	C16:0	1.00	1.00	0.994
Oleoylglycine	C18:2 ⁹	1.00	1.00	0.999
arachidoylglycine	C20:0	1.00	1.00	0.999

Table 3-1. LOD and LOQ for several commercially available NAGs determined by injection of 5 μ L standard solutions from 100 nM to 10 μ M. Calibration curves were linear between 1 - 10 μ M. The LOD and LOQ were determined by a S/N of 5 and 10, respectively.

3.4.4 Reversed Phase Separation of Primary Fatty Acid Amides

Very long chain PFAMs (C12 to C22) were separated via reversed phase chromatography employing a sub 2 μm particle size column (Agilent RP C18 2.1 \times 50 mm, 1.8 μm particle size). The shortest separation achieved was a 4 minute total analysis time (Figure 3-6).

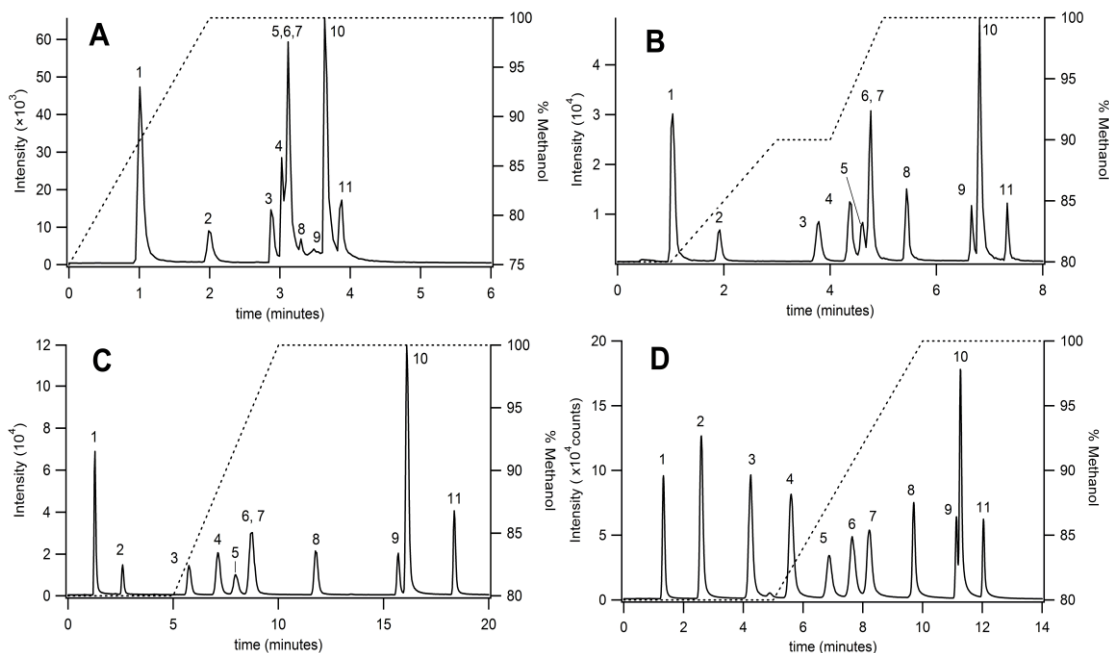


Figure 3-6. Separation of very long chain PFAMs with Agilent RP C18 column (2.1 \times 50 mm, 1.8 μm particle size) using 4 different gradient separations. Peak identities for (A-C) are (1) lauramide, (2) myristamide, (3) palmitamide, (4) oleamide, (5) elaidamide, (6) petroselaidamide, (7) heptadecanoamide, (8) stearamide, (9) erucamide, (10) arachidamide, (11) behenamide. Peak identities for (D) are (1) lauramide, (2) myristamide, (3) linoleamide, (4) palmitamide, (5) oleamide, (6) elaidamide, (7) petroselaidamide, (8) stearamide, (9) erucamide, (10) arachidamide, (11) behenamide. The right axis depicts the gradient elution in % methanol.

Due to the co-elution of oleamide, elaidamide, petroselaidamide, and heptadecanoamide additional gradients were developed (Figure 3-6A-D) in an effort to eliminate co-elution while maintaining the shortest analysis time possible.

A longer gradient elution was established (Figure 3-6C), with a longer initial hold and slower ramp in percent methanol, to determine if petroselaidamide and heptadecanoamide could be resolved. The 20 minute gradient was insufficient to separate the two components; additionally, further increasing the hold, ramp time, or temperature simply increased peak broadening with no increase in resolution (data not shown). Heptadecanoamide was monitored with a separate method in future experiments due to the co-elution with petroselaidamide. A final gradient (Figure 3-6D) was constructed in an effort to maintain the resolution of oleamide, elaidamide, and petroselaidamide as well as reduce the analysis time. The final analysis time was reduced by approximately 2 fold and this gradient method was used in all future experiments for detecting PFAMs.

Utilizing the separation method developed in Figure 3-6D the optimized ionization parameters for greatest detection sensitivity were determined (see **3.5 Reversed Phase Separation of Primary Fatty Acid Amides** for final parameters). The limit of detection for each analyte was determined by 2 μL injection of standards between 500 pM and 10 μM . The results for limit of detection (LOD = signal to noise ratio, S/N, 3) and limit of quantitation (LOQ = S/N 5) are shown in Table 3-2. The calibration curves were linear (see Table 3-2 R^2 value) between 0.500 – 10 μM on average. In cases where the LOD and LOQ were equal the signal was lost below the LOD, however, at this concentration the S/N was above 5.

PFAM	Abbreviation	LOD (nM)	LOQ (nM)	R ²
Lauramide	C12:0	50	100	0.999
Myristamide	C14:0	50	50	0.999
Linoleamide	C18:2 ^{9, 12}	10	50	0.999
Palmitamide	C16:0	20	50	0.999
Oleamide	C18:1 ⁹	400	400	0.999
Elaidamide	C18:1 ^{9trans}	40	400	0.998
Petroselaidamide	C18:1 ^{6trans}	40	400	0.999
Stearamide	C18:0	50	50	0.997
Erucamide	C22:1 ¹³	50	100	0.998
Arachidamide	C20:0	10	50	0.999
behenamide	C22:0	20	20	0.999

Table 3-2. LOD and LOQ for select PFAMs determined by injection of 2 μ L standard solutions from 500 pM to 10 μ M. Calibration curves were linear between 0.500 - 10 μ M. The LOD and LOQ were determined by a S/N of 5 and 10, respectively.

3.5. DISCUSSION AND CONCLUSION

This chapter describes various strategies for efficient separation and detection of saturated and unsaturated fatty acyls. Different subclasses of lipids were resolved with a normal phase separation scheme utilizing a heptane and methyl-tert-butyl ether substituted mobile phase with gradient elution. The addition of isopropanol to the mobile phase was necessary to increase the solubility of these lipids, reducing the carry over between injections. Nonetheless, it was still essential to occasionally wash the column with polar solvents, especially if large injection volumes (> 100 μ L) are used frequently. The fatty acyl subclasses separated via the normal phase method are those commonly extracted with Folch-Pi from biological samples. This method is comparable to previously reported SPE methods¹⁴⁹ and although it has an increased total analysis time the separation is automated and highly reproducible. The eluent can be monitored by MS if a post-column feed is used or collected directly for further separation or analysis. It was found that, with a 200 μ L injection volume, the PFAMs and NAGs would co-elute as one peak between 31 and 38 minutes. This, however, was not problematic as further

analysis conducted with MS/MS found that NAGs ionized in the negative mode while PFAMs were observed in positive mode.

Silver ion chromatographic separation of analytes with various degrees of unsaturation was employed to determine its viability as a technique in multidimensional chromatography of fatty acyls. Argention chromatography by TLC and GC were first described in the 1960's^{151,152}. Later versions involving HPLC were reproduced in our laboratory. In our hands it was observed that the saturated and trans-unsaturated fatty acid phenacyl bromides co-eluted as one peak. Subsequently, mono-unsaturated components eluted, followed by di-unsaturated, and so on. Unlike the saturated components, secondary separation occurred where all components with the same degrees of unsaturation did not co-elute. This was attributed to the column having "uncapped" silinol groups causing a secondary normal phase separation. This separation scheme was found to suffer from irreproducible retention times and, therefore, could not be utilized without a detection system. It was unclear if the reproducibility problem was due to the mobile phase type¹⁴⁶ or silver bleed, but inconsistent elution has been reported by other authors¹³².

Following separation of fatty acyls with either normal phase or silver ion chromatography the individual subclasses (eg. PFAMs or NAGs) can be further separated to determine the distinct analytes present. This was achieved with C18 reversed phase chromatography and detected with tandem MS. The elution order followed the trends observed with fatty acids eluted from reversed phase columns¹⁵³. In general, the lipids elute from shortest to longest acyl chain with one degree of unsaturation causing elution to decrease by the equivalent of 2 carbons. For example, a C16:0 would elute at a similar

retention time to a C18:1. These so called “critical pairs” were able to be separated by adjusting the gradient elution parameters and/or increasing the column theoretical plates. For PFAMs, isobaric compounds (oleamide, elaidamide, and petroselaidamide) differing only in double bond position were unit resolved using a 5 minute hold at 80% methanol followed by a 5 minute linear ramp to 100% methanol. This resulted in LOD of 10 – 400 nM depending on the species. NAGs proved to be difficult to separate on standard C18 columns due to low solubility and increased interaction with the stationary phase. This often resulted in double peaks and both higher peak broadening and tailing. Therefore, a C30 substituted column and a fused-core C18 column with a reduced particle size were employed to determine the optimum conditions for NAG separation. Of note, in our hands NAGs were not found to ionize efficiently or reproducibly in positive ion mode, thus, negative ion mode was used for all studies. The C30 column proved useful in separation of saturated and monounsaturated NAGs with modest tailing, however, the analysis time was undesirable when considering multiple dimensional LC. The 2.6 μm particle size fused-core column was expected to reduce the analysis time, broadening, and tailing factor. As expected, the analysis time was reduced by 6-fold, and peaks were baseline resolved with minimal tailing. Similar to observations of PFAM separation, NAG analysis time could not be reduced below 5 minutes and retain separation. Due to the low ionization efficiency of these compounds the LOD was 1 μM for all species, consequently, limiting the ability to detect biological levels.

Given the experimental limitations of silver ion chromatography, the normal phase chromatography method was chosen as the preferred first dimension separation method due to automation and high reproducibility. An offline approach was favored as

The analysis time by reversed phase separation could not be reduced sufficiently which would lead to larger injection volumes from the first dimension. The small column volume and flow rate of the second dimension would, thus, be incompatible for mixing nonpolar solvents of the first dimension, causing a higher background noise. Additionally fractionation of the NAG and PFAM peaks would lead to overall lower moles being analyzed per unit time and, therefore, may obscure accurate quantitation. By taking time to process samples between separation dimensions all of these caveats were avoided. In summary, we developed an off-line MDLC system for analysis of PFAMs and NAGs in vertebrate samples of complex lipid composition (see **Chapter 4: Analysis of Swiss-Webster Mouse and Sprague-Dawley Rat Tissue via Two Dimensional Liquid Chromatography and Tandem Mass Spectrometry**) for the highest quantitation integrity.

Chapter 4

PFAM and NAG Detection in Tissue Samples and Implications for Future Studies

4.1. ABSTRACT

Primary fatty acid amides (PFAMs) and N-acyl glycines (NAGs) are polar lipids that have been shown to be bioactive in mammals and humans. These compounds are hypothesized to play an important role in bioregulation of physiological processes, such as sleep and mood. Likewise, aberrant metabolism of these lipids may be a diagnostic tool for identifying disease. A group of PFAM and NAG standards, ranging in carbon chain length from 12 to 22 with various degrees of unsaturation, were separated by a normal phase to isolate the PFAM and NAG subclasses. Reconstituted fractions were further separated using reverse phase chromatography with gradient elution by methanol and water. Components were detected by MRM mode to allow for selective detection. The PFAMs were observed in positive mode as the $[M + H]^+$ peak and NAGs were seen in negative mode as the $[M - H]^-$ ion. Heart, liver, and brain tissue obtained from wild type Swiss Webster mice and Sprague-Dawley rats were analyzed via the developed method to determine the biological levels of the target analytes. Samples from mice and rats were found to have levels of PFAMs and NAGs at the periphery of the limit of detection for the described method. Other factors, such as tissue quality and use of inhibitors were found to have a profound effect on sample detection. The knowledge gained from this study has now poised future studies to further correlate the effect of behavioral phenotypes on the biological levels of these bioactive lipids.

4.2. INTRODUCTION

PFAMs are polar lipids that have established physiological properties and neuroreceptor interaction (see **Chapter 1: Metabolism, Physiology, and Analyses of Primary Fatty Acid Amides**). For example, exogenous application of low levels of oleamide to cell lines expressing 5HTR subtypes 1A, 2A, and 2C potentiated the receptors with maximal effects at 100 nM³⁻⁵. Functional studies observed maximum potentiation of PFAMs with acyl tail length 16 to 22 with one degree of unsaturation near the $\Delta 9$ position forming a hairpin-like configuration^{3,6,10}. In addition to interaction with serotonin receptors PFAMs have also been shown to modulate glycine⁶⁴, GABA^{5,10,64,66}, and cannabinoid receptors^{12,13}, gap junctions⁷¹, and cellular calcium signaling^{71,72}. Oleamide and erucamide have been found at elevated levels in the cerebral spinal fluid of sleep deprived rats, cats, and in hibernating squirrels suggesting a physiological role for these PFAMs^{15,52,100,117}. Other physiological effects induced by PFAMs include water modulation⁸⁷, food uptake¹⁸, promote angiogenesis^{55,56} hypolocomotion and decreased body temperature^{17,54}.

Degradation of PFAMs is accomplished by the enzyme FAAH and the mechanism is well defined⁴²⁻⁵¹. Anabolic pathways have been explored exclusively *in vitro* and are still under debate. Proposed pathways include conversion of fatty-CoA substrate to N-acylglycine (NAG) by cytochrome C^{27-29,154}, BAAT³¹, and glycine N-acyl transferase^{32,33}. The NAG can also be formed by an N-acylethanolamine substrate being converted by alcohol dehydrogenase^{36,38}. All of the proposed anabolic pathways for formation of PFAMs include the NAG intermediate being converted by peptidylglycine

α -amidating monooxygenase (PAM)^{22-26,155,156} or cytochrome C. One notable exception was demonstrated by Meuller *et al.* where the fatty-CoA was directly amidated to the corresponding PFAM by cytochrome C^{27-29,154}.

PAM is a bifunctional enzyme primarily responsible for the amidation of glycinated peptides¹⁵⁷⁻¹⁶⁶. It is this amidation action that confers biological activity to the otherwise inactive peptidylglycine. Due to this reflection, NAGs are largely believed to be inactive intermediates in the anabolic pathway of PFAMs. The corresponding NAG was found to be inactive in experiments on oleamide's effect on gap junction communication, supporting this hypothesis⁷⁰. Nonetheless, Bradshaw *et al.* have investigated the distribution of NAGs in biological samples. Skin, lung, spinal cord, kidney, and liver were found to have the highest concentration of select NAGs per weight of dry tissue⁹¹. The approximate concentration range in these tissues was 100 – 1600 pmol/g.

Some reports exist of quantitation of PFAMs in biological samples, such as in human luteal phase plasma², cerebral spinal fluid of sleep deprived cats^{15,117}, and lung, kidney, liver, and brain of pig⁸⁷. However, no comprehensive reports in a single species are available such as those by Bradshaw and co-workers⁹¹. A broad, quantitative screen of PFAM and NAG levels in biological tissues would aid in supporting proposed anabolic pathways and investigating the role of these molecules in behavioral phenotypes. Here we present an analytical strategy for quantitation of PFAMs and NAGs in biological samples.

4.3. MATERIALS AND METHODS

4.3.1 Chemicals

Methanol optima grade, formic acid optima grade, ammonium acetate, hexane, dichloromethane, acetonitrile, and ammonium hydroxide were purchased from Fisher Scientific (Fair Lawn, NJ, USA). Oxalyl chloride, oleic acid, erucic acid, petroselaidic acid, heptane HPLC grade, methyl-tert-butyl-ether HPLC grade, isopropanol HPLC grade, acetic acid, and anhydrous dichloromethane were from Sigma Aldrich (St Louis, MO, USA). N, N-dimethylformamide, heptadecanoic acid, and eicosanoic acid were purchased from Aldrich Chemical Company (Milwaukee, WI, USA). Lauric acid, myristic acid, palmitic acid, stearic acid, and docosanoic acid were purchased from Acros Organics (New Jersey, USA). Elaidic acid was from MP Biomedical Inc. (Solon, OH, USA) and linoleamide was purchased from Enzo Life Sciences (Ann Arbor, MI, USA). Oleoylglycine, Linoleoylglycine, palmitoylglycine, arachidonoylglycine, and arachidoylglycine were purchased from Cayman Chemicals (Ann Arbor, MI, USA).

4.3.2 Lipid Extraction and Normal Phase Separation

Tissue samples of either Swiss-Webster mice or Sprague-Dawley rat (generously donated by Dr. Susan Amara) were weighed while frozen and kept on ice until extraction. Tissue samples between 0.2 – 2.0 g were lipid extracted via a modified Folch-Pi method⁸⁶. Briefly, each sample was homogenized in 20 times the weight (in mL) of 2:1 chloroform:methanol with 1 mM indomethacin additive. Homogenized samples were washed with 0.88% KCl and centrifuged at 2100×g for 60 minutes at 4°C. After centrifugation, the aqueous layer was discarded and the remaining extract was transferred

to a clean tube and dried under nitrogen. All glassware used was vapor silinized to prevent lipid adhesion¹⁶⁷ and any use of plastic was avoided due to contamination by lipid slip additives¹⁶⁸. Each extracted sample was separated via normal phase chromatography utilizing a YMC PVA-Sil column (4.6 × 250 mm, 5 μm particle size). Gradient elution is carried out starting at 95 % mobile phase A (heptane with 0.5% v/v methyl-tert-butyl-ether) and increasing linearly to 50% mobile phase B (methyl-tert-butyl-ether with 10% v/v 2-propanol and 0.2% v/v acetic acid) over 40 minutes with a flow rate of 1 mL/minute (gradient developed by Kroniser and Johnson, unpublished). Fractions were collected at 8 minute intervals and the time corresponding to NAG and PFAM elution was collected, dried under nitrogen, and reconstituted in 100 μL of methanol for further separation with reversed phase chromatography.

4.3.3 Reversed Phase Separation with MRM Detection of PFAMs and NAGs

PFAM and NAG eluent collected from the normal phase separation were further analyzed by reversed phase chromatography. NAGs were separated with a Phenomenex C18 fused-core column (4.6 × 100 mm, 2.6 μm particle size) using a gradient elution starting with 70% methanol hold for 6 minutes, followed by a linear ramp to 80% over 8 minutes and a 1 minute hold at 80%, and ending with a 5 minute linear ramp to 100%. Both methanol and water mobile phases were substituted with 10 mM ammonium acetate to aid in ionization. The flow rate was 1 mL/minute and the injection volume was 5 μL. Ionization was achieved with an ESI source operated in negative mode with optimized parameters: fragmentor voltage 135 V, sheath gas flow 11 L/minute, nebulizer pressure 55 psi, nozzle voltage 500 V, capillary voltage 3500 V, drying gas flow 9 L/minute,

drying gas temperature 275°C, and dwell time of 500 ms. MRM detection mode was used to monitor the $[M-H]^-$ parent ion and 74 m/z product ion.

PFAMs were separated on a Zorbax RP C18 column (2.1 × 50 mm, 1.8 μm particle size) with a gradient elution with methanol:water starting at 80% methanol hold over 5 minutes, followed by a 5 minute linear ramp to 100% methanol, and a final 3 minute hold at 100%. The flow rate was 0.4 mL/minute, a 2 μL injection volume was used, and 0.3% formic acid ionization aid was added to both mobile phases. PFAMs were detected using an Agilent 6460 Triple Quadrupole Mass Spectrometer equipped with an APCI source. Optimized detection parameters are as follows: gas temperature 325°C, vaporization temperature 325°C, gas flow 4 L/minute, nebulizer pressure 22 psi, capillary voltage 3500 V, corona 4 μA, fragmentor 125 V, and dwell time 50 ms. MRM detection was employed to monitor elution of the $[M+H]^+$ parent ions and either product ion 43 m/z for saturated components, or 55 m/z for unsaturated species.

4.4. RESULTS

Swiss-Webster mouse and Sprague-Dawley rat tissue was analyzed according to quantity and availability, therefore, not all samples shown are from the same species nor tissue type. Early attempts at extraction and analysis of PFAMs and NAGs from mouse brain suffered from contamination, obscuring identification even upon blank subtraction (Figure 4-1A). This contamination was found to be leaching from micropipette tips during minor sample transfer steps in the Folch-Pi extraction steps. When all sample contact with plastics was eliminated the contamination profile previously observed was attenuated and sample peaks due to tissue extractions were evident (Figure 4-1B).

Homogenization in SDS prior to Folch extraction was deemed unsuccessful since no analytes were detected from the blank or tissue sample (Figure 4-1C). FAAH inhibitor, indomethacin, was employed to prevent potential degradation (Figure 4-1D). This method of extraction showed the most promising results, with blank response near baseline levels and detection of analytes in the tissue sample. 1 μ M indomethacin was included in all future extractions.

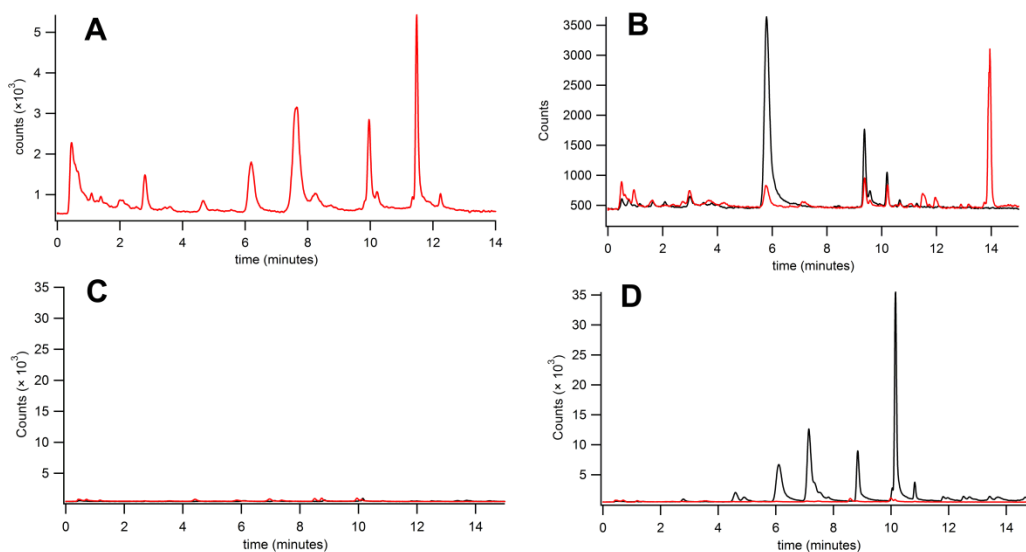


Figure 4-1. Analysis of contamination and use of inhibitors in tissue extracts. (A) Blank extract using extraction solvents with no tissue present (B) Extraction of mouse brain (black) overlaid with blank extract (red) excluding the use of plastic pipet tips in sample preparation. (C) Mouse brain extract (black) versus blank extract (red) using SDS for homogenization and all glass preparation. (D) Mouse brain extract (black) and blank extract (red) by all glass Folch-Pi extraction with 1 μ M indomethacin. All chromatograms shown are analyzed by the reversed phase PFAM method

Rat hearts between 1.2 and 1.4 g were analyzed for the presence of PFAMs and NAGs (Figure 4-2). Three samples analyzed in the same week had very similar chromatographic profiles but the same PFAMs were not present in all samples (Figure 4-2A, B, and C). Two additional samples of rat heart were analyzed one week later with very different chromatographic profiles and nearly no PFAMs detected (Figure 4-2D and

E). Attempts to quantify the PFAMs observed in the heart samples gave a wide variation of concentration ranges (~300 nM to 7 μ M), while some were below the LOQ.

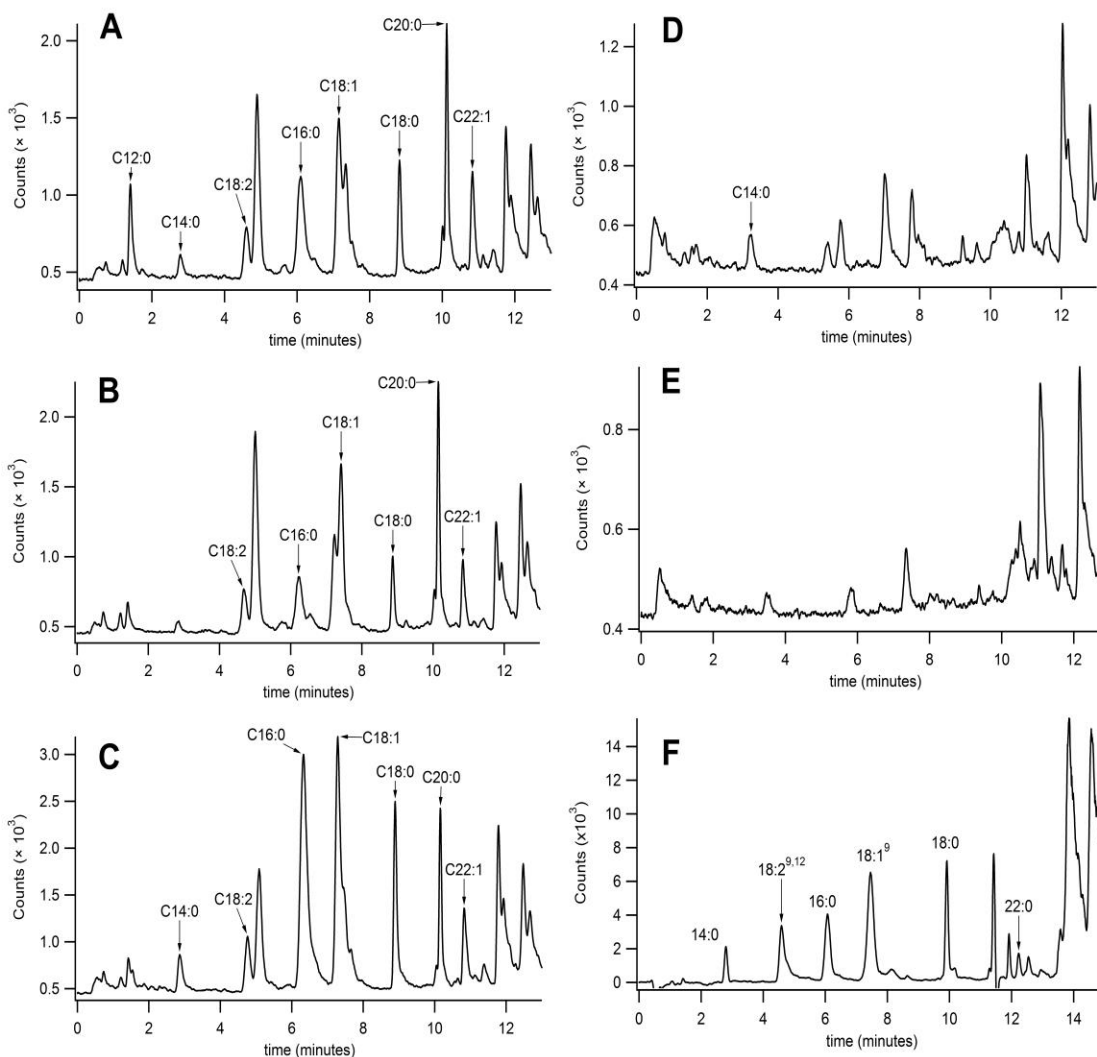


Figure 4-2. Analysis of (A-E) individual Sprague-Dawley rat hearts, and (F) Swiss-Webster mouse brain with mid-brain removed. Peak labels show identified PFAMs using the C:X^Y representation where C shows the acyl chain length, X is the degree of unsaturation, and Y is the position of unsaturation. All unsaturation points are in the cis configuration unless otherwise noted.

Mouse brain was tested because of the known interaction of oleamide with 5HTR. The equivalent of 10 mouse brains (3.7206 g) was analyzed to ensure adequate sample size (Figure 4-2F). All PFAMs identified in the sample were below the LOQ. No NAGs were detected in any of the samples.

Additional sample analysis displayed irreproducible chromatography, thus, the extraction efficiency was tested over a 3 week period with approximately 1 g of rat heart per sample (Figure 3). The first week extraction, following normal protocol, had a percent recovery for an internal standard of 64% for the blank and 73% for the sample Figure 4-3A). The baseline showed a higher variability in dynamic MRM mode for this sample, consequently MRM mode was used in future analysis. Rat hearts for week 2 and 3 extraction experiments were homogenized and kept at 4 °C until analysis.

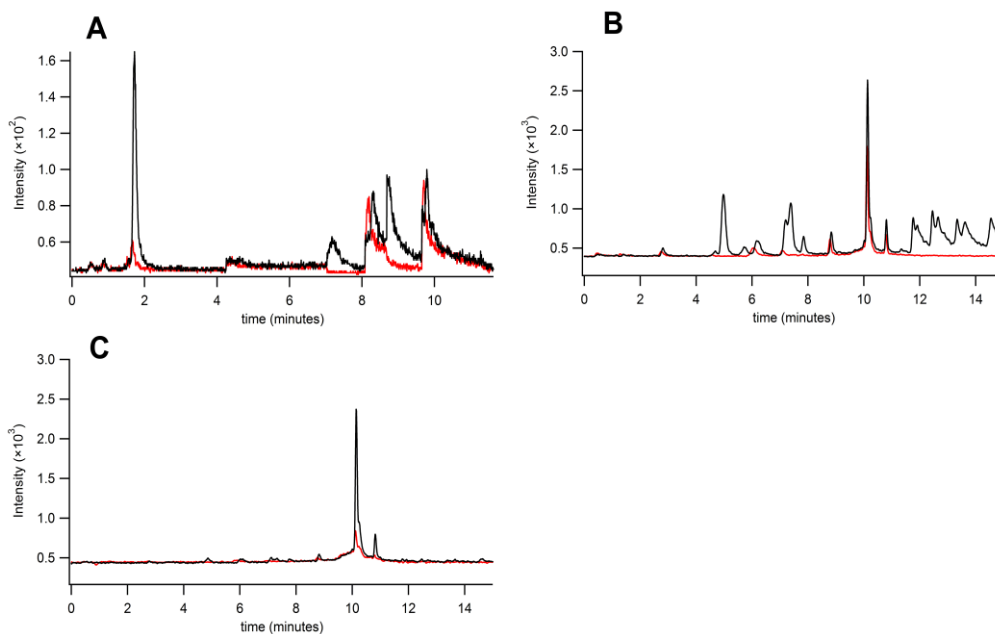


Figure 4-3. Time dependent extraction of individual Sprague-Dawley rat heart samples extracted (A) the same week of homogenization, (B) one week after homogenization, and (C) 2 weeks after homogenization. All samples were homogenized in 2:1 chloroform:methanol with 1 mM indomethacin present. (B) and (C) were stored at 4 °C until analysis. Data for (A) was obtained using dynamic MRM mode while (B) and (C) were collected with MRM mode.

Week 2 samples had a percent recovery of 52% for the blank and 49% for the sample (Figure 4-3B). Week 3 samples were 43% recovery in the blank and the internal standard in the sample solution was not detected (Figure 4-3C).

Reproducibility issues continued after extraction efficiency studies. After normal phase column regeneration protocols were conducted, rat liver was analyzed (Figure 4-4). While each sample had similar chromatographic profiles, no PFAMs or NAGs were detected. All additional tissue analysis for rat brain, liver, and heart displayed no measurable amount of PFAMs nor NAGs.

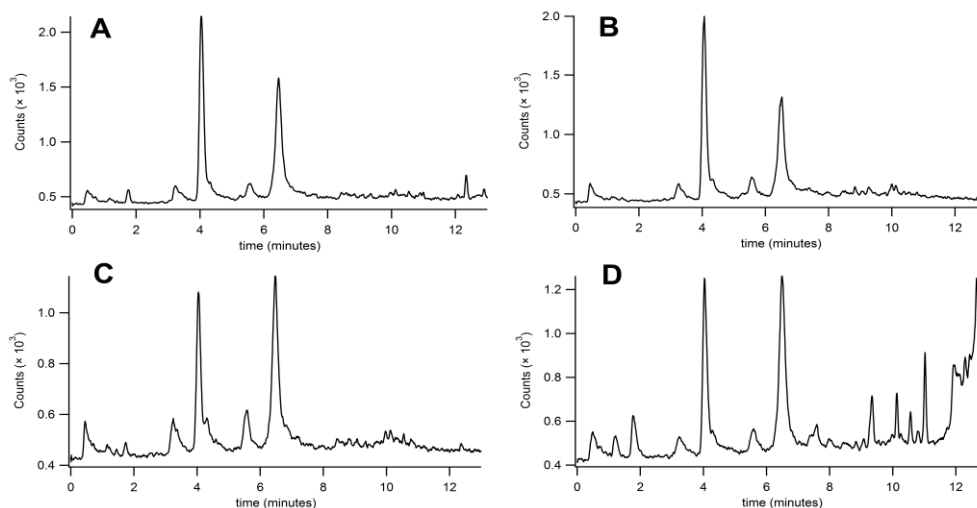


Figure 4-4. Analysis of Sprague-Dawley rat liver. Each figure (A-D) represents one replicate of approximately 2 grams per sample. The peaks present do not match the retention time nor m/z for any known PFAM determined with Agilent Mass Hunter Qualitative Analysis software.

4.5. DISCUSSION AND CONCLUSION

Brain, liver, and heart of Swiss-Webster mice and Sprague-Dawley rats were analyzed for content of PFAMs and NAGs using an off-line normal phase and reversed phase HPLC-MS/MS method. Initial sample extracts of mouse brain showed a high level of contamination evident in both the sample and the blank. This contaminant was found to be extractable lipids in plastic pipette tips (Figure 1A, B). When any tissue sample was extracted and prepared using only glassware, and micropipette transfer steps were eliminated, the blank and sample exhibited very different chromatographic profiles. The addition of an FAAH inhibitor, indomethacin ($IC_{50} = 100 \mu M$)⁴³, was used to prevent

enzymatic degradation of the PFAMs and NAGs present. Addition of 1 mM inhibitor acted to increase the sample signal compared to the blank (Figure 1C, D).

After contamination and inhibitor studies were complete samples were analyzed for identity and quantity of select PFAMs and NAGs. Some preliminary rat heart samples appeared to have comparable chromatographic profiles, possibly indicating similar composition (Figure 2A-E). Future extractions of rat heart failed to reproduce the results obtained in Figure 2A-C. In addition, the quantity and identity of PFAMs observed varied greatly between samples. Attempts to quantitate the observed PFAMs yielded results ranging from 300 nM to over 7 μ M, which could not be reconciled by examining differences in % recovery between samples.

The extraction procedure was tested to determine if a longer extraction time could increase the incidence of PFAMs or NAGs observed (Figure 3). None of the spectra from week 1 to week 3 of extraction had any identifiable PFAMs or NAGs. Because the signal intensities could not be directly compared the % recovery was used as a qualitative measure of extraction efficiency. From week 1 to 3 the % recovery in both the sample and the blank decreased. Reduction in the incidence of heptadecanoamide could be due to a number of factors, including minimal enzymatic degradation or oxidative damage. Therefore, future samples were homogenized, extracted, and dried down within 24 hours.

Over several months of sample preparation the internal standard was increasingly not detected. This issue was resolved by normal phase column regeneration, which removed column build-up. The regeneration procedure was employed after approximately 1 mL of sample extract was injected, or every 5-7 samples. After column cleaning, analysis of rat liver was conducted (Figure 4A-D). Each sample appeared to

exhibit similar chromatographs, however, no PFAMs or NAGs were identified. Indeed, all subsequent analyses of brain, heart, or liver contained no measurable PFAMs or NAGs.

Other authors have reported finding 0.1-5 pmol/100 μ L (approximately 50 nM) oleamide in cerebral spinal fluid^{15,117}, and erucamide in pig lung, kidney, liver, and brain between 0.5 and 12 ng/g (intermediate value of 200 nM)⁸⁷. These values fall just below the LOQ and LOD for oleamide determined in our optimized system. With respect to other PFAMs, the LOD range is from 10 – 400 nM. Thus, a minimum of 4 g of tissue must be extracted to reach the LOQ for oleamide assuming 60% recovery. Separation of 4 g of tissue extract by the normal phase chromatography method developed will require 4 separate injections (approximately 11 hours) for a single tissue sample replicate due to sample viscosity. Additionally, large sample sizes tended to exhibit a white cloudy film after reconstitution in methanol prior to reversed phase analysis. This film was only transparent when dissolved with 2:1 chloroform:methanol. Unfortunately, this solvent caused jamming and clogging of the auto-injection system. One other factor that hindered quantitation was the system LOD and LOQ. The system was optimized, however, there was little difference between many of the LOD and LOQ suggesting that ion transmission dropped off rapidly.

In conclusion, the development of a MDLC-MS/MS method allowed for the analysis of vertebrate tissue samples. The incorporation of an internal standard to the extract aided in the validation of correct fraction collection from the 1st dimension and allowed for stability comparison between samples. From these analyses several important factors in quantitation of PFAMs and NAGs in these samples was determined.

The use of plastics was found to contribute contaminants to the extract and, thus, the use of glass in the preparation was advantageous in reducing background. The addition of inhibitors to prevent degradation of PFAMs by FAAH was found to increase the detection of components in the extract. Additional factors in ensuring reliable quantitation, such as tissue quality and data analysis considerations, are discussed in the following section.

4.6. PROJECT OUTLOOK AND CONCLUDING REMARKS

It is clear, even with careful method selection and sample processing consideration, that quantitation of trace levels of the PFAM and NAG subclasses propose a challenge for conventional separation and detection methods. Several factors were found to have a profound impact on analysis and additional experimental methodology should be further contemplated. One factor found to influence detection was the use of tandem mass spectrometry. Many of the PFAMs and NAGs investigated for determination of LOD and LOQ revealed a steep loss of signal. For NAGs this was observed at 1 μ M and for PFAMs it was variable between 100-400 nM (see **Chapter 3: Chromatographic Separation Methods for Fatty Acyls**). A similar signal drop-off for PFAMs is observed in GC-MS with electron ionization (Davic, A. P., personal communication) and, thus, the LOD seems to be an inherent limitation of these analytes versus quality of MS instrumentation available. This MS LOD may only be capable of being improved for instrumentation with ion trapping capabilities.

Other experimental parameters of consideration are quality and tissue and extraction conditions. Tissue should be excised immediately after sacrifice and flash

frozen in liquid nitrogen within minutes to prevent chemical alteration. If the excised, frozen sample is not processed immediately it should be stored frozen at -80°C. Between removal and usage that sample should not be allowed to thaw until extraction is complete. In addition, the homogenization procedure should be carried out in ice-cold extraction solvents to limit enzymatic hydrolysis. The addition of indomethacin to the 2:1 chloroform/methanol solvent was found to have a positive effect on detection of components in extracted tissue samples. This molecule, while shown effective in reducing FAAH activity, is not an FAAH specific inhibitor, but affects degradation via the COX-2 pathway. A more specific inhibitor should be chosen in future studies to ensure hydrolysis of the analytes is not problematic. Since the FAAH active site is a catalytic triad containing Ser-Ser-Lys, PMSF may be an appropriate choice and has documented inhibition properties on FAAH^{43,44,47}.

The last major consideration of PFAM and NAG quantitation should be data analysis. Endogenous PFAM concentrations have demonstrated fluctuation related to sleep cycle^{15,52,117} and many other mundane events, such as food intake¹⁸, may alter these lipid levels. Therefore, it is not improbable that environmental impact will cause genetically identical animals to display a range of endogenous concentrations. Given these experimental implications the data analysis method is of utmost importance. In evaluation of disease models or behavioral phenotypes, principle component analysis is used to differentiate aberrant levels of biomarkers. Likewise, this approach should be utilized here to determine the range of endogenous variation. These data can then be compared to numerous animal models of disease and behavior to determine if any correlation can be ascertained.

In conclusion, experimental factors, including tissue quality, extraction preparation, and data analysis methods will need to be altered and rigorously conducted to render reliable quantitation results. MS/MS, while a highly sensitive detection method, was not sufficient in this study given the characteristic limitation of PFAM ion transmission. Currently our laboratory is working on a new PFAM detection platform utilizing microdroplet derivitization and laser induced fluorescence detection. In this detection system separated eluents from a chromatographic system are mixed with fluorescent derivitization reagents in nano-droplets formed on a microchip by perpendicular, fast flow of an immiscible phase. The design of the microchip channels enhances mixing of the fluorescent reagents via turbulent convection. The fluorogen tags in this method have no native fluorescence, a large stokes shift, and are selective for primary amines. The un-optimized LOD for this system is in the attomole range (Davic, A. P., personal communication) compared to the above 150 femtomole LOD. This lower LOD combined with the selectivity of the derivitization will enable quantitative measurement of PFAMs with a reduced use of tissue. Therefore, changes in PFAM levels could be tested and compared to behavioral phenotype experiments to determine the significance of these bioactive signal lipids on physiology. The use of fluorescent tagging and sub-attomole detection with microdroplet reaction and laser induced fluorescence platforms being undertaken in our laboratory will provide a more effective means of determining the endogenous trace concentrations of these bioactive lipids.

Appendix 1

Palmitoylethanolamine Stability in Fluorocarbon Emulsions: A Delivery System for Treatment of Chronic Pain

A.1. ABSTRACT

Palmitoylethanolamine (PEA) is an endogenous molecule that has been found in a wide variety of sources including plants, like peanut and soy, as well as various vertebrates. Although PEA does not directly interact with known cannabinoid receptors, it has documented cannabimimetic effects. Treatment or ingestion of this compound is known to produce a myriad of potentially advantageous physiological responses, most notably anti-inflammatory and analgesic effects. PEA was incorporated into nano-emulsions containing fluorocarbon with the intent to trace drug delivery in vivo. A selective and sensitive method was developed utilizing HPLC-MS/MS with MRM detection of the $[M + H]^+$ parent ion and protonated ethanolamine product ion to determine the incorporation and stability of PEA in these nano-emulsions. Detection and quantitation limits for the optimized method reached 1 femtomole.

A.2. INTRODUCTION

N-acyl ethanolamines (NAEs) are congeners of fatty acids containing an ethanolamine moiety and are a subclass of the fatty acyl lipid group outlined by Fahy et al.¹⁶⁹ This group of lipids is biosynthetically produced by cleavage of membrane N-acyl phosphatidylethanolamines to NAEs by a phospholipase D¹⁷⁰⁻¹⁷². Deactivation of these

compounds is achieved by fatty acid amide hydrolase (FAAH) and N-acylethanolamine-hydrolyzing acid amidase (NAAA), preferential for anandamide (AEA) and palmitoylethanolamine (PEA), respectively (for a review see Tsuboi et al¹⁷³), resulting in ethanolamine and the corresponding fatty acid. While both of these enzymes degrade NAEs they are structurally and functionally dissimilar. FAAH and NAAA show no sequence homology and FAAH hydrolyzes compounds optimally at pH 8.5-10, whereas NAAA is most active at pH 4.5-5. Fluorescent tagging experiments of these degradative enzymes show a membrane-like distribution of FAAH and a dispersal of NAAA reminiscent of cytosolic or lysosome residence.

NAEs are endogenous compounds have been characterized in a wide range of species and tissues. Of the discovered NAEs, the endocannabinoid AEA is the most studied. AEA was first isolated from porcine brain and described by Devane *et al.*¹⁷⁴ as an endogenous compound that binds to the cannabinoid receptor, most notorious for its interaction with the psychoactive component in cannabis. The extensive amount of information available on AEA is beyond the scope of this text and will not be covered in detail, except in comparison to PEA (additional information on AEA is reviewed in¹¹³⁻¹¹⁵).

PEA was first described in 1954 as a compound in whole egg yolk and alcohol soluble fractions of egg, but not in protein or acetone fractions, that was found to reduce mean swelling index in joints of guinea pigs and pig weanlings when challenged with anaphylactic arthritis¹⁷⁵. The structural identity of the active component in egg was not identified until several years later by Kuehl *et al.*¹⁷⁶ Since its discovery, PEA has been identified in a wide variety of plant and animal sources, including peanut oil and soy

lechtin¹⁷⁷, sea urchin ovaries¹⁷⁸, central nervous system of leech¹⁷⁹, several species of bivalve molluscs¹⁸⁰, pig¹⁸¹, cow¹⁸¹, sheep¹⁸¹, mouse¹⁸², rat^{183,184}, and human¹²¹. Concentrations of NAEs in these tissues are reported in the pmol/g range.

The most notable physiological properties of PEA identified to date are its propensity for anti-inflammatory and analgesic effects. In models of neuropathic pain induced by chronic constriction injury treatment with subcutaneous injections of 30 mg/kg PEA attenuated pain response from noxious and non-noxious stimuli in wild type mice¹⁸⁵. Additionally, PEA administration prevented changes in number of fibers, myelin thickness, axon diameter, and reduced 50% of edema in nerve fibers. Injections of PEA over a 14 day period also reduced the number of inflammatory infiltrate cells observed at the injury site. These anti-inflammatory and protective effects were not observed in PPAR α null mice. LoVerme and coworkers found similar results for PEA treatment in chronic constriction injury model of neuropathic pain¹⁸⁶. They also described a diminished nociceptive behavioral response to formalin, magnesium sulfate, and carreegan induced hyperalgesia. Reduction of edema was not evident until 1 h post injection, although analgesic effects were evident shortly after treatment. Attenuated pain response was abolished by CB2 antagonist, SR144528, and inhibitors of calcium mediated potassium channels. CB2 knock-out mice were still responsive to anti-inflammatory and analgesic effects of PEA; providing evidence that PEA is not an endogenous ligand for CB2 receptors, but exerts cannabimimetic properties. Paw withdraw latencies of mice administered a single dose of PEA versus those treated with the drug for 7-14 days showed similar results, both of which were higher than mice receiving vehicle, suggesting that PEA does not prompt a developed tolerance over the

time period tested. In line with previous reports, formalin and carrageenan induced edema and hyperalgesia were reduced with PEA treatment¹⁸⁷. PEA was also shown to diminish the number of mast cells present, as well as plasma extravasation caused by substance P. Mast cells were previously shown to be down modulated by exogenous PEA application¹⁸⁸. These effects were revealed to be dose-dependent. Injection of palmitic acid and ethanolamine were ineffective, proving PEA, and not its metabolites, elicited the observed response¹⁸⁷. Interestingly, PEA and AEA co-administered in formalin induced pain models were found to be 100 fold more potent than either compound alone¹⁸⁹. These synergistic effects between PEA and AEA were also demonstrated by enhanced relaxation of rat mesenteric arteries⁷⁸. Attenuated response to pain by AEA and PEA were even more potent when delivered locally, rather than systemically¹⁸⁹. Observed analgesia was reversed by CB2 antagonist SR144528; CB1 antagonist and opioid antagonist, naloxone and SR141716A, were ineffective. Additionally, a selective inhibitor of the main degradative enzyme of PEA, NAAA, was shown to have similar effects as PEA administration in a carrageenan pain and inflammation model¹⁹⁰. Inhibitors of FAAH, the main catabolic enzyme of AEA, had no effect. This data suggests that, while some effects of endogenous NAEs may be ascribed to the so called “entourage effect” (a hypothesis that endogenous NAE properties are due to the increased half-life of AEA), these lipids clearly have their own properties distinct from AEA. PEA treatment has been reported to reduce lipopolysaccharide-induced nitric oxide production in RAW264.7 macrophages¹⁹¹. Thus the analgesic and anti-inflammatory properties of PEA may be attributable to attenuation of nitric oxide production, which is a known pro-inflammatory.

Curiously, other reports of inflammation models and various disease states have shown an endogenous modulation in PEA and other congeners. Intraperitoneal injections of cadmium chloride in Wistar rat testes exhibited a drastic increase in PEA, stearoylethanolamide (SEA), and AEA that was time-dependent with total NAE levels 25 fold higher at 9 h post injection¹⁸³. In patients with osteoarthritis and rheumatoid arthritis, diseases that involve pain and inflammation of the joints, levels of PEA, and to a lesser extent OEA, were found to be dramatically reduced compared to control groups¹⁹². Examination of the CSF of patients with schizophrenia found the PEA and AEA were 2 fold higher versus control groups¹²¹. Tests of stress and anxiety found PEA and OEA concentrations in the serum increased when patients were exposed to a stressful situation¹²². Additionally, in patients characterized as having chronic wide spread pain and chronic neck and shoulder pain that, generally, pain score intensities correlated negatively with PEA and SEA levels¹²⁰. It is unclear in the disease states presented here if aberrant levels of NAEs are due to metabolic defects or are modulated as a downstream response.

There is some evidence that indicates elevated levels of PEA and other NAEs act in a protective manner. PEA, SEA, oleoylethanolamine (OEA), and linoleoylethanolamine were found to increase in infarcted canine myocardium¹⁹³. It is also known that PEA accumulates in ischemic tissues and protects cerebellar granule cells against glutamate excitotoxicity¹⁹⁴. Addition of AEA was found to antagonize the protective effects of PEA in glutamate excitotoxicity. Exogenous application of PEA (1 – 1000 nM) reduced the number of microglial cells and protected dentate gyrus granule cells in excitotoxically lesioned hippocampal slice cultures. These effects were abolished

by PPAR α , but not PPAR γ , antagonists¹⁹⁵. In models of ischemia, administration of 10 mg/kg PEA to rats, either 30 min before or during middle cerebral artery occlusion, significantly reduced the infarct volume and neurological deficit score¹⁹⁶. Several proteins found to be up regulated in ischemia had reduced levels in animals receiving PEA pretreatment. Rats which were given AM404, an NAE uptake inhibitor, were found to have larger infarct volumes and higher neurological deficit scores. Again, PEA and AEA levels were enhanced in the spinal cord of mice in an animal model of multiple sclerosis¹⁸². Intravenous injections of PEA and AEA improved spasticity within 10-30 minutes. PEA was found to dose-dependently reduce impairment, normalize learning profiles and working memory in an animal model of Alzheimer's disease¹⁹⁷. As with the anti-inflammatory and analgesic effects mentioned previously, learning and memory benefits associated with PEA treatment were absent in PPAR α null mice. Finally, intraperitoneal injections of PEA (EC₅₀ 8.9 mg/kg) in maximal electroshock seizure tests were found to have an anticonvulsive property¹⁹⁸. In chemical induced seizures, PEA was only effective against tonic convulsions of pentylenetetrazol and 3-mercaptopropionic acid. Overall, PEA reduced lethality associated with convulsions.

NAEs exert other cannabimimetic effects, such as alteration of food uptake. Guinea pigs and rats deprived of food for 12-18 h had elevated levels of PEA in the brain and liver¹⁹⁹. In contrast to AEA¹⁸, SEA, PEA, and OEA intraperitoneal injection were found to decrease food intake in starved rats²⁰⁰ and mice²⁰¹. Food deprivation acted to reduce the biosynthesis of OEA²⁰⁰. The anorexic effect of OEA was not affected by CB1 or CB2 antagonists, SR141716A and SR144528, respectively. Intracerebroventricular injection did not cause a decrease in food consumption, indicating that the anorexic

effects are not mediated by the central nervous system²⁰⁰. Reduction in food consumption invoked by treatment with SEA (up to 100 mg/kg) was not accompanied by sedation, illness, or diminished motility and body temperature. No other changes in glucose, triglycerides, or cholesterol levels were apparent. Administration of stearic acid did not alter food consumption versus controls. Interestingly, OEA and PEA were found to increase in the white adipose tissue of Wistar rats exposed to 4°C for up to 6 h²⁰². Elevation in NAEs was accompanied by increases in N-acyl transferase, but not FAAH. Exposure of adipocytes to noradrenaline and isoproterenol, beta-adrenergic agonists, elevated levels of OEA and PEA in cells while, the beta-adrenergic antagonist, pranolol, blocked the increases.

Due to the prevalence of these molecules in biological systems and the discovery of multiple orphan G protein coupled receptors, NAE binding has been investigated in orphan GPR55 and GPR119 receptors. Sequencing of GPR55 revealed that rat and mouse shared 75 and 78% identity, respectively, with human²⁰³. GPR55 shares relatively low sequence identity with CB1 and CB2 receptors, 13.5% and 14.4%, respectively²⁰⁴. mRNA levels were highest in the gastrointestinal tract, adrenal gland, central nervous system²⁰³, and large dorsal root ganglion neurons²⁰⁴. Expression of GPR55 in HEK293 cells discovered that AEA, OEA, and PEA were able to bind with EC₅₀ values of 18, 440, and 4 nM via radiolabeled binding assays with GTPγS. Surprisingly, THC was able to bind at an EC₅₀ of 8 nM, which is of higher affinity than its binding with CB1 or CB2 receptors, suggesting this orphan receptor may be a newly discovered cannabinoid receptor^{203,205}. Exogenous application of AEA and THC to HEK293 cells expressing GPR55 acted to increase intracellular calcium and reversibly suppress M type potassium

currents²⁰⁴. PEA had no effect on calcium release. GPR119 is expressed mainly in the gastrointestinal tract, pancreas, and brain²⁰⁶. AEA, SEA, OEA, and PEA were shown to activate human and mouse GPR119 in a yeast fluorescence assay, with OEA being the most potent. Due to this orphan receptors' localization in the gastrointestinal tract and its affinity for OEA, this receptor-ligand interaction was hypothesized to mediate the anorexic effects observed with OEA treatment and indeed synthetic, selective agonists of GPR119 produced a hypophagic effect.

Here we present method development and analysis of PEA stability in fluorocarbon nanoemulsions by HPLC-MS/MS. Fluorocarbon nanoemulsions have been previously demonstrated as drug delivery vehicles for poorly soluble drugs, such as the anti-inflammatory, celecoxib²⁰⁷⁻²⁰⁹. Following this rationale, PEA formulation into fluorocarbon nanoemulsions was undertaken. Here we present development of a sensitive analytical methodology to track incorporation and stability of PEA in new fluorocarbon nanoemulsion formulations. These studies were undertaken in light of the vast evidence for PEA as an analgesic with the intent to deliver and potentially track drug distribution *in vivo* in preclinical models of chronic pain. Tracking drug distribution will aid in determining how much of the drug reaches inflammation sites and how quickly it is degraded *in vivo*.

A.3. MATERIALS AND METHODS

A.3.1 Chemicals

Methanol, optima grade, chloroform, HPLC grade, and formic acid, optima grade were purchased from Fisher Scientific (Fair Lawn, NJ, USA). Palmitoylethanolamine was purchased from Tocris Bioscience (Bristol, UK). Fluorocarbon nano-emulsions were kindly provided by Dr. J. Janjic (Department of Pharmacy, Duquesne University, Pittsburgh, PA)

A.3.2 Methods

PEA extracts were crudely separated on a Zorbax RP C18 column (2.1 × 50 mm, 1.8 μm particle size) with isocratic elution of 80:20 methanol:water containing 0.3% formic acid as an ionization aid. The flow rate was 0.4 mL/minute, a 2 μL injection volume was used, and the eluent was detected using an Agilent 6460 Triple Quadrupole Mass Spectrometer equipped with an ESI source. Optimized detection parameters are as follows: gas temperature 275°C, sheath gas temperature 300°C, gas flow 5 L/minute, sheath gas flow 11 L/h, nebulizer pressure 45 psi, capillary voltage 4000 V, nozzle voltage 450 V, fragmentor 135 V, and dwell time 200 ms. MRM detection was employed to monitor elution of the $[M+H]^+$ parent ion at 300 m/z and product ion 62 m/z at a collision energy of 20 V.

A.4. RESULTS

PEA was directly infused using at Harvard Apparatus syringe pump at a flow of 0.2 mL/min in a 6460 Agilent Triple Quadrupole to determine the compound ionization and optimum collision energy (Figure A-1A). A crude separation method was developed to reduce ion suppression effects and determine the most sensitive ESI ionization parameters and MRM detection (final method described in **Section 3.2 Methods**). The

CID patterns were found to consist of $[M+H]^+$ parent ion, the loss of a hydroxyl group to yield the product ion $283\ m/z$, and fragmentation of the head group giving a protonated ethanolamine moiety at $62\ m/z$ (Figure A-1B). The linear range was found to be $500\ pM$ - $80\ nM$ and the LOD and LOQ were equivalent at $1\ femtomole$ (Figure A-2).

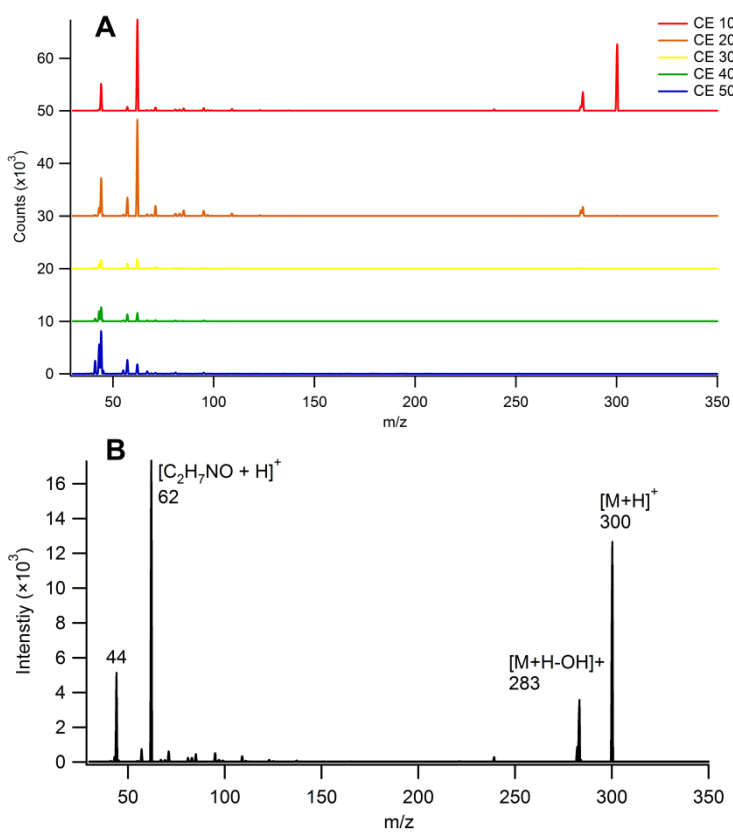


Figure A-1. (A) CID of $1\ \mu M$ PEA directly infused using a Harvard Apparatus syringe pump connected to a 6460 Agilent Triple Quadrupole MS equipped with ESI operated in positive mode. (B) Proposed fragmentation of PEA showing loss of a hydroxyl at $283\ m/z$ and a protonated ethanolamine at $62\ m/z$.

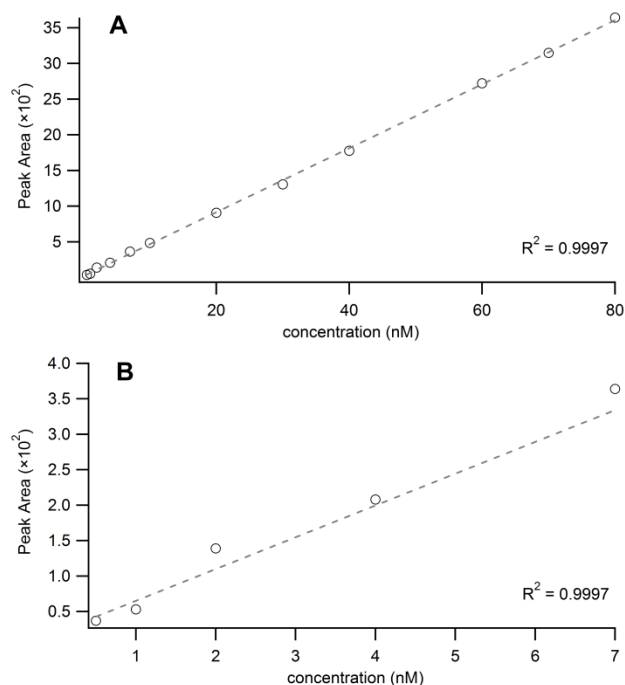


Figure A-2. (A) Concentrations of PEA from 500 pM to 80 nM were used to determine the linear range with isocratic elution in 80:20 methanol/water and an ESI ionization and MRM detection on a 6460 Agilent Triple Quadrupole using the parent ion 300 m/z and product ion 62 m/z . (B) The expanded calibration curve from 500 pM to 7 nM to show linearity in the lower range.

Nano-emulsions were freeze-thawed, extracted with a solution of 2:1 chloroform/methanol (HPLC grade), and an aliquot of the organic phase diluted in methanol to give an expected final concentration within the linear range. As in earlier work, the use of plastic was avoided in the sample preparation process due to use of extractable lipids in the plastic manufacturing process¹⁶⁸. Early formulations of the nano-emulsions contained olive oil to aid in the solubilization of lipophilic PEA, therefore a control sample was prepared with equivalent concentrations of olive oil to determine the possible interferences. The presence of olive oil exerted no negative effects on PEA detection evidenced by matching expected and measured values (Table A-1). Regardless, emulsions Emulsion 1 and 2 contained approximately 10 fold lower detected concentrations than those expected. Further avenues were explored, such as

measurement of PEA in the supernatant versus the pellet of freeze-thawed samples, increasing the concentration of the final sample from 50 to 500 nM (Table A-1), and addition of a normal phase pre-separation step (data not shown). Pre-separation of emulsions compared with a control sample did not increase levels of detection. Addition of ethanol to emulsions Emulsion 3 and 3F (5F is a microfiltered sample identical to Emulsion 3) greatly improved the ability to detect PEA, although, the microfiltered sample showed an almost 2 fold lower than expected value. Ethanol was added only to aid in solubility of the drug into a surfactant mixture and was evaporated from the final sample prior to testing. The same Emulsion 3 and 3F samples were tested again one week post preparation and PEA levels were found to decrease significantly. Lower levels of PEA after one week suggested degradation of PEA in the emulsion.

Sample	Expected (nM)	Measured (nM)
Control	75	72 ± 2
Emulsion 1	500	58 ± 1
Emulsion 2	500	59 ± 1
Emulsion 1		
Supernatant	50	4 ± 2
Pellet	0	5 ± 2
Emulsion 2		
Supernatant	50	5 ± 2
Pellet	0	3 ± 2
Emulsion 3	50	45 ± 1
Emulsion 3F	50	29 ± 1
Emulsion 3 –		
1 week post preparation	50	21 ± 2
Emulsion 3F –		
1 week post preparation	50	8 ± 2

Table A-1. Quantitation of PEA in nano-emulsions. The control sample contained concentrations of PEA and olive oil equivalent to those present in the prepared emulsions. The expected concentration values are those of the final sample after dilution for HPLC-MS/MS. F indicates samples which were filtered after preparation. Measured values show those obtained by peak integration and interpolation from the prepared calibration curved. Statistical values were obtained using the formula for standard error in the least squares fit.

A.5. DISCUSSION AND CONCLUSION

We have successfully determined parameters of a sensitive detection method for PEA. The linear range of 500 pM - 80 nM was chosen due to the high linearity of fit which were greater than 0.9995 (R^2). The LOQ and LOD for PEA with this method was 1 femtomole (500 pM), which is equivalent to those being currently reported for detection of NAEs²¹⁰⁻²¹². Analysis of fragments generated by CID identified a quantitative product ion at 62 m/z matching the mass of a protonated ethanolamine ion. This finding indicates that NAEs can be sensitively and selectively analyzed as the ethanolamine moiety gives a unique point of identification over other lipid classes that frequently yield indistinct acyl fragments. Analysis of nano-emulsions by this method proved challenging as the measured concentration was always less than expected based on the amount of PEA added to initial samples. This could be explained by the strong surfactants used in the dissolution of PEA in the aqueous based solution, since critical micelle index may not have been sufficiently exceeded, thus, impeding the extraction process. Another factor obscuring detection of PEA in nano-emulsions could be the storage or preparation processes. Chemical information available on PEA indicates that this material is light sensitive and therefore stocks or emulsions left in contact with light may have degraded. This may explain the decrease in PEA detection observed of samples 1 week post preparation. The process of freeze-thawing the emulsion before extraction was necessary to remove the fluorocarbon component. This was the layer referred to previously as the “pellet”. Stock solutions of PEA prepared in a 2:1 chloroform/methanol solution and stored at -80°C tend to irreversibly crystallize, signifying degradation (personal

observation). It is possible that repeated freeze-thawing events intended to purify the sample may cause degradation of the active component.

In future analyses of nano-emulsions and animal treatment with such, several important factors should be considered. Samples prepared with PEA should be stored in a location where light exposure is limited. Optimum storage temperature, either room temperature or chilled, would need to be determined with additional stability experiments. Based on previous observations, freeze-thawing of emulsions should be avoided to preserve the chemical integrity of the sample. Due to the unreactive nature of fluorocarbons and use of a selective MRM method it is likely that the presence of this component will not be problematic for the detection or conservation of instrumentation hardware. As surfactant micelle strength may be problematic, matrix conditions should be carefully selected. Many current reports of animal treatment with PEA have employed a mixture of tween 80 and polyethylene glycol or PBS with a final dilution in sterile saline to 20:10 v/v^{182,185,197}. Therefore, it may be of interest to determine PEA stability in a common formulation currently used in *in vivo* experimentation. Additional considerations included brand of extraction solvents, SPE column type, and treatment of tissue samples post-excision. A recent report demonstrated that the brand of SPE column, with identical packing material, resulted in astonishingly different recoveries of NAEs²¹³. This finding carried over into the brand of chloroform used, where some brands resulted in chlorination of unsaturation points, thereby, obscuring true levels of NAEs (OEA in particular). While PEA will not be affected by chlorination, these authors provide great evidence for the importance of rigorous method development. Final concerns are due to post-mortem quantitation of NAEs in animal samples. Several

authors have described an increase in levels of measured NAEs post-mortem in tissue exposed to ambient conditions^{180,181} and generally in necrotized tissue^{193,194}. Schmid et al. reported a linear increase in levels of PEA, OEA, SEA, and AEA with time spent at ambient temperature post-mortem¹⁸¹. Increases were dramatic with 37, 33, and 72 fold in pig, sheep, and cow at 22 h ambient temperature. This finding was corroborated by Sepe with substantial increases in PEA, OEA, AEA, and SEA in bivalve molluscs, but not boiled molluscs, at increasing time at ambient conditions¹⁸⁰. Therefore, excised animal tissue should be used immediately or quickly stored at -20°C. Extractions should be carried out in the shortest time frame possible with ice cold solvents until residual matter can be removed. It would also be prudent to consider the use of enzyme inhibitors for both biosynthesis and degradation of the desired analytes.

In summary, PEA is a lipophilic molecule with a long history of physiological benefits, including anti-inflammatory and analgesic properties. As this compound is endogenously produced, it appears to have few negative side effects that have been reported in *in vivo* tests to date. It is, therefore, an attractive candidate for treatment of afflictions of chronic pain and inflammation. Here we have described a method with sensitive and selective detection of this endogenous compound. Current nano-emulsions analyzed have proved troublesome in the detection and stability of PEA. Even though biosynthesis is prevalent, *ex vivo* preparation is complicated by its lipophilic nature. Nevertheless, the small considerations in sample preparation mentioned previously may prove invaluable in correcting stability hurdles experienced thus far. Additionally, oral dosage, though less effective, has proven successful. Tracking of drug delivery in a solid form may be accomplished with enriched radiolabeled PEA. While small scale

experimentation would be initially expensive; this would not be necessary to carry into clinical settings. Therefore, PEA proves to be a viable treatment strategy with an optimistic future for alleviating individuals afflicted with chronic pain.

REFERENCES

- 1 Fahy, E., Cotter, D., Byrnes, R., Sud, M., Maer, A., Li, J., Nadeau, D., Zhau, Y. & Subramanian, S. Bioinformatics for lipidomics. *Lipidomics and Bioactive Lipids: Mass-Spectrometry-Based Lipid Analysis* **432**, 247-273, (2007).
- 2 Arafat, E. S., Trimble, J. W., Andersen, R. N., Dass, C. & Desiderio, D. M. Identification of fatty acid amides in human plasma. *Life Sci* **45**, 1679-1687, (1989).
- 3 Boger, D. L., Patterson, J. E. & Jin, Q. Structural requirements for 5-HT_{2A} and 5-HT_{1A} serotonin receptor potentiation by the biologically active lipid oleamide. *Proceedings of the National Academy of Sciences of the United States of America* **95**, 4102-4107, (1998).
- 4 Huidobro-Toro, J. P. & Harris, R. A. Brain lipids that induce sleep are novel modulators of 5-hydroxytryptamine receptors. *Proc Natl Acad Sci U S A* **93**, 8078-8082, (1996).
- 5 Huidobro-Toro, J. P., Valenzuela, C. F. & Harris, R. A. Modulation of GABA_A receptor function by G protein-coupled 5-HT_{2C} receptors. *Neuropharmacology* **35**, 1355-1363, (1996).
- 6 Thomas, E. A., Carson, M. J., Neal, M. J. & Sutcliffe, J. G. Unique allosteric regulation of 5-hydroxytryptamine receptor-mediated signal transduction by oleamide. *Proc Natl Acad Sci U S A* **94**, 14115-14119, (1997).
- 7 Thomas, E. A., Cravatt, B. F. & Sutcliffe, J. G. The endogenous lipid oleamide activates serotonin 5-HT₇ neurons in mouse thalamus and hypothalamus. *J Neurochem* **72**, 2370-2378, (1999).
- 8 Hedlund, P. B., Carson, M. J., Sutcliffe, J. G. & Thomas, E. A. Allosteric regulation by oleamide of the binding properties of 5-hydroxytryptamine(7) receptors. *Biochemical Pharmacology* **58**, 1807-1813, (1999).
- 9 Sudhakar, V., Shaw, S. & Imig, J. D. Mechanisms involved in oleamide-induced vasorelaxation in rat mesenteric resistance arteries. *Eur J Pharmacol* **607**, 143-150, (2009).

- 10 Lees, G., Edwards, M. D., Hassoni, A. A., Ganellin, C. R. & Galanakis, D. Modulation of GABA(A) receptors and inhibitory synaptic currents by the endogenous CNS sleep regulator cis-9,10-octadecenoamide (cOA). *Br J Pharmacol* **124**, 873-882, (1998).
- 11 Laposky, A. D., Homanics, G. E., Basile, A. & Mendelson, W. B. Deletion of the GABA(A) receptor beta 3 subunit eliminates the hypnotic actions of oleamide in mice. *Neuroreport* **12**, 4143-4147, (2001).
- 12 Cheer, J. F., Cadogan, A. K., Marsden, C. A., Fone, K. C. & Kendall, D. A. Modification of 5-HT₂ receptor mediated behaviour in the rat by oleamide and the role of cannabinoid receptors. *Neuropharmacology* **38**, 533-541, (1999).
- 13 Mechoulam, R., Fride, E., Hanus, L., Sheskin, T., Bisogno, T., Di Marzo, V., Bayewitch, M. & Vogel, Z. Anandamide may mediate sleep induction. *Nature* **389**, 25-26, (1997).
- 14 Fedorova, I., Hashimoto, A., Fecik, R. A., Hedrick, M. P., Hanus, L. O., Boger, D. L., Rice, K. C. & Basile, A. S. Behavioral evidence for the interaction of oleamide with multiple neurotransmitter systems. *J Pharmacol Exp Ther* **299**, 332-342, (2001).
- 15 Cravatt, B. F., Prosperogarcia, O., Siuzdak, G., Gilula, N. B., Henriksen, S. J., Boger, D. L. & Lerner, R. A. Chemical Characterization of a Family of Brain Lipids That Induce Sleep. *Science* **268**, 1506-1509, (1995).
- 16 Lerner, R. A., Siuzdak, G., Prospero-Garcia, O., Henriksen, S. J., Boger, D. L. & Cravatt, B. F. Cerebrodiene: a brain lipid isolated from sleep-deprived cats. *Proc Natl Acad Sci U S A* **91**, 9505-9508, (1994).
- 17 Huitron-Resendiz, S., Gombart, L., Cravatt, B. F. & Henriksen, S. J. Effect of oleamide on sleep and its relationship to blood pressure, body temperature, and locomotor activity in rats. *Exp Neurol* **172**, 235-243, (2001).
- 18 Martinez-Gonzalez, D., Bonilla-Jaime, H., Morales-Otal, A., Henriksen, S. J., Velazquez-Moctezuma, J. & Prospero-Garcia, O. Oleamide and anandamide effects on food intake and sexual behavior of rats. *Neurosci Lett* **364**, 1-6, (2004).
- 19 Basile, A. S., Hanus, L. & Mendelson, W. B. Characterization of the hypnotic properties of oleamide. *Neuroreport* **10**, 947-951, (1999).

- 20 Bisogno, T., Sepe, N., De Petrocellis, L., Mechoulam, R. & Di Marzo, V. The sleep inducing factor oleamide is produced by mouse neuroblastoma cells. *Biochem Biophys Res Commun* **239**, 473-479, (1997).
- 21 Hanus, L. O., Fales, H. M., Spande, T. F. & Basile, A. S. A gas chromatographic-mass spectral assay for the quantitative determination of oleamide in biological fluids. *Analytical biochemistry* **270**, 159-166, (1999).
- 22 Merkler, D. J., Merkler, K. A., Stern, W. & Fleming, F. F. Fatty acid amide biosynthesis: a possible new role for peptidylglycine alpha-amidating enzyme and acyl-coenzyme A: glycine N-acyltransferase. *Arch Biochem Biophys* **330**, 430-434, (1996).
- 23 Wilcox, B. J., Ritenour-Rodgers, K. J., Asser, A. S., Baumgart, L. E., Baumgart, M. A., Boger, D. L., DeBlassio, J. L., deLong, M. A., Glufke, U., Henz, M. E., King, L., 3rd, Merkler, K. A., Patterson, J. E., Robleski, J. J., Vederas, J. C. *et al.* N-acylglycine amidation: implications for the biosynthesis of fatty acid primary amides. *Biochemistry* **38**, 3235-3245, (1999).
- 24 Merkler, K. A., Baumgart, L. E., DeBlassio, J. L., Glufke, U., King, L., 3rd, Ritenour-Rodgers, K., Vederas, J. C., Wilcox, B. J. & Merkler, D. J. A pathway for the biosynthesis of fatty acid amides. *Adv Exp Med Biol* **469**, 519-525, (1999).
- 25 Carpenter, T., Poore, D. D., Gee, A. J., Deshpande, P., Merkler, D. J. & Johnson, M. E. Use of reversed phase HP liquid chromatography to assay conversion of N-acylglycines to primary fatty acid amides by peptidylglycine-alpha-amidating monooxygenase. *J Chromatogr B Analyt Technol Biomed Life Sci* **809**, 15-21, (2004).
- 26 Merkler, D. J., Chew, G. H., Gee, A. J., Merkler, K. A., Sorondo, J. P. & Johnson, M. E. Oleic acid derived metabolites in mouse neuroblastoma N18TG2 cells. *Biochemistry* **43**, 12667-12674, (2004).
- 27 Driscoll, W. J., Chaturvedi, S. & Mueller, G. P. Oleamide synthesizing activity from rat kidney: identification as cytochrome c. *J Biol Chem* **282**, 22353-22363, (2007).
- 28 Mueller, G. P. & Driscoll, W. J. In vitro synthesis of oleoylglycine by cytochrome c points to a novel pathway for the production of lipid signaling molecules. *J Biol Chem* **282**, 22364-22369, (2007).

- 29 McCue, J. M., Driscoll, W. J. & Mueller, G. P. Cytochrome c catalyzes the in vitro synthesis of arachidonoyl glycine. *Biochemical and biophysical research communications* **365**, 322-327, (2008).
- 30 Sugiura, T., Kondo, S., Kodaka, T., Tonegawa, T., Nakane, S., Yamashita, A., Ishima, Y. & Waku, K. Enzymatic synthesis of oleamide (cis-9, 10-octadecenoamide), an endogenous sleep-inducing lipid, by rat brain microsomes. *Biochemistry and molecular biology international* **40**, 931-938, (1996).
- 31 O'Byrne, J., Hunt, M. C., Rai, D. K., Saeki, M. & Alexson, S. E. The human bile acid-CoA:amino acid N-acyltransferase functions in the conjugation of fatty acids to glycine. *J Biol Chem* **278**, 34237-34244, (2003).
- 32 Waluk, D. P., Schultz, N. & Hunt, M. C. Identification of glycine N-acyltransferase-like 2 (GLYATL2) as a transferase that produces N-acyl glycines in humans. *FASEB journal : official publication of the Federation of American Societies for Experimental Biology* **24**, 2795-2803, (2010).
- 33 Badenhorst, C. P., Jooste, M. & van Dijk, A. A. Enzymatic characterization and elucidation of the catalytic mechanism of a recombinant bovine glycine N-acyltransferase. *Drug metabolism and disposition: the biological fate of chemicals* **40**, 346-352, (2012).
- 34 Huang, S. M., Bisogno, T., Petros, T. J., Chang, S. Y., Zavitsanos, P. A., Zipkin, R. E., Sivakumar, R., Coop, A., Maeda, D. Y., De Petrocellis, L., Burstein, S., Di Marzo, V. & Walker, J. M. Identification of a new class of molecules, the arachidonoyl amino acids, and characterization of one member that inhibits pain. *J Biol Chem* **276**, 42639-42644, (2001).
- 35 Burstein, S. H., Rossetti, R. G., Yagen, B. & Zurier, R. B. Oxidative metabolism of anandamide. *Prostaglandins & other lipid mediators* **61**, 29-41, (2000).
- 36 Bradshaw, H. B., Rimmerman, N., Hu, S. S., Benton, V. M., Stuart, J. M., Masuda, K., Cravatt, B. F., O'Dell, D. K. & Walker, J. M. The endocannabinoid anandamide is a precursor for the signaling lipid N-arachidonoyl glycine by two distinct pathways. *BMC biochemistry* **10**, 14, (2009).
- 37 Aneetha, H., O'Dell, D. K., Tan, B., Walker, J. M. & Hurley, T. D. Alcohol dehydrogenase-catalyzed in vitro oxidation of anandamide to N-arachidonoyl glycine, a lipid mediator: Synthesis of N-acyl glycinals. *Bioorganic & Medicinal Chemistry Letters* **19**, 237-241, (2009).

- 38 Ivkovic, M., Dempsey, D. R., Handa, S., Hilton, J. H., Lowe, E. W., Jr. & Merkler, D. J. N-acylethanolamines as novel alcohol dehydrogenase 3 substrates. *Archives of biochemistry and biophysics* **506**, 157-164, (2011).
- 39 Sanghani, P. C., Robinson, H., Bosron, W. F. & Hurley, T. D. Human glutathione-dependent formaldehyde dehydrogenase. Structures of apo, binary, and inhibitory ternary complexes. *Biochemistry* **41**, 10778-10786, (2002).
- 40 Sanghani, P. C., Bosron, W. F. & Hurley, T. D. Human glutathione-dependent formaldehyde dehydrogenase. Structural changes associated with ternary complex formation. *Biochemistry* **41**, 15189-15194, (2002).
- 41 Chaturvedi, S., Driscoll, W. J., Elliot, B. M., Faraday, M. M., Grunberg, N. E. & Mueller, G. P. In vivo evidence that N-oleoylglycine acts independently of its conversion to oleamide. *Prostaglandins & Other Lipid Mediators* **81**, 136-149, (2006).
- 42 Deutsch, D. G., Ueda, N. & Yamamoto, S. The fatty acid amide hydrolase (FAAH). *Prostaglandins, leukotrienes, and essential fatty acids* **66**, 201-210, (2002).
- 43 Fowler, C. J., Jonsson, K. O. & Tiger, G. Fatty acid amide hydrolase: biochemistry, pharmacology, and therapeutic possibilities for an enzyme hydrolyzing anandamide, 2-arachidonoylglycerol, palmitoylethanolamide, and oleamide. *Biochemical pharmacology* **62**, 517-526, (2001).
- 44 Schlosburg, J. E., Kinsey, S. G. & Lichtman, A. H. Targeting fatty acid amide hydrolase (FAAH) to treat pain and inflammation. *The AAPS journal* **11**, 39-44, (2009).
- 45 Labar, G. & Michaux, C. Fatty acid amide hydrolase: from characterization to therapeutics. *Chemistry & biodiversity* **4**, 1882-1902, (2007).
- 46 Cravatt, B. F. & Lichtman, A. H. Fatty acid amide hydrolase: an emerging therapeutic target in the endocannabinoid system. *Current opinion in chemical biology* **7**, 469-475, (2003).
- 47 McKinney, M. K. & Cravatt, B. F. Structure and function of fatty acid amide hydrolase. *Annual review of biochemistry* **74**, 411-432, (2005).

- 48 Cravatt, B. F. & Lichtman, A. H. The enzymatic inactivation of the fatty acid amide class of signaling lipids. *Chem Phys Lipids* **121**, 135-148, (2002).
- 49 McKinney, M. K. & Cravatt, B. F. Evidence for distinct roles in catalysis for residues of the serine-serine-lysine catalytic triad of fatty acid amide hydrolase. *The Journal of biological chemistry* **278**, 37393-37399, (2003).
- 50 Bracey, M. H., Hanson, M. A., Masuda, K. R., Stevens, R. C. & Cravatt, B. F. Structural adaptations in a membrane enzyme that terminates endocannabinoid signaling. *Science* **298**, 1793-1796, (2002).
- 51 Wei, B. Q., Mikkelsen, T. S., McKinney, M. K., Lander, E. S. & Cravatt, B. F. A second fatty acid amide hydrolase with variable distribution among placental mammals. *The Journal of biological chemistry* **281**, 36569-36578, (2006).
- 52 Stewart, J. M., Boudreaux, N. M., Blakely, J. A. & Storey, K. B. A comparison of oleamide in the brains of hibernating and non-hibernating Richardson's ground squirrel (*Spermophilus richardsonii*) and its inability to bind to brain fatty acid binding protein. *Journal of Thermal Biology* **27**, 309-315, (2002).
- 53 Mendelson, W. B. & Basile, A. S. The hypnotic actions of the fatty acid amide, oleamide. *Neuropsychopharmacology* **25**, S36-39, (2001).
- 54 Murillo-Rodriguez, E., Giordano, M., Cabeza, R., Henriksen, S. J., Mendez Diaz, M., Navarro, L. & Prospero-Garcia, O. Oleamide modulates memory in rats. *Neuroscience letters* **313**, 61-64, (2001).
- 55 Wakamatsu, K., Masaki, T., Itoh, F., Kondo, K. & Sudo, K. Isolation of fatty acid amide as an angiogenic principle from bovine mesentery. *Biochem Biophys Res Commun* **168**, 423-429, (1990).
- 56 Mitchell, C. A., Davies, M. J., Grounds, M. D., McGeachie, J. K., Crawford, G. J., Hong, Y. & Chirila, T. V. Enhancement of neovascularization in regenerating skeletal muscle by the sustained release of erucamide from a polymer matrix. *J Biomater Appl* **10**, 230-249, (1996).
- 57 Rimmerman, N., Bradshaw, H. B., Hughes, H. V., Chen, J. S., Hu, S. S., McHugh, D., Vefring, E., Jahnsen, J. A., Thompson, E. L., Masuda, K., Cravatt, B. F., Burstein, S., Vasko, M. R., Prieto, A. L., O'Dell, D. K. *et al.* N-palmitoyl glycine, a novel endogenous lipid that acts as a modulator of calcium influx and

- nitric oxide production in sensory neurons. *Molecular pharmacology* **74**, 213-224, (2008).
- 58 Popa, D., Lena, C., Fabre, V., Prenat, C., Gingrich, J., Escourrou, P., Hamon, M. & Adrien, J. Contribution of 5-HT₂ receptor subtypes to sleep-wakefulness and respiratory control, and functional adaptations in knock-out mice lacking 5-HT_{2A} receptors. *The Journal of neuroscience : the official journal of the Society for Neuroscience* **25**, 11231-11238, (2005).
- 59 Gardani, M. & Biello, S. M. The effects of photic and nonphotic stimuli in the 5-HT₇ receptor knockout mouse. *Neuroscience* **152**, 245-253, (2008).
- 60 Meyer-Bernstein, E. L. & Morin, L. P. Differential serotonergic innervation of the suprachiasmatic nucleus and the intergeniculate leaflet and its role in circadian rhythm modulation. *The Journal of neuroscience : the official journal of the Society for Neuroscience* **16**, 2097-2111, (1996).
- 61 Hiley, C. R. & Hoi, P. M. Oleamide: a fatty acid amide signaling molecule in the cardiovascular system? *Cardiovasc Drug Rev* **25**, 46-60, (2007).
- 62 Hoi, P. M. & Hiley, C. R. Vasorelaxant effects of oleamide in rat small mesenteric artery indicate action at a novel cannabinoid receptor. *Br J Pharmacol* **147**, 560-568, (2006).
- 63 Macdonald, R. L. & Olsen, R. W. GABA_A receptor channels. *Annual review of neuroscience* **17**, 569-602, (1994).
- 64 Coyne, L., Lees, G., Nicholson, R. A., Zheng, J. & Neufield, K. D. The sleep hormone oleamide modulates inhibitory ionotropic receptors in mammalian CNS in vitro. *British journal of pharmacology* **135**, 1977-1987, (2002).
- 65 Verdon, B., Zheng, J., Nicholson, R. A., Ganelli, C. R. & Lees, G. Stereoselective modulatory actions of oleamide on GABA(A) receptors and voltage-gated Na(+) channels in vitro: a putative endogenous ligand for depressant drug sites in CNS. *British journal of pharmacology* **129**, 283-290, (2000).
- 66 Yost, C. S., Hampson, A. J., Leonoudakis, D., Koblin, D. D., Bornheim, L. M. & Gray, A. T. Oleamide potentiates benzodiazepine-sensitive gamma-aminobutyric acid receptor activity but does not alter minimum alveolar anesthetic concentration. *Anesthesia and analgesia* **86**, 1294-1300, (1998).

- 67 Guan, X., Cravatt, B. F., Ehring, G. R., Hall, J. E., Boger, D. L., Lerner, R. A. & Gilula, N. B. The sleep-inducing lipid oleamide deconvolutes gap junction communication and calcium wave transmission in glial cells. *J Cell Biol* **139**, 1785-1792, (1997).
- 68 Wiles, A. L., Pearlman, R. J., Rosvall, M., Aubrey, K. R. & Vandenberg, R. J. N-Arachidonyl-glycine inhibits the glycine transporter, GLYT2a. *Journal of neurochemistry* **99**, 781-786, (2006).
- 69 Bradshaw, H. B., Lee, S. H. & McHugh, D. Orphan endogenous lipids and orphan GPCRs: a good match. *Prostaglandins & other lipid mediators* **89**, 131-134, (2009).
- 70 Boger, D. L., Patterson, J. E., Guan, X., Cravatt, B. F., Lerner, R. A. & Gilula, N. B. Chemical requirements for inhibition of gap junction communication by the biologically active lipid oleamide. *Proc Natl Acad Sci U S A* **95**, 4810-4815, (1998).
- 71 Lo, Y. K., Tang, K. Y., Chang, W. N., Lu, C. H., Cheng, J. S., Lee, K. C., Chou, K. J., Liu, C. P., Chen, W. C., Su, W., Law, Y. P. & Jan, C. R. Effect of oleamide on Ca²⁺ signaling in human bladder cancer cells. *Biochem Pharmacol* **62**, 1363-1369, (2001).
- 72 Huang, J. K. & Jan, C. R. Linoleamide, a brain lipid that induces sleep, increases cytosolic Ca²⁺ levels in MDCK renal tubular cells. *Life Sci* **68**, 997-1004, (2001).
- 73 Bang, S., Yoo, S., Oh, U. & Hwang, S. W. Endogenous lipid-derived ligands for sensory TRP ion channels and their pain modulation. *Archives of pharmacal research* **33**, 1509-1520, (2010).
- 74 Bradshaw, H. B., Raboune, S. & Hollis, J. L. Opportunistic activation of TRP receptors by endogenous lipids: exploiting lipidomics to understand TRP receptor cellular communication. *Life sciences* **92**, 404-409, (2013).
- 75 Ross, R. A. Anandamide and vanilloid TRPV1 receptors. *British journal of pharmacology* **140**, 790-801, (2003).
- 76 Starowicz, K., Nigam, S. & Di Marzo, V. Biochemistry and pharmacology of endovanilloids. *Pharmacology & therapeutics* **114**, 13-33, (2007).

- 77 Zygmunt, P. M., Petersson, J., Andersson, D. A., Chuang, H., Sorgard, M., Di Marzo, V., Julius, D. & Hogestatt, E. D. Vanilloid receptors on sensory nerves mediate the vasodilator action of anandamide. *Nature* **400**, 452-457, (1999).
- 78 Movahed, P., Jonsson, B. A., Birnir, B., Wingstrand, J. A., Jorgensen, T. D., Ermund, A., Sterner, O., Zygmunt, P. M. & Hogestatt, E. D. Endogenous unsaturated C18 N-acylethanolamines are vanilloid receptor (TRPV1) agonists. *The Journal of biological chemistry* **280**, 38496-38504, (2005).
- 79 Huang, S. M., Bisogno, T., Trevisani, M., Al-Hayani, A., De Petrocellis, L., Fezza, F., Tognetto, M., Petros, T. J., Krey, J. F., Chu, C. J., Miller, J. D., Davies, S. N., Geppetti, P., Walker, J. M. & Di Marzo, V. An endogenous capsaicin-like substance with high potency at recombinant and native vanilloid VR1 receptors. *Proceedings of the National Academy of Sciences of the United States of America* **99**, 8400-8405, (2002).
- 80 Chu, C. J., Huang, S. M., De Petrocellis, L., Bisogno, T., Ewing, S. A., Miller, J. D., Zipkin, R. E., Daddario, N., Appendino, G., Di Marzo, V. & Walker, J. M. N-oleoyldopamine, a novel endogenous capsaicin-like lipid that produces hyperalgesia. *The Journal of biological chemistry* **278**, 13633-13639, (2003).
- 81 Oh, D. Y., Yoon, J. M., Moon, M. J., Hwang, J. I., Choe, H., Lee, J. Y., Kim, J. I., Kim, S., Rhim, H., O'Dell, D. K., Walker, J. M., Na, H. S., Lee, M. G., Kwon, H. B., Kim, K. *et al.* Identification of farnesyl pyrophosphate and N-arachidonylglycine as endogenous ligands for GPR92. *The Journal of biological chemistry* **283**, 21054-21064, (2008).
- 82 Lee, C. W., Rivera, R., Gardell, S., Dubin, A. E. & Chun, J. GPR92 as a new G12/13- and Gq-coupled lysophosphatidic acid receptor that increases cAMP, LPA5. *The Journal of biological chemistry* **281**, 23589-23597, (2006).
- 83 Kohno, M., Hasegawa, H., Inoue, A., Muraoka, M., Miyazaki, T., Oka, K. & Yasukawa, M. Identification of N-arachidonylglycine as the endogenous ligand for orphan G-protein-coupled receptor GPR18. *Biochemical and biophysical research communications* **347**, 827-832, (2006).
- 84 Lu, V. B., Puhl, H. L., 3rd & Ikeda, S. R. N-Arachidonyl glycine does not activate G protein-coupled receptor 18 signaling via canonical pathways. *Molecular pharmacology* **83**, 267-282, (2013).

- 85 Yin, H., Chu, A., Li, W., Wang, B., Shelton, F., Otero, F., Nguyen, D. G., Caldwell, J. S. & Chen, Y. A. Lipid G protein-coupled receptor ligand identification using beta-arrestin PathHunter assay. *The Journal of biological chemistry* **284**, 12328-12338, (2009).
- 86 Folch, J., Lees, M. & Sloane Stanley, G. H. A simple method for the isolation and purification of total lipides from animal tissues. *The Journal of biological chemistry* **226**, 497-509, (1957).
- 87 Hamberger, A. & Stenhagen, G. Erucamide as a modulator of water balance: new function of a fatty acid amide. *Neurochem Res* **28**, 177-185, (2003).
- 88 Kaluzny, M. A., Duncan, L. A., Merritt, M. V. & Epps, D. E. Rapid separation of lipid classes in high yield and purity using bonded phase columns. *Journal of lipid research* **26**, 135-140, (1985).
- 89 Sultana, T. & Johnson, M. E. Sample preparation and gas chromatography of primary fatty acid amides. *J Chromatogr A* **1101**, 278-285, (2006).
- 90 Madl, T. & Mittelbach, M. Quantification of primary fatty acid amides in commercial tallow and tallow fatty acid methyl esters by HPLC-APCI-MS. *The Analyst* **130**, 565-570, (2005).
- 91 Bradshaw, H. B., Rimmerman, N., Hu, S. S., Burstein, S. & Walker, J. M. Novel endogenous N-acyl glycines identification and characterization. *Vitam Horm* **81**, 191-205, (2009).
- 92 Pisitkun, T., Hoffert, J. D., Yu, M. J. & Knepper, M. A. Tandem mass spectrometry in physiology. *Physiology* **22**, 390-400, (2007).
- 93 Gee, A. J., Groen, L. A. & Johnson, M. E. Ion trap mass spectrometry of trimethylsilylamides following gas chromatography. *J Mass Spectrom* **35**, 305-310, (2000).
- 94 Divito, E. B., Davic, A. P., Johnson, M. E. & Cascio, M. Electrospray ionization and collision induced dissociation mass spectrometry of primary fatty acid amides. *Analytical chemistry* **84**, 2388-2394, (2012).

- 95 Lichtman, A. H., Hawkins, E. G., Griffin, G. & Cravatt, B. F. Pharmacological activity of fatty acid amides is regulated, but not mediated, by fatty acid amide hydrolase in vivo. *The Journal of pharmacology and experimental therapeutics* **302**, 73-79, (2002).
- 96 Subramaniam, S., Fahy, E., Gupta, S., Sud, M., Byrnes, R. W., Cotter, D., Dinsarapu, A. R. & Maurya, M. R. Bioinformatics and systems biology of the lipidome. *Chemical reviews* **111**, 6452-6490, (2011).
- 97 Brautigam, A., Wesenberg, D., Preud'homme, H. & Schaumlöffel, D. Rapid and simple UPLC-MS/MS method for precise phytochelatin quantification in alga extracts. *Analytical and bioanalytical chemistry* **398**, 877-883, (2010).
- 98 Neuss, C., Pelzing, M. & Macht, M. A robust approach for the analysis of peptides in the low femtomole range by capillary electrophoresis-tandem mass spectrometry. *Electrophoresis* **23**, 3149-3159, (2002).
- 99 Murphy, R. C., Fiedler, J. & Hevko, J. Analysis of nonvolatile lipids by mass spectrometry. *Chem Rev* **101**, 479-526, (2001).
- 100 Cravatt, B. F. Structure Determination of an Endogenous Sleep-Inducing Lipid, cis-9-octadecenamide (Oleamide): A Synthetic Approach to the Chemical Analysis of Trace Quantities of a Natural Product *Journal of the American Chemical Society* **118**, 580-590, (1996).
- 101 Nichols, K. K., Ham, B. M., Nichols, J. J., Ziegler, C. & Green-Church, K. B. Identification of fatty acids and fatty acid amides in human meibomian gland secretions. *Invest Ophthalmol Vis Sci* **48**, 34-39, (2007).
- 102 Philbrook, G. E. Synthesis of the Lower Aliphatic Amides. *Journal of Organic Chemistry* **19**, 623-625, (1954).
- 103 Wysocki, V. H. R., M. M. Charge Remote Fragmentation of Gas Phase Ions: Mechanistic and Energetic Considerations in the Dissociation of Long-chain Functionalized Alkanes and Alkenes. *International Journal of Mass Spectrometry and Ion Processes* **104**, 179-211, (1991).
- 104 Castro-Perez, J., Roddy, T. P., Nibbering, N. M., Shah, V., McLaren, D. G., Previs, S., Attygalle, A. B., Herath, K., Chen, Z., Wang, S. P., Mitnaul, L., Hubbard, B. K., Vreeken, R. J., Johns, D. G. & Hankemeier, T. Localization of

- fatty acyl and double bond positions in phosphatidylcholines using a dual stage CID fragmentation coupled with ion mobility mass spectrometry. *Journal of the American Society for Mass Spectrometry* **22**, 1552-1567, (2011).
- 105 Griffiths, W. J. Tandem mass spectrometry in the study of fatty acids, bile acids, and steroids. *Mass spectrometry reviews* **22**, 81-152, (2003).
- 106 Griffiths, W. J. A Comparison of Fast-atom Bombardment and Electrospray as Methods of Ionization in the Study of Sulphated- and Sulphonated-lipids by Tandem Mass Spectrometry. *Rapid Commun Mass Spectrom* **10**, 1169-1174, (1996).
- 107 Jensen, N. J. T., K. B.; Gross, M. L. Gas-Phase Ion Decompositions Occuring Remote to a Charge Site. *J Am Chem Soc* **107**, 1863-1868, (1985).
- 108 Crockett, J. S. Collisional Activation of a Series of Homoconjugated Octadecadienoic Acid with Fast Atom Bombardment and Tandem Mass Spectrometry. *Journal of the American Society for Mass Spectrometry* **1**, 183-191, (1990).
- 109 Kerwin, J. L., Wiens, A. M. & Ericsson, L. H. Identification of fatty acids by electrospray mass spectrometry and tandem mass spectrometry. *Journal of mass spectrometry : JMS* **31**, 184-192, (1996).
- 110 Jensen, N. J. G., M. L. Mass spectrometry methods for structural determination and analysis of fatty acids. *Mass Spectrom Rev* **6**, 497-536, (1987).
- 111 Lipid Biochemistry, Metabolism, and Signaling. *Chem Rev* **111**, 5817-6512, (2011).
- 112 Subramaniam, S., Fahy, E., Gupta, S., Sud, M., Byrnes, R. W., Cotter, D., Dinsarapu, A. R. & Maurya, M. R. Bioinformatics and systems biology of the lipidome. *Chem Rev* **111**, 6452-6490, (2011).
- 113 Mechoulam, R. & Parker, L. A. The endocannabinoid system and the brain. *Annual review of psychology* **64**, 21-47, (2013).

- 114 Luchicchi, A. & Pistis, M. Anandamide and 2-arachidonoylglycerol: pharmacological properties, functional features, and emerging specificities of the two major endocannabinoids. *Molecular neurobiology* **46**, 374-392, (2012).
- 115 Ahn, K., McKinney, M. K. & Cravatt, B. F. Enzymatic pathways that regulate endocannabinoid signaling in the nervous system. *Chemical reviews* **108**, 1687-1707, (2008).
- 116 Lambert, D. M., Vandevoorde, S., Jonsson, K. O. & Fowler, C. J. The palmitoylethanolamide family: a new class of anti-inflammatory agents? *Current medicinal chemistry* **9**, 663-674, (2002).
- 117 Lerner, R. A., Siuzdak, G., Prospero-Garcia, O., Henriksen, S. J., Boger, D. L. & Cravatt, B. F. Cerebrodiene: a brain lipid isolated from sleep-deprived cats. *Proceedings of the National Academy of Sciences of the United States of America* **91**, 9505-9508, (1994).
- 118 Fedorova, I., Hashimoto, A., Fecik, R. A., Hedrick, M. P., Hanus, L. O., Boger, D. L., Rice, K. C. & Basile, A. S. Behavioral evidence for the interaction of oleamide with multiple neurotransmitter systems. *The Journal of pharmacology and experimental therapeutics* **299**, 332-342, (2001).
- 119 Wakamatsu, K., Masaki, T., Itoh, F., Kondo, K. & Sudo, K. Isolation of fatty acid amide as an angiogenic principle from bovine mesentery. *Biochemical and biophysical research communications* **168**, 423-429, (1990).
- 120 Ghafouri, N., Ghafouri, B., Larsson, B., Stensson, N., Fowler, C. J. & Gerdle, B. Palmitoylethanolamide and stearoylethanolamide levels in the interstitium of the trapezius muscle of women with chronic widespread pain and chronic neck-shoulder pain correlate with pain intensity and sensitivity. *Pain*, (2013).
- 121 Leweke, F. M., Giuffrida, A., Wurster, U., Emrich, H. M. & Piomelli, D. Elevated endogenous cannabinoids in schizophrenia. *Neuroreport* **10**, 1665-1669, (1999).
- 122 Dlugos, A., Childs, E., Stuhr, K. L., Hillard, C. J. & de Wit, H. Acute stress increases circulating anandamide and other N-acylethanolamines in healthy humans. *Neuropsychopharmacology : official publication of the American College of Neuropsychopharmacology* **37**, 2416-2427, (2012).

- 123 Adlof, R. Analysis of triacylglycerol and fatty acid isomers by low-temperature silver-ion high performance liquid chromatography with acetonitrile in hexane as solvent: limitations of the methodology. *Journal of chromatography. A* **1148**, 256-259, (2007).
- 124 Adlof, R. O. Separation of conjugated linoleic acid methyl esters by silver-ion high performance liquid chromatography in semi-preparative mode. *Journal of Chromatography A* **1033**, 369-371, (2004).
- 125 Christie, W. W., Dobson, G. & Adlof, R. O. A practical guide to the isolation, analysis and identification of conjugated linoleic acid. *Lipids* **42**, 1073-1084, (2007).
- 126 Christie, W. W. Some recent advances in the chromatographic analysis of lipids. *Analisis* **26**, M34-M40, (1998).
- 127 Christie, W. W. in *Lipid Technology* (1998).
- 128 Dobson, G., Christie, W. W. & Nikolovadamyanova, B. Silver Ion Chromatography of Lipids and Fatty-Acids. *Journal of Chromatography B-Biomedical Applications* **671**, 197-222, (1995).
- 129 Momchilova, S., Nikolova-Damyanova, B. & Christie, W. W. Silver ion high-performance liquid chromatography of isomeric cis- and trans-octadecenoic acids - Effect of the ester moiety and mobile phase composition. *Journal of Chromatography A* **793**, 275-282, (1998).
- 130 Nikolova-Damyanova, B., Dobson, G., Momchilova, S. & Christie, W. W. Cyclohexanediol fatty acid diesters as model compounds for mechanistic studies in silver ion high performance liquid chromatography. *Journal of Liquid Chromatography & Related Technologies* **26**, 1905-1912, (2003).
- 131 Mondello, L., Tranchida, P. Q., Stanek, V., Jandera, P., Dugo, G. & Dugo, P. Silver-ion reversed-phase comprehensive two-dimensional liquid chromatography combined with mass spectrometric detection in lipidic food analysis. *Journal of Chromatography A* **1086**, 91-98, (2005).
- 132 Dugo, P., Favoino, O., Tranchida, P. Q., Dugo, G. & Mondello, L. Off-line coupling of non-aqueous reversed-phase and silver ion high-performance liquid chromatography-mass spectrometry for the characterization of rice oil

- triacylglycerol positional isomers. *Journal of Chromatography A* **1041**, 135-142, (2004).
- 133 Dugo, P., Kumm, T., Crupi, M. L., Cotroneo, A. & Mondello, L. Comprehensive two-dimensional liquid chromatography combined with mass spectrometric detection in the analyses of triacylglycerols in natural lipidic matrixes. *Journal of Chromatography A* **1112**, 269-275, (2006).
- 134 Dugo, P., Kumm, T., Fazio, A., Dugo, G. & Mondello, L. Determination of beef tallow in lard through a multidimensional off-line non-aqueous reversed phase-argentation LC method coupled to mass spectrometry. *Journal of Separation Science* **29**, 567-575, (2006).
- 135 Cohen, S. A. *Multidimensional Liquid Chromatography: Theory and Applications in Industrial Chemistry and Life Sciences*. (Wiley Interscience, 2008).
- 136 Giddings, J. C. Two-Dimensional separations: concept and promise. *Analytical Chemistry* **56**, 1258A-1270A, (1984).
- 137 Bushey, M., Jorgenson, J. W. . Automated Instrumentation for Comprehensive Two-Dimensional High Performance Liquid Chromatography of Proteins. *Analytical Chemistry* **62**, 161-167, (1990).
- 138 Dixon, S. P., Pitfield, I. D. & Perrett, D. Comprehensive multi-dimensional liquid chromatographic separation in biomedical and pharmaceutical analysis: a review. *Biomedical Chromatography* **20**, 508-529, (2006).
- 139 Dugo, P., Cacciola, F., Kumm, T., Dugo, G. & Mondello, L. Comprehensive multidimensional liquid chromatography: Theory and applications. *Journal of Chromatography A* **1184**, 353-368, (2008).
- 140 Carr, P. W., Wang, X. & Stoll, D. R. Effect of pressure, particle size, and time on optimizing performance in liquid chromatography. *Anal Chem* **81**, 5342-5353, (2009).
- 141 Karger, B. L. C., W. D. Effect of Particle Size and Average Velocity on Resolution unde Normalized Time Conditions. *Analytical Chemistry* **36**, 991-995, (1964).

- 142 Karger, B. L. C., W. D. Effect of Column Length on Resolution under Normalized Time Conditions. *Analytical Chemistry* **36**, 985-991, (1964).
- 143 Christie, W. W. Silver Ion High-Performance Liquid Chromatography: the mechanism. *Lipid Technology* **10**, 17-19, (1998).
- 144 Momchilova, S. & Nikolova-Damyanova, B. Stationary phases for silver ion chromatography of lipids: Preparation and properties. *Journal of Separation Science* **26**, 261-270, (2003).
- 145 Nikolova-Damyanova, B. Retention of lipids in silver ion high-performance liquid chromatography: Facts and assumptions. *Journal of Chromatography A* **1216**, 1815-1824, (2009).
- 146 Harfmann, R. G., Julka, S. & Cortes, H. J. Instability of hexane-acetonitrile mobile phases used for the chromatographic analysis of triacylglycerides. *Journal of Separation Science* **31**, 915-920, (2008).
- 147 Shan, H. & Wilson, W. K. Ternary gradient elution markedly improves silver-ion high performance liquid chromatography of unsaturated sterols. *Steroids* **67**, 917-923, (2002).
- 148 Adlof, R. & List, G. Analysis of triglyceride isomers by silver-ion high-performance liquid chromatography - Effect of column temperature on retention times. *Journal of Chromatography A* **1046**, 109-113, (2004).
- 149 Sultana, T. & Johnson, M. E. Sample preparation and gas chromatography of primary fatty acid amides. *Journal of chromatography. A* **1101**, 278-285, (2006).
- 150 Wood, R. a. L., T. High-Performance Liquid Chromatography of Fatty Acids: Quantitative Analysis of Saturated, Monoenoic, Polyenoic and Geometrical Isomers. *Journal of Chromatography* **254**, 237-246, (1983).
- 151 Morris, L. J. Separations of lipids by silver ion chromatography. *Journal of lipid research* **7**, 717-732, (1966).
- 152 Herling, J., Shabtai, J. & Gil-Av, E. Gas chromatography with stationary phases containing silver nitrate. III. Isomeric C8 and C9 cyclohexenes and p-menthenes. *Journal of chromatography* **8**, 349-354, (1962).

- 153 Gutnikov, G. Fatty-Acid Profiles of Lipid Samples. *Journal of Chromatography B-Biomedical Applications* **671**, 71-89, (1995).
- 154 Mueller, G. P. & Driscoll, W. J. Biosynthesis of oleamide. *Vitam Horm* **81**, 55-78, (2009).
- 155 Merkler, D. J. C-terminal amidated peptides: production by the in vitro enzymatic amidation of glycine-extended peptides and the importance of the amide to bioactivity. *Enzyme Microb Technol* **16**, 450-456, (1994).
- 156 Owen, T. C. & Merkler, D. J. A new proposal for the mechanism of glycine hydroxylation as catalyzed by peptidylglycine alpha-hydroxylating monooxygenase (PHM). *Med Hypotheses* **62**, 392-400, (2004).
- 157 Eipper, B. A., Glembotski, C. C. & Mains, R. E. Bovine intermediate pituitary alpha-amidation enzyme: preliminary characterization. *Peptides* **4**, 921-928, (1983).
- 158 Eipper, B. A., May, V. & Braas, K. M. Membrane-associated peptidylglycine alpha-amidating monooxygenase in the heart. *J Biol Chem* **263**, 8371-8379, (1988).
- 159 Eipper, B. A., Milgram, S. L., Husten, E. J., Yun, H. Y. & Mains, R. E. Peptidylglycine alpha-amidating monooxygenase: a multifunctional protein with catalytic, processing, and routing domains. *Protein Sci* **2**, 489-497, (1993).
- 160 Eipper, B. A., Stoffers, D. A. & Mains, R. E. The biosynthesis of neuropeptides: peptide alpha-amidation. *Annu Rev Neurosci* **15**, 57-85, (1992).
- 161 Kolhekar, A. S., Bell, J., Shiozaki, E. N., Jin, L., Keutmann, H. T., Hand, T. A., Mains, R. E. & Eipper, B. A. Essential features of the catalytic core of peptidyl-alpha-hydroxyglycine alpha-amidating lyase. *Biochemistry* **41**, 12384-12394, (2002).
- 162 Kolhekar, A. S., Roberts, M. S., Jiang, N., Johnson, R. C., Mains, R. E., Eipper, B. A. & Taghert, P. H. Neuropeptide amidation in *Drosophila*: separate genes encode the two enzymes catalyzing amidation. *J Neurosci* **17**, 1363-1376, (1997).

- 163 Ouafik, L., May, V., Keutmann, H. T. & Eipper, B. A. Developmental regulation of peptidylglycine alpha-amidating monooxygenase (PAM) in rat heart atrium and ventricle. Tissue-specific changes in distribution of PAM activity, mRNA levels, and protein forms. *J Biol Chem* **264**, 5839-5845, (1989).
- 164 Ouafik, L., May, V., Saffen, D. W. & Eipper, B. A. Thyroid hormone regulation of peptidylglycine alpha-amidating monooxygenase expression in anterior pituitary gland. *Mol Endocrinol* **4**, 1497-1505, (1990).
- 165 Prigge, S. T., Kolhekar, A. S., Eipper, B. A., Mains, R. E. & Amzel, L. M. Amidation of bioactive peptides: the structure of peptidylglycine alpha-hydroxylating monooxygenase. *Science* **278**, 1300-1305, (1997).
- 166 Bradbury, A. F., Finnie, M. D. & Smyth, D. G. Mechanism of C-terminal amide formation by pituitary enzymes. *Nature* **298**, 686-688, (1982).
- 167 Seed, B. Silanizing glassware. *Current protocols in molecular biology / edited by Frederick M. Ausubel ... [et al.] Appendix 3*, Appendix 3B, (2001).
- 168 Cooper, I. & Tice, P. A. Migration studies on fatty acid amide slip additives from plastics into food simulants. *Food Addit Contam* **12**, 235-244, (1995).
- 169 Fahy, E., Subramaniam, S., Brown, H. A., Glass, C. K., Merrill, A. H., Murphy, R. C., Raetz, C. R. H., Russell, D. W., Seyama, Y., Shaw, W., Shimizu, T., Spener, F., van Meer, G., VanNieuwenhze, M. S., White, S. H. *et al.* A comprehensive classification system for lipids. *Journal of Lipid Research* **46**, 839-861, (2005).
- 170 Schmid, P. C., Reddy, P. V., Natarajan, V. & Schmid, H. H. Metabolism of N-acylethanolamine phospholipids by a mammalian phosphodiesterase of the phospholipase D type. *The Journal of biological chemistry* **258**, 9302-9306, (1983).
- 171 Di Marzo, V., Fontana, A., Cadas, H., Schinelli, S., Cimino, G., Schwartz, J. C. & Piomelli, D. Formation and inactivation of endogenous cannabinoid anandamide in central neurons. *Nature* **372**, 686-691, (1994).
- 172 Okamoto, Y., Morishita, J., Tsuboi, K., Tonai, T. & Ueda, N. Molecular characterization of a phospholipase D generating anandamide and its congeners. *The Journal of biological chemistry* **279**, 5298-5305, (2004).

- 173 Tsuboi, K., Takezaki, N. & Ueda, N. The N-acylethanolamine-hydrolyzing acid amidase (NAAA). *Chemistry & biodiversity* **4**, 1914-1925, (2007).
- 174 Devane, W. A., Hanus, L., Breuer, A., Pertwee, R. G., Stevenson, L. A., Griffin, G., Gibson, D., Mandelbaum, A., Etinger, A. & Mechoulam, R. Isolation and structure of a brain constituent that binds to the cannabinoid receptor. *Science* **258**, 1946-1949, (1992).
- 175 Coburn, A. F., Graham, C. E. & Haninger, J. The effect of egg yolk in diets on anaphylactic arthritis (passive Arthus phenomenon) in the guinea pig. *The Journal of experimental medicine* **100**, 425-435, (1954).
- 176 Kuehl, F. A. J., T.A.; Ganley, O.H.; Ormond, R.E.; Meisinger, M.A.P. The Identification Of N-(2-Hydroxyethyl)-Palmitamide As s Naturally Occuring Anti-Inflammatory Agent. *J Am Chem Soc* **79**, 5577-5578, (1957).
- 177 Long, D. A. & Martin, A. J. Factor in arachis oil depressing sensitivity to tuberculin in B.C.G.-infected guineapigs. *Lancet* **270**, 464-466, (1956).
- 178 Bisogno, T., Ventriglia, M., Milone, A., Mosca, M., Cimino, G. & Di Marzo, V. Occurrence and metabolism of anandamide and related acyl-ethanolamides in ovaries of the sea urchin *Paracentrotus lividus*. *Biochimica et biophysica acta* **1345**, 338-348, (1997).
- 179 Matias, I., Bisogno, T., Melck, D., Vandenbulcke, F., Verger-Bocquet, M., De Petrocellis, L., Sergheraert, C., Breton, C., Di Marzo, V. & Salzet, M. Evidence for an endocannabinoid system in the central nervous system of the leech *Hirudo medicinalis*. *Brain research. Molecular brain research* **87**, 145-159, (2001).
- 180 Sepe, N., De Petrocellis, L., Montanaro, F., Cimino, G. & Di Marzo, V. Bioactive long chain N-acylethanolamines in five species of edible bivalve molluscs. Possible implications for mollusc physiology and sea food industry. *Biochimica et biophysica acta* **1389**, 101-111, (1998).
- 181 Schmid, P. C., Krebsbach, R. J., Perry, S. R., Dettmer, T. M., Maasson, J. L. & Schmid, H. H. Occurrence and postmortem generation of anandamide and other long-chain N-acylethanolamines in mammalian brain. *FEBS letters* **375**, 117-120, (1995).

- 182 Baker, D., Pryce, G., Croxford, J. L., Brown, P., Pertwee, R. G., Makriyannis, A., Khanolkar, A., Layward, L., Fezza, F., Bisogno, T. & Di Marzo, V. Endocannabinoids control spasticity in a multiple sclerosis model. *FASEB journal : official publication of the Federation of American Societies for Experimental Biology* **15**, 300-302, (2001).
- 183 Kondo, S., Sugiura, T., Kodaka, T., Kudo, N., Waku, K. & Tokumura, A. Accumulation of various N-acylethanolamines including N-arachidonylethanolamine (anandamide) in cadmium chloride-administered rat testis. *Archives of biochemistry and biophysics* **354**, 303-310, (1998).
- 184 Giuffrida, A. & Piomelli, D. Isotope dilution GC/MS determination of anandamide and other fatty acylethanolamides in rat blood plasma. *FEBS letters* **422**, 373-376, (1998).
- 185 Di Cesare Mannelli, L., D'Agostino, G., Pacini, A., Russo, R., Zanardelli, M., Ghelardini, C. & Calignano, A. Palmitoylethanolamide is a disease-modifying agent in peripheral neuropathy: pain relief and neuroprotection share a PPAR-alpha-mediated mechanism. *Mediators of inflammation* **2013**, 328797, (2013).
- 186 LoVerme, J., Russo, R., La Rana, G., Fu, J., Farthing, J., Mattace-Raso, G., Meli, R., Hohmann, A., Calignano, A. & Piomelli, D. Rapid broad-spectrum analgesia through activation of peroxisome proliferator-activated receptor-alpha. *The Journal of pharmacology and experimental therapeutics* **319**, 1051-1061, (2006).
- 187 Mazzari, S., Canella, R., Petrelli, L., Marcolongo, G. & Leon, A. N-(2-hydroxyethyl)hexadecanamide is orally active in reducing edema formation and inflammatory hyperalgesia by down-modulating mast cell activation. *European journal of pharmacology* **300**, 227-236, (1996).
- 188 Facci, L., Dal Toso, R., Romanello, S., Buriani, A., Skaper, S. D. & Leon, A. Mast cells express a peripheral cannabinoid receptor with differential sensitivity to anandamide and palmitoylethanolamide. *Proceedings of the National Academy of Sciences of the United States of America* **92**, 3376-3380, (1995).
- 189 Calignano, A., La Rana, G., Giuffrida, A. & Piomelli, D. Control of pain initiation by endogenous cannabinoids. *Nature* **394**, 277-281, (1998).
- 190 Solorzano, C., Zhu, C., Battista, N., Astarita, G., Lodola, A., Rivara, S., Mor, M., Russo, R., Maccarrone, M., Antonietti, F., Duranti, A., Tontini, A., Cuzzocrea, S., Tarzia, G. & Piomelli, D. Selective N-acylethanolamine-hydrolyzing acid

- amidase inhibition reveals a key role for endogenous palmitoylethanolamide in inflammation. *Proceedings of the National Academy of Sciences of the United States of America* **106**, 20966-20971, (2009).
- 191 Ross, R. A., Brockie, H. C. & Pertwee, R. G. Inhibition of nitric oxide production in RAW264.7 macrophages by cannabinoids and palmitoylethanolamide. *European journal of pharmacology* **401**, 121-130, (2000).
- 192 Richardson, D., Pearson, R. G., Kurian, N., Latif, M. L., Garle, M. J., Barrett, D. A., Kendall, D. A., Scammell, B. E., Reeve, A. J. & Chapman, V. Characterisation of the cannabinoid receptor system in synovial tissue and fluid in patients with osteoarthritis and rheumatoid arthritis. *Arthritis research & therapy* **10**, R43, (2008).
- 193 Epps, D. E., Schmid, P. C., Natarajan, V. & Schmid, H. H. N-Acylethanolamine accumulation in infarcted myocardium. *Biochemical and biophysical research communications* **90**, 628-633, (1979).
- 194 Skaper, S. D., Buriani, A., Dal Toso, R., Petrelli, L., Romanello, S., Facci, L. & Leon, A. The ALIAMide palmitoylethanolamide and cannabinoids, but not anandamide, are protective in a delayed postglutamate paradigm of excitotoxic death in cerebellar granule neurons. *Proceedings of the National Academy of Sciences of the United States of America* **93**, 3984-3989, (1996).
- 195 Koch, M., Kreutz, S., Bottger, C., Benz, A., Maronde, E., Ghadban, C., Korf, H. W. & Dehghani, F. Palmitoylethanolamide protects dentate gyrus granule cells via peroxisome proliferator-activated receptor-alpha. *Neurotoxicity research* **19**, 330-340, (2011).
- 196 Garg, P., Duncan, R. S., Kaja, S. & Koulen, P. Intracellular mechanisms of N-acylethanolamine-mediated neuroprotection in a rat model of stroke. *Neuroscience* **166**, 252-262, (2010).
- 197 D'Agostino, G., Russo, R., Avagliano, C., Cristiano, C., Meli, R. & Calignano, A. Palmitoylethanolamide protects against the amyloid-beta₂₅₋₃₅-induced learning and memory impairment in mice, an experimental model of Alzheimer disease. *Neuropsychopharmacology : official publication of the American College of Neuropsychopharmacology* **37**, 1784-1792, (2012).

- 198 Lambert, D. M., Vandevorode, S., Diependaele, G., Govaerts, S. J. & Robert, A. R. Anticonvulsant activity of N-palmitoylethanolamide, a putative endocannabinoid, in mice. *Epilepsia* **42**, 321-327, (2001).
- 199 Bachur, N. R., Masek, K., Melmon, K. L. & Udenfriend, S. Fatty Acid Amides of Ethanolamine in Mammalian Tissues. *The Journal of biological chemistry* **240**, 1019-1024, (1965).
- 200 Rodriguez de Fonseca, F., Navarro, M., Gomez, R., Escuredo, L., Nava, F., Fu, J., Murillo-Rodriguez, E., Giuffrida, A., LoVerme, J., Gaetani, S., Kathuria, S., Gall, C. & Piomelli, D. An anorexic lipid mediator regulated by feeding. *Nature* **414**, 209-212, (2001).
- 201 Terrazzino, S., Berto, F., Dalle Carbonare, M., Fabris, M., Guiotto, A., Bernardini, D. & Leon, A. Stearoylethanolamide exerts anorexic effects in mice via down-regulation of liver stearyl-coenzyme A desaturase-1 mRNA expression. *FASEB journal : official publication of the Federation of American Societies for Experimental Biology* **18**, 1580-1582, (2004).
- 202 LoVerme, J., Guzman, M., Gaetani, S. & Piomelli, D. Cold exposure stimulates synthesis of the bioactive lipid oleoylethanolamide in rat adipose tissue. *The Journal of biological chemistry* **281**, 22815-22818, (2006).
- 203 Ryberg, E., Larsson, N., Sjogren, S., Hjorth, S., Hermansson, N. O., Leonova, J., Elebring, T., Nilsson, K., Drmota, T. & Greasley, P. J. The orphan receptor GPR55 is a novel cannabinoid receptor. *British journal of pharmacology* **152**, 1092-1101, (2007).
- 204 Lauckner, J. E., Jensen, J. B., Chen, H. Y., Lu, H. C., Hille, B. & Mackie, K. GPR55 is a cannabinoid receptor that increases intracellular calcium and inhibits M current. *Proceedings of the National Academy of Sciences of the United States of America* **105**, 2699-2704, (2008).
- 205 Pertwee, R. G. GPR55: a new member of the cannabinoid receptor clan? *British journal of pharmacology* **152**, 984-986, (2007).
- 206 Overton, H. A., Babbs, A. J., Doel, S. M., Fyfe, M. C., Gardner, L. S., Griffin, G., Jackson, H. C., Procter, M. J., Rasamison, C. M., Tang-Christensen, M., Widdowson, P. S., Williams, G. M. & Reynet, C. Deorphanization of a G protein-coupled receptor for oleoylethanolamide and its use in the discovery of small-molecule hypophagic agents. *Cell metabolism* **3**, 167-175, (2006).

- 207 Janjic, J. M. P., S. K. ; Patrick, M. J. ; Pollock, J. A. ; Divito, E. B. ; Cascio, M. . Suppressing inflammation from inside out with novel NIR visible perfluorocarbon nanotheranostics. *Proc. SPIE* **8596**, (2013).
- 208 Patel, S. K., Patrick, M. J., Pollock, J. A. & Janjic, J. M. Two-color fluorescent (near-infrared and visible) triphasic perfluorocarbon nanoemulsions. *Journal of biomedical optics* **18**, 101312, (2013).
- 209 Patel, S. K., Zhang, Y., Pollock, J. A. & Janjic, J. M. Cyclooxygenase-2 inhibiting perfluoropoly (ethylene glycol) ether theranostic nanoemulsions-in vitro study. *PLoS one* **8**, e55802, (2013).
- 210 Palandra, J., Prusakiewicz, J., Ozer, J. S., Zhang, Y. & Heath, T. G. Endogenous ethanolamide analysis in human plasma using HPLC tandem MS with electrospray ionization. *Journal of chromatography. B, Analytical technologies in the biomedical and life sciences* **877**, 2052-2060, (2009).
- 211 Lam, P. M., Marczylo, T. H. & Konje, J. C. Simultaneous measurement of three N-acylethanolamides in human bio-matrices using ultra performance liquid chromatography-tandem mass spectrometry. *Analytical and bioanalytical chemistry* **398**, 2089-2097, (2010).
- 212 Lin, L., Yang, H. & Jones, P. J. Quantitative analysis of multiple fatty acid ethanolamides using ultra-performance liquid chromatography-tandem mass spectrometry. *Prostaglandins, leukotrienes, and essential fatty acids* **87**, 189-195, (2012).
- 213 Skonberg, C., Artmann, A., Cornett, C., Hansen, S. H. & Hansen, H. S. Pitfalls in the sample preparation and analysis of N-acylethanolamines. *Journal of lipid research* **51**, 3062-3073, (2010).